Direct Methods For Solving the Schrödinger Equation

Explicitly Correlated Wavefunctions

Mohammad Mostafanejad

Research School of Chemistry

College of Physical and Mathematical Sciences

A thesis submitted for the degree of

Master of Philosophy

of the Australian National University

November 2016

Declaration

I hereby declare that to my best knowledge, the contents of this thesis are original and have not been submitted in whole or in part for consideration for any other degree or qualification at ANU, or any other university. Also, necessary citations have been carefully and explicitly made throughout the text whenever they referred to the work of other persons. This dissertation contains fewer than 60,000 words excluding appendices, bibliography, footnotes, tables, figures and equations.

Mohammad Mostafanejad

November 2016

To my parents . . .

Acknowledgements

I would like to thank ANU for the IPRS scholarship. Inspiring and fruitful discussions with our sabbatical visitors Prof. Patrick Bultinck from Ghent University which led to an interesting project on the performance of the Hylleraas-configuration interaction wavefunction, and Prof. Vitaly Rassolov from University of South Carolina which resulted in a deeper understanding of mine about the electron correlation problem and correlation operators are also acknowledged. I am indebted to our physicist visitor Prof. Nimrod Moiseyev for the fascinating discussion about complex and stability analyses and sending me valuable papers from his PhD project. I am also grateful to Dr. Andrew Thomas Beresford Gilbert for his expertise in mathematics who was a great source of learning for me and Dr. Marat Sibaev for his useful suggestions.

Abstract

The notions of electron correlation and correlation problem arising in the framework of approximate solutions to the Schrödinger equation are presented. Then, we briefly review the original ideas of explicit inclusion of the interelectronic distance, r_{12}, into the wavefunction as a solution to this problem.

Exemplifying the efficiency of the explicit correlation for achieving high accuracy, we analyze the Nakatsuji's free-complement (FC) method. We demonstrate that at each FC order, fewer number of complement functions is required to get lower energies compared with those resulting from the conventional FC method. Applying the FC method to the triplet excited state of the He atom, we have discovered the appearance of permanents in addition to the determinants in the FC expansion of the wavefunction. These permanents are shown to be important for the energy convergence.

To achieve a better understanding about the explicitly correlated methods, especially, the R12 and F12 methods, we analyzed three possible candidates with various correlation functions $F(r_{12})$ for a compact and efficient ansatz. Our main focus on the linear correlation factor r_{12} has led this analysis to the investigation of the correlated molecular orbital (CMO)

theory of the Frost and Braunstein (FB). We revisit CMO theory within both restricted (R) and unrestricted formalisms (U). We also introduce the unrestricted FB (UFB) ansatz for the first time and derive the necessary expressions for both RFB and UFB overlap, kinetic, nuclear-attraction and interelectronic Coulomb repulsion matrix elements. All integrals have been obtained in closed form except one for which, we have used an accurate one-dimensional quadrature.

Finally, we investigate the potential energy curve (PEC) of UFB for H_2 at small, intermediate and large internuclear distances. Then, we compare its performance with that of RFB, restricted Hartree-Fock (RHF), unrestricted Hartree-Fock (UHF) and configuration interaction (CI) wavefunctions. Reproducing the RFB results for a much wider range of bond lengths in H_2 reveals that the calculations of FB contain significant errors. We have also found a pole in the RFB linear correlation coefficient. Our UFB ansatz provides significant improvement over the RFB where passing the symmetry breaking point it completely removes the hump in the RFB PEC. The UFB ansatz also shows surprising features such as the presence of multiple solutions, non-smooth PEC, symmetry-broken solutions that are higher in energy than the restricted solution and RFB→UFB stability in the presence of lower UFB solutions. These phenomena can have significant impacts on the explicitly correlated calculations such as R12 and F12 within the unrestricted framework. Also, a detailed discussion on the large-R asymptotic analysis of these five wavefunctions shows that none of these PECs has the correct $O(R^{-6})$ decay within the minimal basis model. The UFB energy, however, demonstrates dispersion-like $O(R^{-8})$ decay which is an improvement over the CI and UHF with exponential decays. Considering the generalized FB (GFB) wavefunction where r_{12}^n is the correlation factor and n is a positive integer, we have shown that no analytic function of r_{12} can capture the dispersion within the minimal basis.

Table of Contents

List of Figures

List of Tables

List of Abbreviations and Nomenclatures

Acronyms / Abbreviations

AO Atomic Orbital

BO Born-Oppenheimer

CC Coupled Cluster

CCS Coupled Cluster Singles

CCSD Coupled Cluster Singles and Doubles

CHGF Confluent Hypergeometric Function

CI Configuration Interaction

CMO Correlated Molecular Orbital

CSF Configuration State Function

FB Frost-Braunstein

FC Free Complement

FCI Full-Configuration Interaction

GTO Gaussian-Type Orbital

HF Hartree-Fock

HP Hartree Product

ICI Iterative Configuration Interaction

ISE Inverse Schrödinger Equation

LSE Local Schrödinger Equation

LYP Lee–Yang–Parr

MO Molecular Orbital

PEC Potential Energy Curve

RFB Restricted Frost-Braunstein

RHF Restricted Hartree-Fock

SB Symmetry-Broken

SCF Self-Consistent Field

SE Schrödinger Equation

SSE Scaled Schrödinger Equation

STO Slater-Type Orbital

UFB Unrestricted Frost-Braunstein

UHF Unrestricted Hartree-Fock

CHAPTER 1

Electron Correlation and Explicitly Correlated Wavefucntions

The electron correlation problem as one of the central challenges in modern quantum chemistry has been briefly reviewed. Various definitions and concepts for describing the electron correlation including those which are based on probabilistic or statistical interpretation have been discussed. Furthermore, qualitative electron correlation concepts such as radial, angular, left-right, static and dynamic correlations have been summarized. We also briefly refer to the quantitative tools for measuring the electron correlation. Considering one of the main drawbacks of standard approximate quantum mechanical methods which are based on the configuration interaction (CI)-type expansions *of the wavefunction, i.e., the slow convergence of the energy to the basis set limit, the origins of the ideas of introducing the interelectronic distance into the wavefunction were discussed. Atomic units have been used throughout this thesis.*

1.1 Introduction to the Correlation Problem

As one of the most fundamental characteristics of the many-electron systems and based on the probabilistic interpretation of the quantum mechanics, [1] the electron correlation can find its roots in the correlation concept arising in probability theory [2, 3]. This issue is of crucial importance in quantum chemistry possibly because most popular approximate methods in this field are based on independent particle model or mean–field approach to describe the N-electron systems. [1, 4] Therefore, because of relying on the independent particle or mean–field models, one makes an error that is considered as *correlation problem*. [1, 5, 6] There are two main sources responsible for the electron correlation: [1, 5]

i. Fermi Correlation: Electrons as countable but indistinguishable fermions should obey Fermi statistics and satisfy the Pauli principle meaning that the N-electron wavefunction should be antisymmetric with respect to the simultaneous exchange of the (spatial and spin) coordinates of any pairs of electrons.

ii. Coulomb Correlation: Electrons as charged particles repel each other through (pair-wise) Coulombic electrostatic forces.

In relation to the concept of electron correlation, one can refer to the Löwdin's classical definition of the *correlation energy* which is the difference between the exact non-relativistic energy and the restricted Hartree-Fock (RHF) energy: the lowest variational energy obtainable with a single-determinant wavefunction. [7] Pople and Binkley extended the scope of this definition to the unrestricted HF (UHF) wavefunctions. [8] However, these definitions have been criticized by several authors for various ambiguities in them. [1, 5] Kutzelnigg encourages the quantum chemistry community to abandon these traditional definitions in favor of a modern definition of the correlation energy which intrinsically arises in the second-quantization formulation in Fock-space using the cumulants [9–14] of the density matrices. [1]

1.1.1 Electron Correlation in Statistical Sense

Let us assume two variables, say, $\mathbf{x}_1$ and $\mathbf{x}_2$ in a two-variable distribution with the (joint or pair) probability distribution function $P_{12}(\mathbf{x}_1,\mathbf{x}_2)$. The individual (or marginal) probability distribution functions for each variable can be obtained by integrating out the other variable, *i.e.*, [3]

$$P_1(\mathbf{x}_1) = \int P_{12}(\mathbf{x}_1,\mathbf{x}_2)\, d\mathbf{x}_2 \qquad \text{or} \qquad P_2(\mathbf{x}_2) = \int P_{12}(\mathbf{x}_1,\mathbf{x}_2)\, d\mathbf{x}_1 \tag{1.1}$$

The two variables, $\mathbf{x}_1$ and $\mathbf{x}_2$ are independent from each other if [15, 16]

$$P_{12}(\mathbf{x}_1,\mathbf{x}_2) = P_1(\mathbf{x}_1)\, P_2(\mathbf{x}_2) \tag{1.2}$$

For distinguishable particles, the individual probability distribution functions $P_1(\mathbf{x}_1)$ and $P_2(\mathbf{x}_2)$ can be different from each other and hence, the pair probability distribution function $P_{12}(\mathbf{x}_1,\mathbf{x}_2)$ may be different for every particle pair. [5] Let $\Psi(\mathbf{x}_1,\mathbf{x}_2,\mathbf{x}_3,\ldots,\mathbf{x}_N)$ be an N-electron wavefunction in which, $\mathbf{x}_i$ collectively shows the spatial, $\mathbf{r}_i$ and spin, ω_i coordinates. The electrons are indistinguishable particles and therefore, $P_1(\mathbf{x}_1) = P_2(\mathbf{x}_2)$. Hence, the normalized one-electron $\rho(\mathbf{x})$ and pair densities $\rho_2(\mathbf{x}_1,\mathbf{x}_2)$ can be defined as

$$\rho(\mathbf{x}) = NP_1(\mathbf{x}_1) \tag{1.3}$$

$$\rho_2(\mathbf{x}_1,\mathbf{x}_2) = N(N-1)\, P_{12}(\mathbf{x}_1,\mathbf{x}_2) \tag{1.4}$$

where

$$P_1(\mathbf{x}_1) = \int d\mathbf{x}_2 \cdots \int d\mathbf{x}_N \ \Psi^*(\mathbf{x}_1, \mathbf{x}_2, \mathbf{x}_3, \ldots, \mathbf{x}_N)\Psi(\mathbf{x}_1, \mathbf{x}_2, \mathbf{x}_3, \ldots, \mathbf{x}_N) \tag{1.5}$$

$$P_{12}(\mathbf{x}_1, \mathbf{x}_2) = \int d\mathbf{x}_3 \cdots \int d\mathbf{x}_N \ \Psi^*(\mathbf{x}_1, \mathbf{x}_2, \mathbf{x}_3, \ldots, \mathbf{x}_N)\Psi(\mathbf{x}_1, \mathbf{x}_2, \mathbf{x}_3, \ldots, \mathbf{x}_N) \tag{1.6}$$

Here, $P_1(\mathbf{x}_1)$ shows the probability of finding an electron at $\mathbf{x}_1$, and the pair density $P_{12}(\mathbf{x}_1, \mathbf{x}_2)$ is the probability of finding an electron at $\mathbf{x}_1$ and simultaneously, another electron at $\mathbf{x}_2$. [5] When the electrons are (statistically) uncorrelated or independent, one can write

$$\rho_2(\mathbf{x}_1, \mathbf{x}_2) = \frac{N-1}{N} \rho(\mathbf{x}_1)\rho(\mathbf{x}_2) \tag{1.7}$$

In the non-relativistic regime, each electron can be described by a spin-orbital $\chi(\mathbf{x})$ which is the product of a spatial function $\psi(\mathbf{r})$ of the position vector $\mathbf{r}$ and one of the two orthonormal spin functions $\alpha(\omega)$ (spin-up) or $\beta(\omega)$ (spin-down), *i.e.* [17]

$$\chi(\mathbf{x}) = \begin{cases} \psi(\mathbf{r})\alpha(\omega) \equiv \psi(\mathbf{r}) \\ \qquad \text{or} \\ \psi(\mathbf{r})\beta(\omega) \equiv \overline{\psi}(\mathbf{r}) \end{cases} \tag{1.8}$$

Also, an equivalent notation has been presented in Eq. 1.8 by which, each spin-orbital is indicated by its spatial part and lacking or having the bar denotes the presence of the $\alpha(\omega)$ or $\beta(\omega)$ spin function, respectively. Since the spatial probability densities are of more interest in the non-relativistic framework, one can obtain $\rho(\mathbf{r})$ and $\rho_2(\mathbf{r}_1, \mathbf{r}_2)$ from $\rho(\mathbf{x})$ and $\rho_2(\mathbf{x}_1, \mathbf{x}_2)$, respectively, through integration over all spin variables ω_i. [18]

1.1.2 Hartree Product and Slater Determinants

The general form for the Hartree product (HP) can be written as [1, 5, 17]

$$\Psi^{\mathrm{HP}}(\mathbf{x}_1, \mathbf{x}_2, \mathbf{x}_3, \ldots, \mathbf{x}_N) = \prod_{i=1}^{N} \chi_i(\mathbf{x}_i) \tag{1.9}$$

where $\chi(\mathbf{x})$ are orthonormal spin-orbitals. The form of the HP wavefunction implicitly assigns each electron to a specific spin-orbital and thus, incorrectly assumes that the electrons are distinguishable particles. Hence, for every pair of electrons i and j, there is a different set of one- and two-particle probability distribution functions

$$P_i(\mathbf{x}_i) = \chi_i^*(\mathbf{x}_i)\, \chi_i(\mathbf{x}_i) \tag{1.10a}$$

$$P_j(\mathbf{x}_j) = \chi_j^*(\mathbf{x}_j)\, \chi_j(\mathbf{x}_j) \tag{1.10b}$$

$$P_{ij}(\mathbf{x}_i, \mathbf{x}_j) = P_i(\mathbf{x}_i)\, P_j(\mathbf{x}_j) \tag{1.10c}$$

Here, the contentious issue of the presence of the electron correlation in the electronic HP wavefunction arises. Based on Eqs. 1.10a-1.10c, a large group of quantum chemists believe that the HP wavefunction is statistically uncorrelated. [17] However, the second group of scientists, for which, we directly quote Hättig *et al.*'s [5] comments as an example, show that the HP wavefunction for an electronic system is statistically correlated. Considering Eqs. 1.10a-1.10c, they say: "*Since for every pair (of electrons), the two-particle probability distribution function factorizes into a product of one-particle distribution functions, one may be tempted to say that the electrons are statistically uncorrelated (Eq. 1.2). This is only true if the electronic coordinates are treated as distinguishable. However, because electrons are in fact indistinguishable, the correct measure for statistical correlation between electrons is*

Eq. 1.7. For the HP wavefunction, the density and pair density functions take the form of

$$\rho(\mathbf{x}_1) = \sum_{i=1}^{N} P_i(\mathbf{x}_1) \tag{1.11}$$

$$\rho_2(\mathbf{x}_1, \mathbf{x}_2) = \sum_{\substack{i,j=1 \\ i \neq j}}^{N} P_{ij}(\mathbf{x}_1, \mathbf{x}_2) \tag{1.12}$$

which leads to

$$\rho_2(\mathbf{x}_1, \mathbf{x}_2) = \rho(\mathbf{x}_1)\rho(\mathbf{x}_2) - \sum_{i=1}^{N} P_i(\mathbf{x}_1)P_i(\mathbf{x}_2) \tag{1.13}$$

Regarding Eq. 1.13, Hättig *et al.* [5] then add: "*Thus, the electron pair probability distribution derived from a Hartree product wavefunction is statistically correlated.*" Note that in Eq. 1.12, one must exclude the $i = j$ term from the summation. In order to provide further understanding of the nature of the correlation, existing in HP wavefunction, the authors of Ref. [5] present another example in which, they consider HP wavefunction for a specific state of bosonic particles. In this bosonic system, all particles can occupy the same orbitals. It can be easily shown that in such a system, described by the HP wavefunction, the particles are statistically uncorrelated. [5] Kutzelnigg also comments on this issue using the same strategy. [1] He mentions: "*With the just given definition of independent electrons (Eq. 1.7), even a Hartree product does not generally describe independent electrons, since the density and the pair density given by Eqs. 1.11 and 1.12, respectively, do not satisfy Eq. 1.7.*" [1] He refers to the ground state of the two-electron atom described by the HP wavefunction and the electron gas described by a HP of plane wave states as exceptions where the HP can describe them as systems of independent particles. [1]

There are positive [1] and negative criticisms [1, 5] about the HPs. The criticisms are mainly focused on three major aspects:

i. The HP does not fulfill the Pauli principle and implies that the electrons are distinguishable particles. There is a different effective one-particle operator for each spin-orbital.

ii. The HP is not invariant with respect to a unitary transformation among the occupied spin-orbitals. [1]

iii. The HP wavefunction is an eigenfunction of the $\hat{S}_z$ operator but not an eigenfunction of the total spin operator $\hat{S}^2$, generally.

As noted by Slater, [19], an improvement over the HP ansatz can be made by using a linear combination of HPs [17] which satisfies the Pauli principle. Considering a set of M (orthonormal) spatial orbitals $\{\psi_i | i = 1, 2, \ldots, M\}$, one can construct a set of $2M$ (orthonormal) spin-orbitals $\{\chi_i | i = 1, 2, \ldots, 2M\}$. Using this set of spin-orbitals, a *Slater determinant*, describing the simplest antisymmetric wavefunction [20] for a N-electron system, can be constructed as [4, 17]

$$\Psi(\mathbf{x}_1, \mathbf{x}_2, \ldots, \mathbf{x}_N) = \frac{1}{\sqrt{N!}} \begin{vmatrix} \chi_i(\mathbf{x}_1) & \chi_j(\mathbf{x}_1) & \ldots & \chi_k(\mathbf{x}_1) \\ \chi_i(\mathbf{x}_2) & \chi_j(\mathbf{x}_2) & \ldots & \chi_k(\mathbf{x}_2) \\ \vdots & \vdots & & \vdots \\ \chi_i(\mathbf{x}_N) & \chi_j(\mathbf{x}_N) & \ldots & \chi_k(\mathbf{x}_N) \end{vmatrix} \tag{1.14}$$

$$= \frac{1}{\sqrt{N!}} \mathcal{A} \prod_{i=1}^{N} \chi_i(\mathbf{x}_i) \tag{1.15}$$

in which, the N-electron antisymmetrizer, $\mathcal{A}$, is defined as [1, 5]

$$\mathcal{A} = \sum_{q=1}^{N!} \varepsilon_q \mathscr{P}_q \tag{1.16}$$

where depending on the parity of the permutation, $\mathscr{P}_q$, the Levi-Civita symbol ε takes the value of [3]

$$\varepsilon_q = \begin{cases} +1 & \text{even permutation} \\ -1 & \text{odd permutation} \end{cases} \tag{1.17}$$

Compared with the HP, the wavefunction approximated by the Slater determinant(s) satisfies the Pauli principle and is invariant under the unitary transformation among the occupied spin-orbitals, [1]. The Slater determinants are the eigenfunction of $\hat{S}_z$ operator, and also, the eigenfunctions of the total spin operator $\hat{S}^2$ for electronic states with closed-shell or high-spin open-shell configurations. However, for low-spin open-shell configurations, one can use configuration state functions (CSFs) that can be the eigenfunctions of both $\hat{S}_z$ and $\hat{S}^2$ operators. Generally, CSFs are defined as the linear combination of the Slater determinants. [21]

For a wavefunction approximated by a single Slater determinant, the one-electron and pair densities can be expressed as

$$\rho(\mathbf{x}) = NP_i(\mathbf{x}) = \sum_{i=1}^{N} \chi_i(\mathbf{x})\chi_i^*(\mathbf{x}) \tag{1.18}$$

$$\begin{aligned} \rho_2(\mathbf{x}_1,\mathbf{x}_2) &= \rho(\mathbf{x}_1)\rho(\mathbf{x}_2) - \sum_{i=1}^{N} P_i(\mathbf{x}_1)P_i(\mathbf{x}_2) \\ &= \sum_{\substack{i,j=1 \\ i\neq j}}^{N} \left[\chi_i(\mathbf{x}_1)\chi_j(\mathbf{x}_2)\chi_i^*(\mathbf{x}_1)\chi_j^*(\mathbf{x}_2) - \chi_i(\mathbf{x}_1)\chi_j(\mathbf{x}_2)\chi_j^*(\mathbf{x}_1)\chi_i^*(\mathbf{x}_2)\right] \end{aligned} \tag{1.19}$$

Note that the inclusion of the $i = j$ term in Eq. 1.19 leaves the pair density unchanged because this contribution would be canceled between the first (direct) and second (exchange) terms in the square brackets. Therefore, one can safely remove the $i \neq j$ restriction from the summation. However, exclusion of the self-pairing contribution in the HP case was necessary because of the Pauli principle. [1] Considering a Slater determinant for a two-electron wavefunction and Eq. 1.19, one can easily verify that there is a finite probability of finding two electrons with opposite spin at the same point in space, *i.e.*, $\rho_2(\mathbf{r}_1,\mathbf{r}_1) \neq 0$. However, for electrons of parallel spins, $\rho_2(\mathbf{r}_1,\mathbf{r}_1) = 0$ and one can speak of the existence of the *Fermi hole* around each electron. [5, 17] Kutzelnigg criticizes statements such as "there is a negative Fermi correlation for electrons with the same spin and no correlation for electrons with opposite spin." [1] He shows that what is crucial is not the individual spins of the electrons but the total spin to which, their spins are coupled.

1.1.3 Electron Correlation in Qualitative Sense

The conceptual explanation and pictorial intuition can be achieved for the electron correlation using simple descriptors which are based on the pair density functions and arise in both Fermi and Coulomb correlation contexts. These are [1, 5]

i. Radial (or in-out) correlation: If an electron spends most of its time close to a nucleus, it is more probable for the other electron(s) to be found far out from the nucleus.

ii. Angular correlation: If one electron is on one side of the nucleus, the other electron is more likely to be found on the opposite side.

iii. Left-right correlation: If an electron spends most of its time close to a nucleus, it is more probable for the other electron to be found close to the other nucleus.

The radial and angular descriptors are convenient for describing the electron correlation in atoms or for regions which are close to nuclei in molecules. The left-right correlation, however, is useful for describing the electron correlation in the regions between atoms in molecules. [5] To exemplify these concepts, one can consider the leading configuration in the ground state of the H_2 molecule, which is $1\sigma_g^2$, the admixture of which with the $2\sigma_g^2$ and $1\pi_u^2$ configurations can account for the radial and angular correlation, respectively. [1]

In chapter 4, we will see in the configuration interaction (CI) calculation on the ground state energy of the H_2 molecule that mixing the $1\sigma_g^2$ state with $1\sigma_u^2$ state leads to a negative left-right correlation and reduces the probability of finding the electrons being found close to each other in space. This correlation is purely due to the Coulombic repulsion force between the electrons. [5] From this CI picture, in which different CSFs can mix, the notion of *static correlation* emerges. On the other hand, one can speak of *dynamic correlation* when (compared to the mean-field picture) an electron can "feel" the instantaneous interaction with another electron when they are in similar regions of space.

1.1.4 Electron Correlation in Quantitative Sense

Probability theory not only provides us a way to define the electron correlation from the statistical point of view, but also a tool to "measure" it. Considering the two variables x and y of individual probability densities $P_1(x)$ and $P_2(y)$, respectively, and the joint probability density $P_{12}(x,y)$, one can define the mean values $\langle x\rangle$ and $\langle y\rangle$, the variances σ_x^2 and σ_y^2 [3]

$$\langle x\rangle = \int_{-\infty}^{\infty} x\, P_1(x)\, dx \qquad \langle y\rangle = \int_{-\infty}^{\infty} y\, P_2(y)\, dy \tag{1.20a}$$

$$\sigma^2(x) = \int_{-\infty}^{\infty} (x-\langle x\rangle)^2 P_1(x)\, dx \qquad \sigma^2(y) = \int_{-\infty}^{\infty} (y-\langle y\rangle)^2 P_2(y)\, dy \tag{1.20b}$$

and covariance, $\mathrm{cov}(x,y)$, as [3]

$$\mathrm{cov}(x,y) = \int_{-\infty}^{\infty}\int_{-\infty}^{\infty} (x-\langle x\rangle)(y-\langle y\rangle)\ P_{12}(x,y)dxdy \tag{1.21}$$

It can be easily shown that the normalized covariance (or correlation coefficient, τ) is bounded between -1 and 1. [3], In other words

$$\tau = \frac{\mathrm{cov}(x,y)}{\sigma(x)\,\sigma(y)}; \qquad -1 \leq \tau \leq +1 \tag{1.22}$$

Here, $\tau = -1$ and $\tau = +1$ indicate perfect negative and positive correlations, respectively. Although $\tau = 0$ shows that the variables x and y are uncorrelated, it should not be mixed up with the statistical independence of the variables (Eq. 1.7). In order to define quantitative measures of the electron correlation such as radial, τ_r, and angular, τ_a, correlation coefficients, the vector variables $\mathbf{r}_1$, $\mathbf{r}_2$ and $\mathbf{r}_1 \cdot \mathbf{r}_2$ can be used in τ instead of the variables x, y and xy, respectively. [15, 16] For example, for the ground state of the helium atom, the radial and angular correlation coefficients are equal to $\tau_r = -0.112$ and $\tau_a = -0.054$, respectively. [1] Other measures of correlation such as correlation entropy have also been proposed for the quantitative description of the electron correlation. [22]

1.2 Explicit Correlation in Electronic Wavefunctions

After about nine decades from the discovery of the most fundamental equation in quantum mechanics, the Schrödinger equation (SE), [23] the mystery of having the exact solution to this equation, describing the correlated motion of N interacting particles, stands still except for a small number of special cases. Considering the astonishing technological advancements in the computational resources and albeit of numerical accuracy that one can achieve for some small systems, even for the helium atom, [24] the exact analytic solution to SE is still unknown. Consequently, adopting pragmatic approximations for solving the SE has been the main focus of the quantum chemistry community so far. [4]

In construction of the trial wavefunction for variational calculations, one should retain as many symmetries and properties of the exact wavefunction as possible. [4] For instance, the wavefunction of fermions should be antisymmetric with respect to the permutation of any pair of electrons. Some of the properties of the exact wavefunction have more crucial impacts on the variational calculations with trial wavefunctions than the others, especially, when one deals with highly accurate calculations. For example, based on the Kato's analysis of the properties of the exact wavefunction [25] near Coulomb singularities, [26] the eigenfunctions of the N-electron SE are continuous and have bounded continuous first derivatives. [6] The results of his work showed that the structure of the first derivative of the wavefunction can be universally described in terms of the interparticle coordinates. Therefore, the trial wavefunctions with the same types of singularities would be a more efficient approximation to the exact solution. [6]

In 1927, for the first time, Slater proposed an approximate wavefunction including the interelectronic distance which turned out to be a proper candidate for both core and Rydberg limits of a two-electron atom. [27] About the same time, Hylleraas performed a calculation on the ground state of the helium atom. [28] Hylleraas' calculation showed that compared with the slow convergence rate for the energy of the CI-type expansions, a rapid convergence to the basis set limit can be achieved for the energy using explicitly correlated wavefunctions. Adopting a three-term wavefunction, he managed to achieve a variational energy of $E = -2.90243$. [28] Following Hylleraas' ideas, James and Coolidge designed a 13-term explicitly correlated wavefunction and used it for the ground state of the H_2 molecule to obtain $E = -1.173465$ at $R = 1.4$. They also generalized Hylleraas' expansion for Li atom [29] which has been considered as the essence of the Hylleraas-configuration interaction (Hy-CI) method [5] introduced by Preiskorn and Woźnicki. [30] Since then, there were numerous improvements in the field of explicitly correlated calculations in general and on Hylleraas-type expansions, in particular. An interesting survey can be found in Refs. [5, 6, 31]. Because of the complexity and difficulty of the many-electron integrals arising in the explicitly correlated methods, the application of these methods has been mainly restricted to highly accurate calculations on small systems.

Recent developments, however, have been mostly focused on invention of the practically affordable methods for larger systems. The key paper on this route was published in 1985 by Kutzelnigg [32] who introduced the R12 method to show that the augmentation of the reference determinant in the traditional CI expansion with the linear r_{12} correlation factor, satisfying the cusp condition, results in the rapid convergence of the energy to its basis set limit value. [32] Kutzelnigg not only presented his result for the He atom and He-like ions, but also proposed a way for generalization of this ansatz toward many-electron systems. [5] Today, the R12 and (and its modified modern version F12) method [33, 34] and its combinations with various standard correlated methods such as second-order Møller-Plesset (MP2) perturbation and coupled cluster (CC) theories, [35] armed with mathematical approximations and numerical methods to avoid direct calculation of many-electron integrals, [5] have made it possible to have an acceptable balance between accuracy and computational resources for larger systems of chemical interest.

1.3 Concluding Remarks

A brief introduction to the correlation problem in quantum chemistry is presented. Considering both qualitative and quantitative aspects of the electron correlation, different definitions and concepts such as statistical interpretation of the electron correlation, radial, angular, left-right, static and dynamic correlation were discussed. Regarding the slow rate of convergence of the energy toward its basis set limit value in the CI-type expansions of the wavefunction, the explicit insertion of the interelectronic distance in the wavefunction has been considered as an efficient solution.

In the next chapter, we consider the free-complement (FC) method, which is based on the theory of the structure of the exact wavefunctions presented by Nakatsuji. Through a careful analysis, we will discuss the strengths and weaknesses of the FC method to be able to think about the best way to construct a compact but efficient ansatz which is generalizable for large systems.

CHAPTER 2

Structure of the Exact Wavefunction: Free Complement Method

We present a brief review on the structure of the exact wavefunction investigated by Nakatsuji. Exploring the fundamental aspects of the free complement (FC) or iterative configuration interaction (ICI) method, we try to understand its mechanism of work. Through reproducing the results of the FC method for helium atom and H_2^+ *molecular ion, we analyze this method to identify its strengths and weaknesses. Similar to the works of Koga on finding the optimal and compact Hylleraas and Kinoshita expansions, we have found that FC method produces some energetically unimportant complement functions in each iteration the population of which, are rapidly increasing with iteration* *number. It can be shown that at a specific FC order, lower energies can be obtained using fewer complement functions. In the study of the first triplet excited state of the He atom, we have found that in addition to the determinants, permanents also appear in the FC expansion of the wavefunction. We have demonstrated that the presence of permanents in the FC expansion is important for the energy convergence. However, they have either been overlooked in Nakatsuji's works or discarded because of their computational costs without any comments. These results led us to think about designing a new correlation factor $F(r_{12})$ with which one can have an optimally compact and efficient wavefunction.*

2.1 Introduction

In 2000, H. Nakatsuji began to report a series of studies under the topic of the structure of the exact wavefunction. [36–40] He based the foundation of this research on the fact that the exact *"Hamiltonian is composed of only one- and two- particle operators and there are no physical operators that involve more-than-three body interactions"*. [36] That is

$$\mathscr{H} = \mathscr{F} + \mathscr{G} \tag{2.1}$$

in which, the one-electron operator $\mathscr{F}$ and two-electron operator $\mathscr{G}$ have been defined in the first-quantization as

$$\mathscr{F} = \sum_i -\frac{1}{2}\nabla_i^2 - \sum_i \sum_A Z_A / r_{iA} \tag{2.2}$$

$$\mathscr{G} = \sum_{i>j} 1/r_{ij} \tag{2.3}$$

or in the second-quantized form as

$$\mathscr{F} = \sum_{PQ} f_{PQ}\, a_P^\dagger a_Q \tag{2.4}$$

$$\mathscr{G} = \frac{1}{2}\sum_{PQ} g_{PQRS}\, a_P^\dagger a_R^\dagger a_S a_Q \tag{2.5}$$

where in Eqs. 2.4 and 2.5, summations are over all spin-orbitals. [4, 41] Here, the creation operator $a^\dagger$, and annihilation operator a, satisfy the anticommutation relations

$$\begin{aligned} a_P^\dagger a_Q + a_Q a_P^\dagger &= [a_P^\dagger, a_Q]_+ = \delta_{PQ} \\ a_P^\dagger a_Q^\dagger + a_Q^\dagger a_P^\dagger &= [a_P^\dagger, a_Q^\dagger]_+ = 0 \\ a_P a_Q + a_Q a_P &= [a_P, a_Q]_+ = 0 \end{aligned} \tag{2.6}$$

He then proposed two theorems to indicate the possibility of the description of the exact wavefunction in terms of single and double excitations. [36] The first theorem is

Theorem 2.1.1 *The wavefunction* Ψ *that satisfies both conditions*

$$\langle\Psi|(\mathscr{H} - \mathscr{E})a_P^\dagger a_Q|\Psi\rangle = 0 \tag{2.7a}$$

$$\langle\Psi|(\mathscr{H} - \mathscr{E})a_P^\dagger a_R^\dagger a_S a_Q|\Psi\rangle = 0 \tag{2.7b}$$

is exact in a necessary and sufficient sense.

and the second theorem states that

Theorem 2.1.2 *Assume that* Ψ *has the variables of the order of only singles and doubles*

$$\Psi = \Psi(c_Q^P\, a_P^\dagger a_Q,\; c_{QS}^{PR}\, a_P^\dagger a_R^\dagger a_S a_Q, \Phi_i) \tag{2.8a}$$

where Φ_i is the given reference wavefunction. If Ψ satisfies the variational condition for the coefficients c_Q^P and c_{QS}^{PR}, i.e.,

$$\frac{\partial \Psi}{\partial c_Q^P} = a_P^{\dagger} a_Q \Psi \tag{2.8b}$$

$$\frac{\partial \Psi}{\partial c_{QS}^{PR}} = a_P^{\dagger} a_R^{\dagger} a_S a_Q \Psi \tag{2.8c}$$

then Ψ is exact in the sufficient sense.

Note that theorem 2.1.2 is not a necessary condition because the space defined by Ψ in this theorem may be smaller than the real space of the exact wavefunction. Proof of both theorems is presented by Nakatsuji. [36] Based on theorem 2.1.2, he considered the variational exponential ansatz [36, 38, 39] and examined coupled-cluster singles (CCS), coupled-cluster singles and doubles (CCSD) and full-configuration interaction (FCI) wavefunctions for these conditions. [36] After this analysis, he proposed an ansatz based on the structure of the exact wavefunction which satisfies both theorems 2.1.1 and 2.1.2. This is the starting point for his free complement (FC) method's proposal.

In his second paper in this series, Nakatsuji generalized the second theorem by dividing the Hamiltonian into N_D parts to obtain a set of N_D equations which are equivalent to the Schrödinger (SE) equation. [37] In this way, the FC method could be generalized to calculate the exact wavefunction with N_D variables where $1 \leq N_D \leq m^2 + \left[\frac{m(m-1)}{2}\right]^2$ in which, m is the number of active orbitals. [37] This method has been applied to molecular systems using finite basis-sets. [40] Armed with inverse Schrödinger equation (ISE) [42] and scaled Schrödinger equation (SSE) [43] which are equivalent to the SE and are proposed to remove the nuclear and electronic singularity problems, the FC method has been further generalized to its final form. This method is now considered as an analytic way of generating arbitrarily accurate wavefunctions and energies the scope of which is again restricted to small systems where the necessary integrals are available in closed form. [5, 6, 24]

When the analytic form of the overlap and Hamiltonan matrix elements are not available, Nakatsuji proposes the use of local SE (LSE) with the standard Monte Carlo sampling. [44–46] In the present thesis, in order to be able to propose a compact form for an accurate wavefunction for molecular systems, the analytic solutions to the explicitly correlated problems will be the main focus. Consequently, integral-free methods such as FC-LSE will not be considered further.

2.2 Free-Complement Method and Scaled-Schrödinger Equation

We now embark on a more detailed analysis of the FC method within the framework of the SSE. [24] The original form of SE

$$\mathscr{H}\Psi = \mathscr{E}\Psi \tag{2.9}$$

where the general Hamiltonian defined in Eq. 2.1, has nuclear (Eq. 2.2) and electronic (Eq. 2.3) singularities. Since the right-hand side of Eq. 2.9 has no singularities, these sharp changes must be canceled out in the left hand side of this equation. In the case of the exact wavefunction, satisfying the Kato's cusp conditions, [26] no such singularities exist in the SE. However, in case of an approximate wavefunction, this precise cancelation does not happen and some of the matrix elements (*e.g.*, those involving $-1/r^m$ factor where $m \geq 3$ or matrix elements in different ansätze) may diverge. [43] In the ISE scheme, one uses $\mathscr{H}^{-1}$ instead of $\mathscr{H}$ and therefore, no such difficulties regarding to the singularities occur. [42] One of the issues which arises in the ISE approach is that one needs to know how to write the inverse Hamiltonian in closed form. [42] The SSE is free from such problems [43] and can be written as

$$g(\mathscr{H} - \mathscr{E})\Psi = 0 \tag{2.10}$$

in which, g stands for the scaling factor which is a function of electron coordinates. [43] This multiplicative operator, g, does not generally commute with Hamiltonian and is always non-zero except at singular point r_0 where it can be zero. The g factor also satisfies

$$\lim_{r \to r_0} gV \neq 0 \tag{2.11}$$

where V is the potential operator in the Hamiltonian. This condition is necessary because g should not eliminate information at singularity. There are various possible forms for g function, [47] however, Nakatsuji favors the following form [24]

$$g = \sum_i \sum_A r_{iA} + \sum_{i>j} r_{ij} \tag{2.12}$$

The construction of the FC wavefunction in the SSE framework begins with the simplest ICI (SICI) formula

$$\Psi_{n+1} = [1 + C_n g(\mathscr{H} - E_n)]\Psi_n \tag{2.13}$$

where C_n is the variational parameter at each order n. The FC wavefunction is guaranteed to converge to the exact solution of the SSE without encountering the singularity problem. [43, 47] Applying the g and $g\mathscr{H}$ operators for n times on Ψ_0 in Eq. 2.13, the right-hand side of this equation becomes a sum of analytical *complement functions* ϕ_i

$$\Psi_n = \sum_{i=1}^{M_n} c_i^{(n)} \phi_i^{(n)} \tag{2.14}$$

Here, the coefficients $\{c_i^{(n)}\}$ are determined variationally [47] and M_n is the number of complement functions. This is important to note that when one uses g and $g\mathscr{H}$ operators in Eq. 2.13, some diverging functions are also generated in Eq. 2.14. Nakatsuji points out that they should be discarded because the wavefunction must be integrable and finite. [24, 47] Considering Eq. 2.14, in the FC method, the Hamiltonian itself is responsible for generating the basis (complement) functions. [24] The functional form of the complement functions is determined by the form of the initial wavefunction Ψ_0. [24]

2.2.1 Free-Complement Electronic Energies

In the present section, we apply the FC method to calculate the energy of the H_2^+ molecular ion [48, 49], and He atom in both singlet ground [47] and triplet excited states. [50] We also use spatial representation for constructing our initial wavefunctions because of its simplicity and convenience in the absence of external fields. [18]

2.2.1.1 Hydrogen Molecular Ion: The Ground State

The H_2^+ molecular ion is a special case of a molecular system for which, the exact solution to the non-relativistic SE is known. [48, 49, 51] Because of the Born-Oppenheimer (BO) approximation, this three-body problem can be reduced to one-body two-center problem in (confocal spheroidal or) elliptic coordinate system shown in Fig. 2.1. [52]

$$\lambda = \frac{r_A + r_B}{R}, \qquad \mu = \frac{r_A - r_B}{R}, \qquad \omega \tag{2.15}$$

where λ, μ and ω are defined on the ranges of $[1,\infty)$, $[-1,1]$ and $[0,2\pi]$, respectively and the volume element is $R^3(\lambda^2-\mu^2)/8$. [52] Also, r_A stands for the distance of the electron from center A, r_B is the distance of the electron from center B and R is the distance between two centers A and B (Fig. 2.1). In this coordinate system, the Hamiltonian operator can be written as

$$\mathscr{H} = -\frac{2}{R^2(\lambda^2-\mu^2)}\left[\frac{\partial}{\partial\lambda}(\lambda^2-1)\frac{\partial}{\partial\lambda} + \frac{\partial}{\partial\mu}(1-\mu^2)\frac{\partial}{\partial\mu} + \frac{(\lambda^2-\mu^2)}{(\lambda^2-1)(1-\mu^2)}\frac{\partial^2}{\partial\omega^2}\right] - \frac{4\lambda}{R(\lambda^2-\mu^2)} \tag{2.16}$$

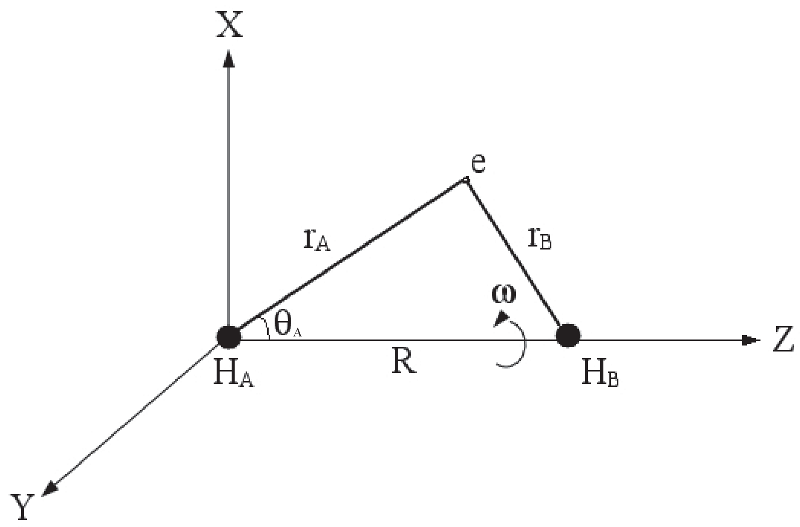

Fig. 2.1 The hydrogen molecular ion H_2^+ aligned on the Z axis in the elliptic coordinate system.

where the first line of Eq. 2.16 comes from the kinetic part and the second line results from the nuclear-attraction term. [49] We need to choose an appropriate g factor to eliminate the singularity issue arising from the nuclear attraction term in the Hamiltonian. Therefore, based on Eq. 2.12, the g factor takes the form of [49]

$$g = -\frac{1}{V_{Ne}} = \frac{R\left(\lambda^2 - \mu^2\right)}{4\lambda} \tag{2.17}$$

The sign of the V_{Ne} is inverted to make g positive everywhere except at singularity. Using spatial notation, [18] the initial wavefunction Ψ_0 for $X^2\Sigma_g^+$ (or $1\sigma_g$) gerade ground state of H_2^+ can be constructed as

$$\Psi_0 = \exp[-\zeta'(r_\mathrm{A} + r_\mathrm{B})] = \exp(-\zeta\lambda) \tag{2.18}$$

where $\zeta' = \zeta/R$. Successive application of the g and $g\mathscr{H}$ operators on Ψ_0 (Eq. 2.13) and removing the duplications and singular terms results in the general form (Eq. 2.14) of the FC wavefunction

$$\Psi = \sum_{i=1}^{M_n} c_i \lambda^{m_i} \mu^{n_i} \exp(-\zeta\lambda) \tag{2.19}$$

in which, m_i can be a positive or negative integer and n_i can be zero or positive even integer for the gerade ground state ($X^2\Sigma_g^+$) of H_2^+. [49] Considering the general form of the FC wavefunction, the Hamiltonian and overlap matrix elements over complement functions $\{\phi_i\}$ become

$$\langle\phi_i|\mathscr{H}|\phi_j\rangle = \frac{R^3}{8}\int_0^{2\pi}\int_{-1}^{1}\int_1^{\infty}\left(\lambda^{m_i}\mu^{n_i}e^{-\zeta\lambda}\right)\mathscr{H}\left(\lambda^{m_j}\mu^{n_j}e^{-\zeta\lambda}\right)\left(\lambda^2-\mu^2\right)\,d\lambda\,d\mu\,d\omega \tag{2.20a}$$

$$\langle\phi_i|\phi_j\rangle = \frac{R^3}{8}\int_0^{2\pi}\int_{-1}^{1}\int_1^{\infty}\left(\lambda^{m_i}\mu^{n_i}e^{-\zeta\lambda}\right)\left(\lambda^{m_j}\mu^{n_j}e^{-\zeta\lambda}\right)\left(\lambda^2-\mu^2\right)\,d\lambda\,d\mu\,d\omega \tag{2.20b}$$

The explicit forms for the integrals can be obtained using a symbolic mathematical program package such as *Mathematica* [53] or can be found in Nakatsuji's paper. [48] Solving the generalized eigenvalue equation and diagonalizing the Hamiltonian matrix with respect to the overlap matrix gives the energies that are shown in Table 2.1.

Table 2.1 The free-complement ground state ($X^2\Sigma_g^+$) electronic energy E, and exponent ζ, for the hydrogen molecular ion H_2^+ at $R=2$.

n	M_n	ζ^a	$-E^a$	$-E_\zeta{}^b$	$\Delta E = E_\zeta - E$
0	1	1.3	**1.0**79 384 965 831 435	**1.0**79 384 965 831 435	0
1	4	1.1	**1.10**1 421 270 731 672	**1.10**0 681 090 163 764	7.4×10^{-4}
2	13	0.8	**1.102 6**27 432 357 877	**1.102 6**23 480 965 489	4.0×10^{-6}
3	26	1.2	**1.102 634 2**08 423 548	**1.102 634 2**08 390 056	3.4×10^{-11}
4	43	1.1	**1.102 634 214 49**3 685	**1.102 634 214 49**2 225	1.5×10^{-12}

[a] Refs. [48, 49]
[b] E_ζ is the FC energy calculated using a fixed value of $\zeta = 1.3$ for the exponent.

The first row of this table shows a simple variational calculation using Ψ_0 in minimal basis model. In order to find the optimized energy and the exponent for the minimal basis, one can normalize Ψ_0

$$1 = \langle\Psi_0|\Psi_0\rangle = \frac{R^3}{8}C^2\int_0^{2\pi}\int_{-1}^{1}\int_1^{\infty}\exp(-2\zeta\lambda)\left(\lambda^2-\mu^2\right)\,d\lambda\,d\mu\,d\omega \tag{2.21}$$

to get

$$\Psi_0 = \left[\frac{24\zeta^3 e^{2\zeta}}{\pi R^3 \left(4\zeta^2 + 6\zeta + 3\right)} \right]^{1/2} \exp(-\zeta\lambda) \tag{2.22}$$

Assuming $\zeta > 0$, the Hamiltonian matrix element in Eq. 2.20b becomes

$$\begin{aligned} E &= \frac{\langle\Psi_0|\mathscr{H}|\Psi_0\rangle}{\langle\Psi_0|\Psi_0\rangle} \\ &= \frac{R^3}{8} \left[\frac{24\zeta^3 e^{2\zeta}}{\pi R^3 \left(4\zeta^2 + 6\zeta + 3\right)} \right] \int_0^{2\pi} \int_{-1}^{1} \int_1^{\infty} \exp(-\zeta\lambda) \mathscr{H} \exp(-\zeta\lambda) \left(\lambda^2 - \mu^2\right) \, d\lambda \, d\mu \, d\omega \\ &= \frac{6\zeta(2\zeta+1)(\zeta-2R)}{\left(4\zeta^2+6\zeta+3\right) R^2} \end{aligned} \tag{2.23}$$

The potential energy curve (PEC) is produced after adding the $1/R$ nuclear repulsion term to the optimized electronic energy at each specific bond length. At $R_e \approx 2.00$, [54] the optimized exponent and the electronic energy for the minimal basis model are $\zeta = 1.3337\cdots$ and $E = -1.079\,754\,641\cdots$, respectively. Note that the difference in the calculated energy presented here compared with that demonstrated in the first row of the Table 2.1 comes from the difference between the number of digits considered for ζ in the corresponding calculations.

The FC energies in the fourth column of Table 2.1 were reproduced using the optimal values for ζ reported in Refs. [48, 49] and agree perfectly with the energies presented in these references. The number of accurate digits, shown in boldface, increases as the structure of the FC wavefucntion converges to the exact solution of the SE with increasing the FC order, n.

The FC energies calculated using the fixed exponent $\zeta = 1.3$ and energy differences are collected in fifth and sixth columns of Table 2.1, respectively. These values demonstrate that fixing the exponent to its initially optimized value has small effect on the calculated FC energy at higher orders. In fact, the number of accurate digits remains unchanged in this case. Hence, one can choose a reasonable value as an initial guess for the exponent and keep it fixed during the FC calculations. The initial guess exponents can be obtained in a minimal–basis variational calculation or can be estimated from Slater's rules [55]. This eliminates the cost of non-linear optimization which is both time-consuming and difficult at higher orders.

2.2.1.2 Helium Atom: The Ground State

Since the ground state of the helium atom has zero spatial angular momentum or S symmetry, we adopt Hylleraas $\{s,t,u\}$ interparticle coordinates defined as

$$\begin{aligned} s &= r_1 + r_2 \\ t &= r_1 - r_2 \\ u &= |\mathbf{r}_1 - \mathbf{r}_2| = r_{12} \end{aligned} \tag{2.24}$$

to solve the SSE (or equivalently SE) using FC method. In this coordinate system, [56] the nucleus is considered to be fixed at the origin. Hence, the Hamiltonian can be written as

$$\begin{aligned} \mathscr{H} = &-\left(\frac{\partial^2}{\partial s^2}+\frac{\partial^2}{\partial t^2}+\frac{\partial^2}{\partial u^2}\right) - 2\frac{s(u^2-t^2)}{u(s^2-t^2)}\frac{\partial^2}{\partial s \partial u} - 2\frac{t(s^2-u^2)}{u(s^2-t^2)}\frac{\partial^2}{\partial u \partial t} - \frac{4s}{s^2-t^2}\frac{\partial}{\partial s} \\ &-\frac{2}{u}\frac{\partial}{\partial u} + \frac{4t}{s^2-t^2}\frac{\partial}{\partial t} - \frac{4sZ}{s^2-t^2} + \frac{1}{u} \end{aligned} \tag{2.25}$$

where the last two terms in this equation belong to the Coulomb potential

$$V = V_{Ne} + V_{ee} = -\frac{4sZ}{s^2-t^2} + \frac{1}{u} \tag{2.26}$$

in which, Z is the nuclear charge. The remaining terms in Eq. 2.25 come from the kinetic part. According to Eq. 2.12, we choose g such that

$$g = \left(\frac{8s}{s^2-t^2}\right)^{-1} + \left(\frac{1}{u}\right)^{-1} \tag{2.27}$$

where for the He atom, $Z = 2$. The sign of the V_{Ne} is inverted to make g positive everywhere except at singularity. Neglecting the spin part, our initial guess in spatial form would be the product of two atomic orbitals (AOs) for two electrons

$$\Psi_0 = \exp[-\zeta(r_1 + r_2)] = \exp(-\zeta s) \tag{2.28}$$

Applying the g and $g\mathscr{H}$ operators on Ψ_0 in Eq. 2.13 and removing the duplications and singular terms, one finds that Eq. 2.14 becomes

$$\Psi_1 = \left[c_1\, s^0 t^0 u^0 + c_2\, s^{-1} t^2 u^0 + c_3\, s^1 t^0 u^0 + c_4\, s^0 t^0 u^1\right] \exp(-\zeta s) \tag{2.29}$$

continuing the FC process to higher orders, *i.e.*, applying g and $g\mathscr{H}$ operators in a consecutive way, one discovers that the generated FC wavefunctions have the general form of

$$\Psi = \sum_{i=1}^{M_n} c_i s^{l_i} t^{m_i} u^{n_i} \exp(-\zeta s) \tag{2.30}$$

where c_i is the variational parameter. For singlet state, l_i runs over all integers while, m_i is a non-negative and even integer and n_i runs over all non-negative integers. [47] By the present choice of the g factor (Eqs. 2.12 and 2.27), the negative powers of the variable s are also generated in the $\{s,t,u\}$ expansion of the FC wavefunction (Eq. 2.30). In 1957, Kinoshita [57] reported the importance of the inclusion of the negative powers of s in the wavefunction expansion for which, the resulting energy was remarkably improved compared with the ansätze that were bereft of these terms.

Instead of the tedious way of applying the FC operators, Nakatsuji proposed a combination of equalities and inequalities- the conditions imposed on $\{l_i, m_i, n_i\}$ for generating the complement functions at each specific order. [46, 50] Using these rules seem to have some ramifications for the first triplet excited state of the helium atom. This issue will be discussed in the next subsection.

The general Hamiltonian and overlap matrix elements over the complement functions $\{\phi_i\}$ become [56]

$$\langle\phi_i|\mathscr{H}|\phi_j\rangle = 2\pi^2 \int_0^\infty \int_0^s \int_t^s \left(s^{l_i} t^{m_i} u^{n_i} e^{-\zeta s}\right) \mathscr{H} \left(s^{l_j} t^{m_j} u^{n_j} e^{-\zeta s}\right) \left(s^2 - t^2\right)\; u\, du\, dt\, ds \tag{2.31a}$$

$$\langle\phi_i|\phi_j\rangle = 2\pi^2 \int_0^\infty \int_0^s \int_t^s \left(s^{l_i} t^{m_i} u^{n_i} e^{-\zeta s}\right) \left(s^{l_j} t^{m_j} u^{n_j} e^{-\zeta s}\right) \left(s^2 - t^2\right)\; u\, du\, dt\, ds \tag{2.31b}$$

The explicit forms for the integrals can be achieved using *Mathematica* [53] or can be looked up in Nakatsuji's paper. [47] Diagonalizing the Hamiltonian matrix with respect to the overlap matrix gives the energies that are shown in Table 2.2.

Table 2.2 The free-complement singlet ground state (^1S) electronic energy E, and exponent ζ, for the helium atom.

n	M_n	ζ	-E	-$E_\zeta{}^a$	$\Delta E = E_\zeta - E$
0	1	1.688	**2**.847 656 250	**2**.847 656 250	0
1	4	1.690	**2.90**1 338 005	**2.90**1 337 708	3.0×10^{-7}
2	16	1.736	**2.903** 642 984	**2.903** 638 631	4.4×10^{-6}
3	37	1.779	**2.903 72**0 264	**2.903 71**9 381	8.8×10^{-7}
4	71	1.837	**2.903 724** 019	**2.903 723** 761	2.6×10^{-7}

^{a} E_ζ is a FC energy calculated using a fixed value of $\zeta = 27/16$ for the exponent.

Here, the boldface digits show the exact and accurate digits (after rounding up to a specific decimal place) in the energy. Normalizing $\Psi_0 = Ce^{-\zeta s}$ (Eq. 2.28) using Eq. 2.31b and solving the equation for C,

$$1 = \langle\Psi_0|\Psi_0\rangle = 2\pi^2 C^2 \int_0^\infty \int_0^s \int_t^s e^{-2\zeta s} \left(s^2 - t^2\right)\; u\, du\, dt\, ds \tag{2.32}$$

one can find that $C = \zeta^3/\pi$. Assuming $\zeta > 0$, the minimization of the energy with respect to ζ using Rayleigh-Ritz technique [3]

$$\begin{aligned} E &= \frac{\langle \Psi_0 | \mathscr{H} | \Psi_0 \rangle}{\langle \Psi_0 | \Psi_0 \rangle} \\ &= 2\pi^2 \int_0^\infty \int_0^s \int_t^s \left(s^2 - t^2\right) \, u \, \left(\frac{\zeta^3}{\pi} e^{-\zeta s}\right) \mathscr{H} \left(\frac{\zeta^3}{\pi} e^{-\zeta s}\right) du \, dt \, ds \\ &= \zeta^2 - \frac{27}{8}\zeta \end{aligned} \tag{2.33}$$

gives the well-known [58] values of $E = -(27/16)^2$ and $\zeta = 27/16$ for the helium atom.

The first-order FC energy (second row in Table 2.2) can be obtained through diagonalization of the 4×4 Hamiltonian matrix with respect to the overlap matrix in the generalized eigenvalue equation. The process is almost the same for higher orders as well. The fifth column of the Table 2.2 shows the FC energies E_ζ calculated using the fixed value of $\zeta = 27/16$ for the exponent. As is shown by the last column of the Table 2.2, the non-linear optimization of the exponent can contribute to the energy at sixth decimal place or higher. Thus, depending on the accuracy that we are seeking and/or the number of non-linear parameters that may be optimized, fixing the exponent(s) to a reasonable value makes the FC calculations faster because the bottleneck of the FC calculations becomes the diagonalization of the Hamiltonian matrix.

In Table 2.2, one can see that as we increase the order, the energy and the structure of the FC wavefunction become closer to being exact as it is guaranteed by the theorems 2.1.1 and 2.1.2. Comparing the data in Tables 2.2 and 2.1 and considering the boldface digits, one can see that the convergence rate for the H_2^+ is faster than that of the helium atom. This is possibly because of the presence of the electronic cusp in the He atom. Although initially, the rate of convergence in terms of acquiring more accurate digits is quite rapid with increasing the order, it becomes slower at higher orders. For example, going from $n = 9$ to $n = 12$, by almost doubling the number of complement functions from $M_n = 541$ to $M_n = 1171$, one can add only one more exact digits (at the tenth decimal place) to the energy. As discussed by Bartlett, [59] Gronwall [60] and Fock, [61, 62] fulfilling the three-body collision conditions may become an important factor for obtaining highly-accurate results. Nakatsuji adopted various ansätze inserting the interelectronic distance in the logarithmic form into the initial wavefunction to achieve an accuracy of over 40 digits in the energy of the ground state of the helium atom using $M_n = 22709$ complement functions generated at the order of $n = 27$. [47]

It is important to note that at a specific FC order, lower energies can be obtained using fewer complement functions. For instance, the energy of the first-order FC wavefunction (Table 2.2) with four terms ($E = -2.9013$) can be compared with that of the optimized three-terms Hylleraas wavefunction ($E = -2.9024$)) [63]. We have verified this fact for second-order where lower energy was obtained with the number of terms fewer than 16. Although the structure of the FC wavefunction converges to that of the exact wavefunction at the $n \to \infty$ limit, one can be more efficient by generating fewer but energetically more important functions.

2.2.1.3 Helium Atom: The Triplet Excited State

The FC method is equally applicable to both ground and excited states in the sense that when one tries to find the variational energies by diagonalizing a $M_n \times M_n$ Hamiltonian, the approximate ground and excited state energies (of the same symmetry) are obtained within a same eigenvalue problem. [50] Therefore, similar to the helium in the ground state, we can use the FC method to calculate the first triplet excited state energy with the electronic configuration $1s2s$. The Hamiltonian operator $\mathscr{H}$ and the g factor remain the same as those introduced in Eqs. 2.25 and 2.27 for $\{s,t,u\}$ coordinate system. As noted by Nakatsuji, [50], in order to calculate the energy of the $1sNs$ state of the helium atom, at least about N different exponential functions should be included in the initial wavefuntion Ψ_0 to mimic the $1s$ and higher Ns atomic orbitals. [50] Therefore, a different Ψ_0 should be considered because of the antisymmetric spatial part of the triplet state [18] and also the fact that the $2s$ orbital is more diffuse than the $1s$ orbital. Dropping the spin part, the initial wavefunction can be expressed as

$$\Psi_0 = \begin{vmatrix} e^{-\alpha r_1} & e^{-\beta r_1} \\ e^{-\alpha r_2} & e^{-\beta r_2} \end{vmatrix} = \begin{vmatrix} e^{-\alpha(s+t)/2} & e^{-\beta(s+t)/2} \\ e^{-\alpha(s-t)/2} & e^{-\beta(s-t)/2} \end{vmatrix} \tag{2.34}$$

The normalization factor for Ψ_0 can be found through

$$1 = \langle\Psi_0|\Psi_0\rangle = 2\pi^2 C^2 \int_0^\infty \int_0^s \int_t^s \begin{vmatrix} e^{-\alpha(s+t)/2} & e^{-\beta(s+t)/2} \\ e^{-\alpha(s-t)/2} & e^{-\beta(s-t)/2} \end{vmatrix}^2 \left(s^2 - t^2\right) u\, du\, dt\, ds \tag{2.35}$$

to give the normalized Ψ_0 as

$$\Psi_0 = \left[2\pi^2 \left(\frac{1}{\alpha^3\beta^3} - \frac{64}{(\alpha+\beta)^6}\right)\right]^{-1/2} \begin{vmatrix} e^{-\alpha(s+t)/2} & e^{-\beta(s+t)/2} \\ e^{-\alpha(s-t)/2} & e^{-\beta(s-t)/2} \end{vmatrix} \tag{2.36}$$

Assuming $\alpha > 0$ and $\beta > 0$, the Rayleigh-Ritz expression for obtaining the variational energy is

$$\begin{aligned} E &= \frac{\langle\Psi_0|\mathscr{H}|\Psi_0\rangle}{\langle\Psi_0|\Psi_0\rangle} \\ &= 2\pi^2 \left[2\pi^2 \left(\frac{1}{\alpha^3\beta^3} - \frac{64}{(\alpha+\beta)^6}\right)\right]^{-1} \\ &\times \int_0^\infty \int_0^s \int_t^s \left(s^2 - t^2\right) u \begin{vmatrix} e^{-\alpha(s+t)/2} & e^{-\beta(s+t)/2} \\ e^{-\alpha(s-t)/2} & e^{-\beta(s-t)/2} \end{vmatrix} \mathscr{H} \begin{vmatrix} e^{-\alpha(s+t)/2} & e^{-\beta(s+t)/2} \\ e^{-\alpha(s-t)/2} & e^{-\beta(s-t)/2} \end{vmatrix} du\, dt\, ds \\ &= \frac{\alpha^2}{2} + \frac{\beta^2}{2} - 2\alpha - 2\beta + \frac{\alpha\beta\left(\alpha^3 + 8\alpha^2\beta + 32\alpha^2\beta^2 + 8\alpha\beta^2 + \beta^3\right)}{\alpha^4 + 8\alpha^3\beta + 30\alpha^2\beta^2 + 8\alpha\beta^3 + \beta^4} \end{aligned} \tag{2.37}$$

Minimizing the energy expression with respect to the exponents α and β can result in the variational energy of $E = -2.160\,645\,710\cdots$ and optimized exponents $\alpha = 1.9686\cdots$ and

$\beta = 0.3210\cdots$ to arbitrary accuracy. The difference between the variational energy value presented here and the energy value reported in the first row and third column of the Table 2.3 comes from the different number of digits considered for the exponents.

Table 2.3 The first triplet excited state (^3S) FC electronic energy (E or E' [b]) [a] of the helium atom with the electronic configuration $1s2s$.

n	M_n	-E	M'_n [b]	-E' [b]	$\Delta E = E'^{\,b} - E$
0	1	**2.1**60 644 009	1	**2.1**60 644 009	0
1	4	**2.1**61 240 437	5	**2.1**63 221 387	-0.001 980 950
2	16	**2.16**8 856 982	21	**2.17**3 532 754	-0.004 675 772
6[c]	5724	**2.175 229 378 236 791 305 738 9**66	–	–	–

[a] The exponents of the $1s$ and $2s$ orbitals were optimized for the minimal basis and kept fixed to $\alpha = 1.97$ and $\beta = 0.32$ during the FC calculations.
[b] The primed values were calculated using FC wavefunctions that included the permanents in addition to the usual complement functions generated during the FC process.
[c] Ref. [48] The initial wavefunction Ψ_0 included 6 exponential functions in this calculation.

Beginning the FC procedure by applying the g and $g\mathscr{H}$ operators on Ψ_0 in Eq. 2.34 and removing the duplications and singular terms, one finds that the general form of the FC wavefunction becomes different from our expectations. That is, in addition to having a usual sum over antisymmetric determinants of Slater orbitals in Ψ_0, the symmetric anti-determinants or "permanents" also appear in the FC expansion.

Before presenting a simple definition for the permanents, we shall consider the Laplacian development of a general $n \times n$ determinant D_n in terms of minors M_{ij} [3]

$$D_n = \begin{vmatrix} a_{11} & a_{12} & \dots & a_{1n} \\ a_{21} & a_{22} & \dots & a_{2n} \\ \dots & \dots & \dots & \dots \\ a_{n1} & a_{n2} & \dots & a_{nn} \end{vmatrix} = \sum_{j=1}^{n} (-1)^{i+j} M_{ij} a_{ij} \tag{2.38}$$

where the minor M_{ij}, corresponding to the element a_{ij}, is defined as a determinant of order $n-1$ generated through striking out the ith row and jth column of the original determinant.

The factor $(-1)^{i+j}M_{ij}$ is called *cofactor* of the element a_{ij}. In this way, determinants (as well as permanents) are polynomials in entries of the matrix. [3]

Permanents can be considered as an analog of a determinant in which, all signs in the expansion by minors in Eq. 2.38 are taken as positive. For example, the permanent of a 2×2 matrix A will be

$$perm(A) = \begin{vmatrix} a_{11} & a_{12} \\ a_{21} & a_{22} \end{vmatrix}_{+} = a_{11}a_{22} + a_{12}a_{21} \qquad (2.39)$$

where the "perm()" as well as the vertical bars with plus signs, $|\ \ |_{+}$, indicate permanents. [64, 65] After this short digression, we get back to the FC expansion (Eq. 2.14) which now includes both determinants and permanents

$$\Psi' = \sum_{i=1}^{M_n'} c_i\, s^{l_i} t^{m_i} u^{n_i} \begin{vmatrix} e^{-\alpha(s+t)/2} & e^{-\beta(s+t)/2} \\ e^{-\alpha(s-t)/2} & e^{-\beta(s-t)/2} \end{vmatrix} + c_i'\, s^{l_i'} t^{m_i'} u^{n_i'} \begin{vmatrix} e^{-\alpha(s+t)/2} & e^{-\beta(s+t)/2} \\ e^{-\alpha(s-t)/2} & e^{-\beta(s-t)/2} \end{vmatrix}_{+} \qquad (2.40)$$

where m_i' and m_i run over odd and even positive integers, respectively. Also, l_i and l_i' vary over all integers and n_i and n_i' run over all non-negative integers. Note that the multiplications of either the odd polynomial part with permanents or even polynomial part with determinants generates correct symmetry for the spatial part of the triplet state. The new FC wavefunction Ψ' should be compared with that which results from applying Nakatsuji's rules and conditions (Table 1 in Ref. [50]) imposed on $\{l_i, m_i, n_i\}$ using different numbers of exponential functions in Ψ_0. Based on his FC method, we have used the minimum number of exponential functions ($N = 2$) in the initial wavefunction to calculate the energy of the $1s2s$ triplet state of the helium atom. The results of these calculations are gathered in Table 2.3. This table clearly shows that including the permanents in the FC calculations although is not favorable from computational and technical point of view, is energetically important. For example, at $n = 1$ by adding one permanent, the energy gain is about 2 mE_h. Thus, keeping permanents in the

FC wavefunction seems necessary for obtaining a faster convergence to the desired accuracy in the calculated energy values.

2.2.2 Examples of Compact Explicitly Correlated Wavefucntions: A Case Study

Seeking the optimal forms for the N-term Hylleraas [66–68, 63] and the Kinoshita wavefunctions, [67, 69, 70], Koga performed several investigations with different optimization techniques on these two wavefunctions for the helium atom and helium-like ions. He showed that, for positive integer values of $\{l_i, m_i, n_i\}$ in Eq. 2.30, the optimal form of a N-term Hylleraas wavefunction depends on the nuclear charge Z. [68, 63] The reason of this observation has been related to the different significance in the radial and angular correlation effects. In this way, based on Eq. 2.24, it may be inferred that the terms including the variables s and t contribute mainly to the radial correlation energy whereas terms involving the variable u mainly contribute to the angular correlation energy. [68, 63]

An important lesson than can be learnt from Koga's studies on the N-term Hylleraas wavefunctions is that the perturbational approaches are inappropriate for finding the optimal form of the Hylleraas expansion shown in Eq. 2.30. [68, 63] This is because of the fact that the terms that appear in the optimal N-term Hylleraas expansion does not necessarily appear in the optimal N'-term expansion of the same form where $N' > N$. [68, 63] Kong *et al.* [6] performed an experiment (Tables 2 and 3 in Ref. [6]) on the calculation of the energy of the helium atom using the 3-term Hylleraas expansion of the form

$$\Psi = C\left[1 + c_1(r_1 - r_2)^2 + c_2 F(r_{12})\right]\ \Psi_0 \tag{2.41}$$

where C is the normalization factor, and $\Psi_0 = \phi(r_1)\phi(r_2)$ in which, $\phi(r)$ is a spherically symmetric orbital. They demonstrated that there are three factors that play crucial roles in the calculation of the electronic energy of the helium atom:

i. For having a compact wavefunction suitable for high-precision calculations, the inclusion of both second and third term in Eq. 2.41 is necessary.

ii. Reoptimization of the orbitals $\phi(r)$ in the explicitly correlated ansatz of Eq. 2.41 is also important for high-precision calculations.

iii. The functional form of the correlation factor $F(r_{12})$ does not seem to be important as long as its Taylor expansion includes linear r_{12} terms. [6]

Although these results seem plausible, care must be taken in their interpretation. Based on Koga's results in his study on finding the optimal N-term Hylleraas expansions, [63] the optimal form for the 3-term Hylleraas expansion has different terms for $Z = 1$ and $Z \in \{2,3,5,10\}$. Therefore, all results may become different due to the nuclear charge (or in general, system-) dependency of the optimal form of the N-term Hylleraas wavefunction. [63]

Although we have found that it is possible to construct shorter expansions than those generated by FC method at each order which can give lower energies, finding the optimal form of the FC wavefunction at each FC order and the best way of doing it is not our goal. The plan here is to consider 3 different ansätze as possible candidates for constructing a compact explicitly correlated wavefunction applicable for large systems which can give us accurate energies. [5, 6] Hence, assuming the general form of

$$\Psi = [1 + pF(u)]\Psi_0 \tag{2.42}$$

where p is the linear variational parameter and Ψ_0 is defined in Eq. 2.28, we now seek a suitable form for the correlated part $F(u)\Psi_0$ of our two-term explicitly correlated wavefunction. The test ground will be the helium atom in its singlet ground state considered in the interparticle $\{s,t,u\}$ or Hylleraas coordinate system. In order to extract maximum information from each ansatz,

$$\Psi_a = [1 + p_a \ln(u)]\Psi_0 \tag{2.43}$$

$$\Psi_b = [1 + p_b u]\Psi_0 \tag{2.44}$$

$$\Psi_c = [1 + p_c \exp(-\beta u)]\Psi_0 \tag{2.45}$$

all non-linear as well as linear parameters in each trial wavefunction were fully optimized and their corresponding variationally optimized energies and parameters are shown in Table 2.4.

Table 2.4 The variational electronic energy E, exponents ζ and β and linear correlation coefficient p for the singlet ground state of the helium atom.

Ψ_i	ζ	β	p	$-E$	$\Delta E = E_i - E_0$
Ψ_0	1.6875	–	0	2.847 656	0
Ψ_a	1.7553	–	0.1174	2.875 318	-0.027 661
Ψ_b	1.8497	–	0.3658	2.891 121	-0.043 464
Ψ_c	1.8487	0.0156	-0.9598	2.891 125	-0.043 468

Here, the energy of the Ψ_0 (Table 2.2) has been added as a reference value. The calculated electronic energies shown in Table 2.4 indicate that the idea of having logarithmic correlation factor, originating from the three-particle coalescence condition, [59–62] may play an important role in highly-accurate calculations but not in a compact two-terms wavefunction designed for more moderate accuracies.

The ΔE values shown in the last column of the Table 2.4 are consistent with the third result coming from the Kong *et al.* report (mentioned after Eq. 2.41) because the second term in the Taylor expansion of the exponential function is the linear r_{12} term. Hence, one can see that the difference in the calculated correlation energies corresponding to the linear correlation factor in Ψ_b and exponential correlation factor in Ψ_c is of the order of 10^{-6}. This energy lowering can be related to the contributions from quadratic, cubic *etc*. powers of the r_{12} in the Taylor expansion of the exponential correlation factor. [71, 33] In the minimal basis, the values of the linear coefficients resulting from Kato's cusp condition for Ψ_b and Ψ_c are $p_b = 0.3658$ and $-\beta p_c/(p_c+1) = 0.3725$, respectively. These values are different from Kato's cusp value (1/2) for the exact wavefunction. [26]

Armed with the results gathered in this section for small one- and two-electron systems, we are now in a position to propose a general compact form for an explicitly correlated wavefunction which can be applied to many-electron (atomic and molecular) systems. Among the ansätze proposed in Eqs. 2.43, 2.44 and 2.45, a good candidate can be the wavefnction shown in Eq. 2.44. This is because of its simple form and the presence of the linear term in the correlated part of the wavefunction. Also, as we will show in the final chapter, the results of the wavefunction with linear correlation factor can be generalized to any positive integer powers of r_{12} as a correlation factor. Moreover, our experiments with combinations of different powers of r_{12} produce the outcomes that are consistent with our expectations. These studies are presented in Chapter 4 where we analyzed the behavior of the Frost and Braunstein (FB) wavefunction for a simple molecular system, H_2.

2.3 Concluding Remarks

The details and mechanism of the work of the FC method proposed by Nakatsuji based on his series of studies on the structure of the exact wavefunction have been reviewed. Presenting the necessary foundations of this theory, the strengths and weaknesses of the FC method were discussed. Also, we analyzed the FC method through the calculation of the electronic energy of the ground state ($X^2\Sigma_g^+$) of the H_2^+ molecular ion and helium atom in its singlet ground state (^1S–with the electronic configuration $1s^2$) and triplet excited state (^3S–with the electronic configuration $1s2s$).

In our experiments on the triplet excited state of the helium atom, it has been found that the presence of a group of terms involving permanents in the FC expansion of the wavefunction were neglected (or ruled out) so far. This is probably because of the conditions which are imposed on the polynomial part of the Hylleraas expansion in order to automatize the generation of the FC functions. We also showed that considering permanents in the Hylleraas expansion of the helium atom wavefunction is energetically important in a sense that their inclusion seems necessary to have a more rapid convergence of the energy to its basis set limit. The presence of permanents while energetically beneficial, is not computationally favorable for large FC orders where the number of terms in the Hylleraas expansion rapidly increases.

Finally, based on our experiences with FC methods and Koga's studies on the optimal form of the Hylleraas and Kinoshita expansions, it can be shown that at a specific FC order, lower energies can be obtained using fewer complement functions. In this way, we have proposed three ansätze as suitable candidates for a compact explicitly correlated wavefunction which can simply be generalized and applied to many-electron systems. Among these candidates, the wavefunction with linear correlation factor, will be subject of our careful analysis in Chapter 4 for a simple molecular system, H_2.

CHAPTER 3

Investigation of the Frost-Braunstein Wavefunction for H_2: Theory

The analysis of the compact wavefunctions, presented in the previous chapter, has led us to the ideas of "Correlated Molecular Orbital" (CMO) theory of Frost and Braunstein (FB) to achieve a better understanding about the mechanism of work of correlation functions in the explicitly correlated methods such as R12 (and F12). Therefore, we revisit the CMO theory within both restricted (R) and unrestricted (U) formalisms. Our investigation involves five approximate wavefunctions: restricted Hartree-Fock (RHF), unrestricted Hartree-Fock (UHF), configuration interaction (CI), restricted Frost-Braunstein (RFB), which is equivalent to the CMO ansatz, and unrestricted Frost-Braunstein

(UFB) wavefunctions among which, the last one has been introduced by us for the first time. To be able to analyze the performance of each of these wavefunctions, in describing the electron correlation effects in H_2*, one needs to calculate all necessary one- and two-electron integrals. Since some of the two-electron integrals in the FB calculations are problematic, we have modeled our exponential atomic wavefunctions by their STO-nG expansions and used an extrapolation formula to predict the Slater-type orbitals' (STOs) energy limit* $(n = \infty)$*. We believe that our extrapolated results are indistinguishable from those from exact STOs. We provide most of the required integrals over the Gaussian-type orbitals (GTOs) in closed form while the most difficult ones (nuclear-attraction integrals with* r_{12}*) can be reduced to a straightforward one-dimensional quadrature.*

3.1 Introduction

Following the pioneering works of Hylleraas on helium atom [28], and James and Coolidge [72] on the hydrogen molecule, Frost, Braunstein and Schwemer introduced the concept of the "correlated molecular orbital" (CMO) in 1948 [73] in favor of explicit inclusion of the interelectronic distances in the molecular wavefunctions. After three years, Frost and Braunstein (FB) published a paper [74] in which, they calculated the electronic energy of H_2 using the CMO wavefunction defined in Eq. 3.4. The motivation for introducing the CMO ansatz is that the r_{12} factor can bring some electron correlation which is known to be present at normal bond lengths. Furthermore, adding the linear correlation factor provides the advantage of leading to the correct asymptotic limit at infinitely large internuclear distances over the ordinary molecular orbital (MO) wavefunctions. [74] Minimizing the energy with respect to the orbital exponents ζ, and the linear correlation coefficient p, FB managed to calculate the potential energy curve (PEC) of the H_2 molecule. The minimum of the CMO PEC was found to be at $R = 1.34$ bohr with the energy of -1.151 E_h which correspond to the internuclear distance of 0.71 Å and the binding energy of 4.11 eV. [74]

Throughout the present chapter, we might switch between spin-orbital or spatial orbital frameworks: Using spin-orbitals is more general and one can greatly simplify and reduce algebraic manipulations which is useful for the formulation of many theories of quantum chemistry in the first-quantization regime. [4] On the other hand, one has to integrate out the spin functions to reduce the spin-orbital formulations to those which involve only spatial orbitals that are more suitable for computational and numerical purposes. [17]

3.2 Theoretical Framework

For deep understanding of the effect of the explicit correlation factor r_{12} in the CMO or FB wavefunction, we will consider five approximate ansätze:

$$\Psi_{\text{RHF}} = \psi_1(\mathbf{r}_1)\psi_1(\mathbf{r}_2) \tag{3.1}$$

$$\Psi_{\text{UHF}} = \psi_\alpha(\mathbf{r}_1,t)\psi_\beta(\mathbf{r}_2,t) \tag{3.2}$$

$$\Psi_{\text{CI}} = \psi_1(\mathbf{r}_1)\psi_1(\mathbf{r}_2)\cos(\tfrac{\theta\pi}{4}) - \psi_2(\mathbf{r}_1)\psi_2(\mathbf{r}_2)\sin(\tfrac{\theta\pi}{4}) \tag{3.3}$$

$$\Psi_{\text{CMO}} \equiv \Psi_{\text{RFB}} = \psi_1(\mathbf{r}_1)\psi_1(\mathbf{r}_2)(1+p\,r_{12}) \tag{3.4}$$

$$\Psi_{\text{UFB}} = \psi_\alpha(\mathbf{r}_1,t)\psi_\beta(\mathbf{r}_2,t)(1+p\,r_{12}) \tag{3.5}$$

where the RHF, UHF, CI, RFB and UFB stand for restricted Hartree-Fock, unrestricted Hartree-Fock, configuration interaction, restricted Frost-Braunstein and unrestricted Frost-Braunstein wavefunctions, respectively. Also, we have rewritten the CMO wavefunction in its more compact but equivalent RFB form by using the definition of the spin-restricted MOs [75, 76] given by

$$\psi_1(\mathbf{r}) = \left[\phi_{\text{A}}^{S}(\mathbf{r}) + \phi_{\text{B}}^{S}(\mathbf{r})\right] / \sqrt{2(1+S_{\text{AB}})} \tag{3.6a}$$

$$\psi_2(\mathbf{r}) = \left[\phi_{\text{A}}^{S}(\mathbf{r}) - \phi_{\text{B}}^{S}(\mathbf{r})\right] / \sqrt{2(1-S_{\text{AB}})} \tag{3.6b}$$

Rotations of these spin-restricted MOs yield the spin-unrestricted MOs [77]

$$\psi_\alpha(\mathbf{r},t) = \psi_1(\mathbf{r})\cos(\tfrac{t\pi}{4}) + \psi_2(\mathbf{r})\sin(\tfrac{t\pi}{4}) \tag{3.7a}$$

$$\psi_\beta(\mathbf{r},t) = \psi_1(\mathbf{r})\cos(\tfrac{t\pi}{4}) - \psi_2(\mathbf{r})\sin(\tfrac{t\pi}{4}) \tag{3.7b}$$

where t is the symmetry-breaking or mixing parameter. Our basis functions are the $1s$ Slater-type orbitals (STOs)

$$\phi_{\mathrm{A}}^{S}(\mathbf{r}) = \sqrt{\zeta^3/\pi}\exp(-\zeta|\mathbf{r}-\mathbf{R}/2|) \tag{3.8a}$$

$$\phi_{\mathrm{B}}^{S}(\mathbf{r}) = \sqrt{\zeta^3/\pi}\exp(-\zeta|\mathbf{r}+\mathbf{R}/2|) \tag{3.8b}$$

Where $\mathbf{R}$ is a vector that joins the two centers A and B. The overlap integral is therefore [4, 78, 3]

$$S_{\mathrm{AB}} = (1+\lambda^{-1}+\lambda^{-2}/3)\exp(-1/\lambda) \tag{3.9}$$

where $\lambda = (\zeta R)^{-1}$.

In this chapter, we study the FB model within both spin-restricted and unrestricted formalisms. We derive the Hamiltonian and overlap matrix elements for both RFB and UFB within the same section due to their similarities. For the sake of completeness, we will also provide a brief theoretical background for RHF, UHF and CI ansätze. However, a comprehensive introduction to each of these methods can be found in various textbooks. [4, 17, 79]

3.2.1 Restricted Hartree-Fock

The HF ground-state wavefunction of the H_2 molecule within the minimal basis model can be written as

$$|\Psi_0\rangle = |\chi_1\chi_2\rangle = |\psi_1\overline{\psi}_1\rangle = |1\bar{1}\rangle \tag{3.10}$$

The Hamiltonian for such a two-electron system is

$$\begin{aligned}\mathscr{H} &= \left(-\frac{1}{2}\nabla_1^2 - \sum_A \frac{Z_A}{r_{1A}}\right) + \left(-\frac{1}{2}\nabla_2^2 - \sum_A \frac{Z_A}{r_{2A}}\right) + \frac{1}{r_{12}} \\ &= h(1) + h(2) + \frac{1}{r_{12}}\end{aligned} \tag{3.11}$$

where the kinetic and potential energies of the ith electron in the field of the nuclei have been incorporated in $h(i)$ which is called *core-Hamiltonian* for this reason. As shown in Eq. 3.11, one can write the total Hamiltonian as a sum of one-electron $\mathscr{F}$ and two-electron $\mathscr{G}$ operators

$$\mathscr{F} = h(1) + h(2) \tag{3.12}$$

$$\mathscr{G} = r_{12}^{-1} \tag{3.13}$$

Using the orthonormality of the spin functions, the matrix element expressions of the one- and two-electron operators in terms of spin-orbitals,

$$\langle i|h|j\rangle = \langle \chi_i|h|\chi_j\rangle = \int \chi_i^*(\mathbf{x}_1)h(\mathbf{r}_1)\chi_j(\mathbf{x}_1)d\mathbf{x}_1 \tag{3.14a}$$

$$\langle ij|kl\rangle = \langle \chi_i\chi_j|\chi_k\chi_l\rangle = \int \chi_i^*(\mathbf{x}_1)\chi_i^*(\mathbf{x}_2)r_{12}^{-1}\chi_k(\mathbf{x}_1)\chi_l(\mathbf{x}_2)d\mathbf{x}_1d\mathbf{x}_2 \tag{3.14b}$$

can be further reduced to the integral expressions that involve only the spatial functions

$$\langle i|h|i\rangle = h_{ii} = \int \psi_i^*(\mathbf{r}_1)h(\mathbf{r}_1)\psi_i(\mathbf{r}_1)d\mathbf{r}_1 \tag{3.15a}$$

$$\langle ij|ij\rangle = J_{ij} = \int |\psi_i(\mathbf{r}_1)|^2 r_{12}^{-1}|\psi_j(\mathbf{r}_2)|^2 d\mathbf{r}_1 d\mathbf{r}_2 \tag{3.15b}$$

$$\langle ij|ji\rangle = K_{ij} = \int \psi_i^*(\mathbf{r}_1)\psi_j^*(\mathbf{r}_2)r_{12}^{-1}\psi_j(\mathbf{r}_1)\psi_i(\mathbf{r}_2)d\mathbf{r}_1 d\mathbf{r}_2 \tag{3.15c}$$

where J_{ij} and K_{ij} are the Coulomb repulsion and exchange integrals, respectively. Note that in case of the one-electron operator h, the matrix element between spin-orbitals of different spin functions is zero. Whether $\langle ij|kl\rangle$ refers to an integral over spin-orbitals or spatial orbitals can only be determined from the context. [17] The RHF energy E_{RHF} of the ground state $|\Psi_0\rangle$ and the first doubly excited state $|\Psi_{1\bar{1}}^{2\bar{2}}\rangle$ of the H_2 molecule can be written as

$$\begin{aligned} E_0 &= \langle\Psi_0|\mathscr{H}|\Psi_0\rangle \\ &= 2\langle\psi_1|h|\psi_1\rangle + \langle\psi_1\psi_1|\psi_1\psi_1\rangle \\ &= 2h_{11} + J_{11} \end{aligned} \tag{3.16}$$

and

$$\begin{aligned} &\langle\Psi_{1\bar{1}}^{2\bar{2}}|\mathscr{H}|\Psi_{1\bar{1}}^{2\bar{2}}\rangle \\ &= 2\langle\psi_2|h|\psi_2\rangle + \langle\psi_2\psi_2|\psi_2\psi_2\rangle \\ &= 2h_{22} + J_{22} \end{aligned} \tag{3.17}$$

respectively. Using exponential integral functions, [3, 80, 81] Sugiura [82] presented analytic expressions for all necessary integrals over STOs in closed form for H_2 within the minimal basis model. We provide these expressions in the Appendix A for the sake of clarity and completeness. In the next chapter, using Eq. 3.16 and the expressions given in Appendix A, we will calculate RHF PEC by minimizing E_{RHF} with respect to orbital exponents at various bond lengths for further investigations.

3.2.2 Unrestricted Hartree-Fock

The RHF wavefunction (Eq. 3.1) considers identical spatial distributions for the electrons of opposite spin in the MO description of the ground state wavefunction of H_2. Mathematically, this means that the coefficients of the STO basis functions ϕ_A^S and ϕ_B^S in the spin-restricted MOs (Eqs. 3.6a and 3.6b) have to be the same. [75, 76] However, there are special situations such as homolytic cleavage of the H_2 bond in which, we need to relax the symmetry restriction for a more proper description of the process. This relaxation can be performed by rotating the spin-restricted MOs to obtain the spin-unrestricted MOs. [77] In other words, the rotation or mixing parameter t in Eqs. 3.7a and 3.7b relaxes the restriction over the coefficients of STOs to generate asymmetric MOs. If required, the mixing coefficient t can change between $0 \leq t \leq 1$. Assuming different spatial distributions for electrons with different spin states in the wavefunction, the mixing coefficient t takes the effect of spin-polarization into account. Therefore, E_{UHF} can be expressed as [17]

$$E_{\text{UHF}} = \langle \psi_\alpha | h | \psi_\alpha \rangle + \langle \psi_\beta | h | \psi_\beta \rangle + \langle \psi_\alpha \psi_\beta | \psi_\alpha \psi_\beta \rangle \tag{3.18}$$

or more explicitly,

$$\begin{aligned} E_{\text{UHF}} = 2h_{11} \cos^2(\tfrac{t\pi}{4}) + 2h_{22} \sin^2(\tfrac{t\pi}{4}) + J_{11} \cos^4(\tfrac{t\pi}{4}) \\ + J_{22} \sin^4(\tfrac{t\pi}{4}) + (2J_{12} - 4K_{12}) \cos^2(\tfrac{t\pi}{4}) \sin^2(\tfrac{t\pi}{4}) \end{aligned} \tag{3.19}$$

Minimization of E_{UHF} with respect to both the orbital exponents ζ and the mixing coefficient t at various internuclear distances R enables us to calculate the UHF PEC of H_2 for our future analysis in the next chapter. Calculation of the UHF energy (Eq. 3.19) within the minimal basis model requires exactly the same one- and two-electron integral expressions as provided in Appendix A.

3.2.3 Configuration Interaction

Considering the spatial orbitals ψ_1 and ψ_2 in the H_2 molecule within the minimal basis model, one can construct a set of $2M = 4$ (Sec. 2.2.1) spin-orbitals

$$\begin{aligned} \chi_1 &\equiv \psi_1 \qquad & \chi_2 &\equiv \overline{\psi}_1 \\ \chi_3 &\equiv \psi_2 \qquad & \chi_4 &\equiv \overline{\psi}_2 \end{aligned} \tag{3.20}$$

Since the exact ground state of the H_2 molecule is of gerade symmetry, one might impose this symmetry condition on the CI wavefunction to be of the same spatial symmetry. [4] Therefore, the CI ground state wavefunction (Eq. 3.3) will be the linear combination of the HF ground state, $|\Psi_0\rangle = |\chi_1\chi_2\rangle = |1\bar{1}\rangle$, and the doubly excited state $|\Psi_{1\bar{1}}^{2\bar{2}}\rangle = |\chi_3\chi_4\rangle = |2\bar{2}\rangle$. The determinantal mixing parameter θ allows the HF ground state determinant to mix with the first doubly excited state determinant. Hence, the 2×2 CI Hamiltonian matrix, $\mathbf{H}$, can be constructed in the basis of the $|\Psi_0\rangle$ and $|\Psi_{1\bar{1}}^{2\bar{2}}\rangle$ determinants [17]

$$\mathbf{H} = \begin{bmatrix} \langle\Psi_0|\mathscr{H}|\Psi_0\rangle & \langle\Psi_0|\mathscr{H}|\Psi_{1\bar{1}}^{2\bar{2}}\rangle \\ \langle\Psi_{1\bar{1}}^{2\bar{2}}|\mathscr{H}|\Psi_0\rangle & \langle\Psi_{1\bar{1}}^{2\bar{2}}|\mathscr{H}|\Psi_{1\bar{1}}^{2\bar{2}}\rangle \end{bmatrix} \tag{3.21}$$

which, using Eqs. 3.15, 3.16 and 3.17, one can simplify this matrix a bit more

$$\mathbf{H} = \begin{bmatrix} 2h_{11} + J_{11} & K_{12} \\ K_{12} & 2h_{22} + J_{22} \end{bmatrix} \tag{3.22}$$

Finally, E_{CI} can be obtained through diagonalizing the CI Hamiltonian matrix $\mathbf{H}$. Equivalently, it is possible to minimize the Rayleigh-Ritz expression

$$E_{\mathrm{CI}} = (2h_{11} + J_{11}) \cos^2\left(\frac{\theta\pi}{4}\right) + (2h_{22} + J_{22}) \sin^2\left(\frac{\theta\pi}{4}\right) - 2K_{12} \sin\left(\frac{\theta\pi}{4}\right) \cos\left(\frac{\theta\pi}{4}\right) \tag{3.23}$$

with respect to both orbital exponent ζ and mixing coefficient t at different bond lengths R. Again, the necessary integral expressions are given in Appendix A. Since the restricted MOs have been used in the construction of the CI wavefunction, we use acronyms CI and RCI interchangeably throughout the thesis.

3.3 Frost-Braunstein Wavefunction

So far, the basic concepts of the three wavefunctions RHF, UHF, and CI (Eqs. 3.1–3.3) have been reviewed. All these methods belong to a group of quantum mechanical theories called *algebraic approximations* which are based on the expansions in terms of antisymmetrized products (Eq. 1.14) of orthonormal spin-orbitals. [5, 6] These spin-orbitals can be obtained through a self-consistent field (SCF) procedure such as the HF method. [17] These traditional single- and/or multi-determinant CI-type expansions suffer from a known problem [34]- a frustratingly slow rate of convergence of the calculated energies toward the one-particle basis set limit [83–87] which is due to the improper description of the electronic cusp (see Sec. 1.2). [26] Since this slow convergence rate of the CI-type expansions happens because of the linear dependence of the exact wavefunction on the interelectronic distance in the region of the electron-electron coalescence, the explicit inclusion of the r_{12} correlation factor into the approximate wavefunction can be a natural way of dealing with this problem. [28, 27] Mathematically, in the simplest but still general case, one can represent the electronic wavefunction for atoms and molecules through adding an explicit function of interelectronic distance to the wavefunction [88]

$$\Psi = \Phi F(r_{12}) \tag{3.24}$$

where Φ is the CI-type expansion part in terms of spin-orbitals or MOs. Note that in case of the CMO or RFB wavefunction, Φ corresponds to the ground state Slater determinant and $F(r_{12}) = (1 + r_{12})$. Although such an explicitly correlated wavefuction converges rapidly to the basis set limit with basis set size, the matrix elements of the $\mathscr{H}$ operator can no longer be factorized into products of only one- and two-electron integrals. Thus, one needs a completely different strategy to deal with this new group of integrals as we will see in the next subsection.

3.3.1 Frost-Braunstein Integrals

For calculating E_{FB} at different bond lengths and obtaining the corresponding FB PEC, one needs to construct the Hamiltonian **H**, and overlap **S**, matrices. The electronic energies can be obtained through solving the generalized 2 × 2 eigenvalue equation of the form

$$\mathbf{HC} = \mathscr{E}\mathbf{SC} \tag{3.25}$$

where $\mathscr{E}$ and **C** are 2 × 2 matrices of eigenvalues (energies) and eigenfunctions. The Hamiltonian and overlap matrices for the RFB take the form of,

$$\mathbf{H} = \begin{bmatrix} \langle \psi_1 \psi_1 | \mathscr{H} | \psi_1 \psi_1 \rangle & \langle \psi_1 \psi_1 | \mathscr{H} r_{12} | \psi_1 \psi_1 \rangle \\ \langle \psi_1 \psi_1 | r_{12} \mathscr{H} | \psi_1 \psi_1 \rangle & \langle \psi_1 \psi_1 | r_{12} \mathscr{H} r_{12} | \psi_1 \psi_1 \rangle \end{bmatrix} \tag{3.26}$$

and

$$\mathbf{S} = \begin{bmatrix} \langle \psi_1 \psi_1 | r_{12}^0 | \psi_1 \psi_1 \rangle & \langle \psi_1 \psi_1 | r_{12}^1 | \psi_1 \psi_1 \rangle \\ \langle \psi_1 \psi_1 | r_{12}^1 | \psi_1 \psi_1 \rangle & \langle \psi_1 \psi_1 | r_{12}^2 | \psi_1 \psi_1 \rangle \end{bmatrix} \tag{3.27}$$

and for the UFB,

$$\mathbf{H} = \begin{bmatrix} \langle \psi_\alpha \psi_\beta | \mathscr{H} | \psi_\alpha \psi_\beta \rangle & \langle \psi_\alpha \psi_\beta | \mathscr{H} r_{12} | \psi_\alpha \psi_\beta \rangle \\ \langle \psi_\alpha \psi_\beta | r_{12} \mathscr{H} | \psi_\alpha \psi_\beta \rangle & \langle \psi_\alpha \psi_\beta | r_{12} \mathscr{H} r_{12} | \psi_\alpha \psi_\beta \rangle \end{bmatrix} \tag{3.28}$$

and

$$\mathbf{S} = \begin{bmatrix} \langle \psi_\alpha \psi_\beta | r_{12}^0 | \psi_\alpha \psi_\beta \rangle & \langle \psi_\alpha \psi_\beta | r_{12}^1 | \psi_\alpha \psi_\beta \rangle \\ \langle \psi_\alpha \psi_\beta | r_{12}^1 | \psi_\alpha \psi_\beta \rangle & \langle \psi_\alpha \psi_\beta | r_{12}^2 | \psi_\alpha \psi_\beta \rangle \end{bmatrix} \tag{3.29}$$

For the sake of clarity and convenience, it is best to break the Hamiltonian matrix into different pieces, *i.e.*

$$\mathbf{H} = \mathbf{T} + \mathbf{U}_1 + \mathbf{U}_2 + \mathbf{V} \tag{3.30}$$

and consider each of those terms separately. Here, $\mathbf{T}$ is the kinetic matrix, $\mathbf{U}_1$ and $\mathbf{U}_2$ are the nuclear attraction matrices in the field of both nuclei for the electron 1 and 2, respectively, and $\mathbf{V}$ stands for the electron-electron Coulomb repulsion matrix.

In the following subsections, we will consider each of these four $\mathbf{T}$, $\mathbf{U}_1$, $\mathbf{U}_2$, and $\mathbf{V}$ matrices and try to find a way to calculate them accurately. Since some of the two-electron integrals in the FB calculations in the single-ζ basis are problematic, we have modeled our exponential atomic wavefunctions by their STO-nG expansions. Therefore, we need to consider these integrals over 1s primitive Gaussian type-orbitals (GTOs). A normalized 1s GTO centered at $\mathbf{A}$ can be written as [17]

$$\phi_{\mathrm{A}}^{G}(\mathbf{r} - \mathbf{A}) = (2\alpha/\pi)^{3/4} \exp(-\alpha|\mathbf{r} - \mathbf{A}|^2) \tag{3.31}$$

where α is the Gaussian orbital exponent.

3.3.1.1 Overlap and Coulomb Repulsion Integrals

In quantum mechanics or more generally, in mathematical physics, there are situations in which, we face problems such that if they can be solved at all, it can be done only with difficulty. However, sometimes it is possible to transform our problem from its *ordinary*, *direct* or *physical* space to a *transformed* space where the solution of that problem might become relatively easier. After obtaining the solution in the transformed space, the reverse transformation into its direct space can be performed. [3] In such cases, it is often possible to consider pairs of functions f and g which are related to each other through

$$g(x) = \int_a^b f(t)K(x,t)dt \tag{3.32}$$

where a, b and the kernel $K(x,t)$ are the same for such pairs of functions. [3] In the calculation of FB matrix elements, the method of (3-dimensional) Fourier transform proved itself very useful as we show here. In this method, the kernel is an exponential function of the form $\exp(i\mathbf{x}\cdot\mathbf{t})$ and the integration is over the whole 3-D space.

Suppose in the ordinary space, we are given a function $f(\mathbf{r})$ of the vector $\mathbf{r}$ pointing at the position of an electron. The 3-D Fourier transform of this function, $g(\mathbf{k})$, is given by

$$g(\mathbf{k}) = \int f(\mathbf{r})e^{-i\mathbf{k}\cdot\mathbf{r}}d\mathbf{r} \tag{3.33}$$

where the vector $\mathbf{k}$ is the transform variable in the transformed space. The Fourier transformation allows us to back-transform to the ordinary space by

$$f(\mathbf{r}) = (2\pi)^{-3}\int g(\mathbf{k})e^{i\mathbf{k}\cdot\mathbf{r}}d\mathbf{k} \tag{3.34}$$

Thus, according to Eq. 3.32, $f(\mathbf{r})$ and $g(\mathbf{k})$ are called a Fourier transform pair. [3] In order to calculate the FB overlap matrix elements, the Fourier (integral) representations of r^{-1} and r^0 can be used, from which, the following formal Fourier representations are formed as

$$\begin{aligned}
\delta(\mathbf{r}) &= \int \left(\frac{\Gamma(1)}{8\pi^3 k^0}\right) e^{i\mathbf{k}\cdot\mathbf{r}}d\mathbf{k} & r^{-2} &= \int \left(\frac{1}{4\pi k}\right) e^{i\mathbf{k}\cdot\mathbf{r}}d\mathbf{k} \\
r^{-1} &= \int \left(\frac{\Gamma(1)}{2\pi^2 k^2}\right) e^{i\mathbf{k}\cdot\mathbf{r}}d\mathbf{k} & r^{0} &= \int \delta(\mathbf{k}) e^{i\mathbf{k}\cdot\mathbf{r}}d\mathbf{k} \\
r^{+1} &= -\int \left(\frac{\Gamma(3)}{2\pi^2 k^4}\right) e^{i\mathbf{k}\cdot\mathbf{r}}d\mathbf{k} & r^{+2} &= -\int \nabla_{\mathbf{k}}^2 \delta(\mathbf{k}) e^{i\mathbf{k}\cdot\mathbf{r}}d\mathbf{k}
\end{aligned} \tag{3.35}$$

Here, we have used the Laplacian identity

$$\nabla^2_{\mathbf{r}} \int k^{-n} e^{i\mathbf{k}\cdot\mathbf{r}} d\mathbf{k} = -\int k^{-(n-2)} e^{i\mathbf{k}\cdot\mathbf{r}} d\mathbf{k} \tag{3.36}$$

Armed with these relations, the overlap matrix elements over primitive GTOs can take the form of

$$S_{\text{mn}} = \langle r_{12}^m e^{-\alpha(\mathbf{r}_1-\mathbf{A})^2} e^{-\beta(\mathbf{r}_2-\mathbf{B})^2} | e^{-\gamma(\mathbf{r}_1-\mathbf{C})^2} e^{-\delta(\mathbf{r}_2-\mathbf{D})^2} r_{12}^n \rangle \tag{3.37}$$

which can be further simplified using $p = m + n$

$$S_{\text{p}} = \langle e^{-\alpha(\mathbf{r}_1-\mathbf{A})^2} e^{-\beta(\mathbf{r}_2-\mathbf{B})^2} | r_{12}^p | e^{-\gamma(\mathbf{r}_1-\mathbf{C})^2} e^{-\delta(\mathbf{r}_2-\mathbf{D})^2} \rangle \tag{3.38}$$

For $p = 0$ case, one can write

$$\begin{aligned}
S_0 &= \langle e^{-\alpha(\mathbf{r}_1-\mathbf{A})^2} e^{-\beta(\mathbf{r}_2-\mathbf{B})^2} | r_{12}^0 | e^{-\gamma(\mathbf{r}_1-\mathbf{C})^2} e^{-\delta(\mathbf{r}_2-\mathbf{D})^2} \rangle \\
&= G_{\text{AC}} G_{\text{BD}} \int\int e^{-\zeta(\mathbf{r}_1-\mathbf{P})^2} \left[r_{12}^0 \right] e^{-\eta(\mathbf{r}_2-\mathbf{Q})^2} d\mathbf{r}_1 d\mathbf{r}_2 \\
&= G_{\text{AC}} G_{\text{BD}} \int\int e^{-\zeta(\mathbf{r}_1-\mathbf{P})^2} \left[\int \delta(\mathbf{k}) e^{i\mathbf{k}\cdot(\mathbf{r}_1-\mathbf{r}_2)} d\mathbf{k} \right] e^{-\eta(\mathbf{r}_2-\mathbf{Q})^2} d\mathbf{r}_1 d\mathbf{r}_2 \\
&= G_{\text{AC}} G_{\text{BD}} \int \delta(\mathbf{k}) \left[\int e^{-\zeta(\mathbf{r}_1-\mathbf{P})^2 + i\mathbf{k}\cdot\mathbf{r}_1} d\mathbf{r}_1 \right] \left[\int e^{-\eta(\mathbf{r}_2-\mathbf{Q})^2 - i\mathbf{k}\cdot\mathbf{r}_2} d\mathbf{r}_2 \right] d\mathbf{k} \\
&= G_{\text{AC}} G_{\text{BD}} (\pi/\zeta)^{3/2} (\pi/\eta)^{3/2} \int \delta(\mathbf{k}) e^{i\mathbf{k}\cdot(\mathbf{P}-\mathbf{Q})} e^{-(k^2/4\zeta)-(k^2/4\eta)} d\mathbf{k} \\
&= G_{\text{AC}} G_{\text{BD}} (\pi/\zeta)^{3/2} (\pi/\eta)^{3/2} \left[\frac{2\,\Gamma(\frac{3}{2}+\frac{0}{2})}{\sqrt{\pi}} \right] \left(\frac{\zeta\eta}{\zeta+\eta} \right)^{0/2} M\left(\frac{0}{2}, \frac{3}{2}, -\frac{\zeta\eta}{\zeta+\eta} (\mathbf{P}-\mathbf{Q})^2 \right)
\end{aligned} \tag{3.39}$$

where $\Gamma(n+1) = n!$ and $M(a,b,z)$ is the confluent hypergeometric function (CHGF) or Kummer function defined as [3, 80, 81]

$${}_1F_1(a;b;z) = M(a,b,z) = \sum_{n=0}^{\infty} \frac{(a)_n}{(c)_n} \frac{z^n}{n!} \tag{3.40}$$

in which, $(a)_n$ is the Pochhammer symbol. $M(a,b,z)$ is convergent for all finite z (real or complex) and becomes a polynomial if the parameter a is 0 or a negative integer. [3, 80, 81]. It has a regular singularity at $z=0$ and an irregular one at $z=\infty$. Also, M becomes indeterminate for certain parameter values, *e.g.*, when c is an integer. [3]

Going from the first line to the second line of the set of Eqs. 3.39, the G_{AC} and G_{BD} were introduced as

$$\begin{aligned} G_{\text{AC}} &= \exp\left(-\frac{\alpha\gamma}{\alpha+\gamma}|\mathbf{A}-\mathbf{C}|^2\right) \\ G_{\text{BD}} &= \exp\left(-\frac{\beta\delta}{\beta+\delta}|\mathbf{B}-\mathbf{D}|^2\right) \end{aligned} \tag{3.41}$$

and the exponents ζ and η were defined as

$$\begin{aligned} \zeta &= \alpha+\gamma \\ \eta &= \beta+\delta \end{aligned} \tag{3.42}$$

Here, we have used an important property of the $1s$ Gaussian functions which simplifies the multi-center integrals like the overlap integral in the first line of Eqs. 3.39: The product of two $1s$ Gaussian functions ϕ_{A}^G and ϕ_{B}^G, focused on different nuclei A and B centered at **A** and **B**, is another $1s$ Gaussian function (apart from a constant factor) with the new exponent p on a third center P. In other words, for unnormalized $1s$ Gaussians

$$\exp\left(-\alpha|\mathbf{r}-\mathbf{A}|^2\right)\exp\left(-\beta|\mathbf{r}-\mathbf{B}|^2\right) = K\exp\left(-p|\mathbf{r}-\mathbf{P}|^2\right) \tag{3.43}$$

where the proportionality constant K is

$$K = \exp\left(-\frac{\alpha\beta}{\alpha+\beta}|\mathbf{A}-\mathbf{B}|^2\right) \tag{3.44}$$

and the new center P is located on a line that joins centers A and B

$$\mathbf{P} = \frac{\alpha\mathbf{A} + \beta\mathbf{B}}{\alpha + \beta} \tag{3.45}$$

Also, the exponent of the new Gaussian becomes

$$p = \alpha + \beta \tag{3.46}$$

Passing to the third line of Eqs. 3.39, we substituted r_{12}^0 by its Fourier representation provided in Eq. 3.35. The off-diagonal elements of the FB overlap matrices (Eqs. 3.27 and 3.29) can be calculated in the same manner

$$\begin{aligned}
S_1 &= \langle e^{-\alpha(\mathbf{r}_1-\mathbf{A})^2} e^{-\beta(\mathbf{r}_2-\mathbf{B})^2} | r_{12}^1 | e^{-\gamma(\mathbf{r}_1-\mathbf{C})^2} e^{-\delta(\mathbf{r}_2-\mathbf{D})^2} \rangle \\
&= G_{\mathrm{AC}} G_{\mathrm{BD}} \int\int e^{-\zeta(\mathbf{r}_1-\mathbf{P})^2} \left[r_{12}^1\right] e^{-\eta(\mathbf{r}_2-\mathbf{Q})^2} d\mathbf{r}_1 d\mathbf{r}_2 \\
&= G_{\mathrm{AC}} G_{\mathrm{BD}} \int\int e^{-\zeta(\mathbf{r}_1-\mathbf{P})^2} \left[-\frac{\Gamma(3)}{2\pi^2} \int \frac{e^{i\mathbf{k}\cdot(\mathbf{r}_1-\mathbf{r}_2)}}{k^4} d\mathbf{k}\right] e^{-\eta(\mathbf{r}_2-\mathbf{Q})^2} d\mathbf{r}_1 d\mathbf{r}_2 \\
&= G_{\mathrm{AC}} G_{\mathrm{BD}} \left(-\frac{\Gamma(3)}{2\pi^2}\right) \int k^{-4} \left[\int e^{-\zeta(\mathbf{r}_1-\mathbf{P})^2 + i\mathbf{k}\cdot\mathbf{r}_1} d\mathbf{r}_1\right] \left[\int e^{-\eta(\mathbf{r}_2-\mathbf{Q})^2 - i\mathbf{k}\cdot\mathbf{r}_2} d\mathbf{r}_2\right] d\mathbf{k} \\
&= G_{\mathrm{AC}} G_{\mathrm{BD}} (\pi/\zeta)^{3/2} (\pi/\eta)^{3/2} \left(-\frac{\Gamma(3)}{2\pi^2}\right) \int k^{-4} e^{i\mathbf{k}\cdot(\mathbf{P}-\mathbf{Q})} e^{-\left(k^2/4\zeta\right) - \left(k^2/4\eta\right)} d\mathbf{k} \\
&= G_{\mathrm{AC}} G_{\mathrm{BD}} (\pi/\zeta)^{3/2} (\pi/\eta)^{3/2} \left[\frac{2\,\Gamma(\frac{3}{2}+\frac{1}{2})}{\sqrt{\pi}}\right] \left(\frac{\zeta\eta}{\zeta+\eta}\right)^{-1/2} M\left(-\frac{1}{2}, \frac{3}{2}, -\frac{\zeta\eta}{\zeta+\eta}(\mathbf{P}-\mathbf{Q})^2\right)
\end{aligned} \tag{3.47}$$

in which, we have again used Gaussian product rule (Eqs. 3.43–3.46) and the Fourier representation of the r_{12}^1 given in Eqs. 3.35. Finally, the last FB overlap matrix element can be obtained in a slightly different fashion as

$$
\begin{aligned}
S_2 &= \langle e^{-\alpha(\mathbf{r}_1-\mathbf{A})^2} e^{-\beta(\mathbf{r}_2-\mathbf{B})^2} | r_{12}^2 | e^{-\gamma(\mathbf{r}_1-\mathbf{C})^2} e^{-\delta(\mathbf{r}_2-\mathbf{D})^2} \rangle \\
&= G_{\mathrm{AC}} G_{\mathrm{BD}} \int\int e^{-\zeta(\mathbf{r}_1-\mathbf{P})^2} \left[r_{12}^2 \right] e^{-\eta(\mathbf{r}_2-\mathbf{Q})^2} d\mathbf{r}_1 d\mathbf{r}_2 \\
&= G_{\mathrm{AC}} G_{\mathrm{BD}} \int\int e^{-\zeta(\mathbf{r}_1-\mathbf{P})^2} \left[-\int \nabla_{\mathbf{k}}^2 \delta(\mathbf{k}) e^{i\mathbf{k}\cdot(\mathbf{r}_1-\mathbf{r}_2)} d\mathbf{k} \right] e^{-\eta(\mathbf{r}_2-\mathbf{Q})^2} d\mathbf{r}_1 d\mathbf{r}_2 \\
&= G_{\mathrm{AC}} G_{\mathrm{BD}} \int \left[-\nabla_{\mathbf{k}}^2 \delta(\mathbf{k}) \right] \left[\int e^{-\zeta(\mathbf{r}_1-\mathbf{P})^2 + i\mathbf{k}\cdot\mathbf{r}_1} d\mathbf{r}_1 \right] \left[\int e^{-\eta(\mathbf{r}_2-\mathbf{Q})^2 - i\mathbf{k}\cdot\mathbf{r}_2} d\mathbf{r}_2 \right] d\mathbf{k} \\
&= G_{\mathrm{AC}} G_{\mathrm{BD}} (\pi/\zeta)^{3/2} (\pi/\eta)^{3/2} \int \left[-\nabla_{\mathbf{k}}^2 \delta(\mathbf{k}) \right] e^{i\mathbf{k}\cdot(\mathbf{P}-\mathbf{Q})} e^{-\left(k^2/4\zeta\right)-\left(k^2/4\eta\right)} d\mathbf{k}
\end{aligned}
\tag{3.48a}
$$

Integrating by parts twice, one can write

$$
\begin{aligned}
S_2 &= G_{\mathrm{AC}} G_{\mathrm{BD}} (\pi/\zeta)^{3/2} (\pi/\eta)^{3/2} \int \left(-\nabla_{\mathbf{k}}^2 \right) \left[e^{i\mathbf{k}\cdot(\mathbf{P}-\mathbf{Q})} e^{-\left(k^2/4\zeta\right)-\left(k^2/4\eta\right)} \right] \delta(\mathbf{k}) \, d\mathbf{k} \\
&= G_{\mathrm{AC}} G_{\mathrm{BD}} (\pi/\zeta)^{3/2} (\pi/\eta)^{3/2} \int \Big[-k^2/4 \left(\zeta^{-1} + \eta^{-1} \right)^2 + i \left(\zeta^{-1} + \eta^{-1} \right) \mathbf{k}\cdot(\mathbf{P}-\mathbf{Q}) \\
&\quad + 3/2 \left(\zeta^{-1} + \eta^{-1} \right) + (\mathbf{P}-\mathbf{Q})^2 \Big] \left[e^{i\mathbf{k}\cdot(\mathbf{P}-\mathbf{Q})} e^{-\left(k^2/4\zeta\right)-\left(k^2/4\eta\right)} \right] \delta(\mathbf{k}) \, d\mathbf{k} \\
&= G_{\mathrm{AC}} G_{\mathrm{BD}} (\pi/\zeta)^{3/2} (\pi/\eta)^{3/2} \left[3/2 \left(\zeta^{-1} + \eta^{-1} \right) + (\mathbf{P}-\mathbf{Q})^2 \right] \\
&= G_{\mathrm{AC}} G_{\mathrm{BD}} (\pi/\zeta)^{3/2} (\pi/\eta)^{3/2} \left[\frac{2\,\Gamma(\frac{3}{2}+\frac{2}{2})}{\sqrt{\pi}} \right] \left(\frac{\zeta\eta}{\zeta+\eta} \right)^{-2/2} M\left(-\frac{2}{2}, \frac{3}{2}, -\frac{\zeta\eta}{\zeta+\eta} (\mathbf{P}-\mathbf{Q})^2 \right)
\end{aligned}
\tag{3.48b}
$$

Looking at the final lines of Eqs. 3.39, 3.47 and 3.48, one can easily see that there is a certain pattern in the final form of the FB overlap matrix element's formulas. It can be shown that the general overlap matrix element, S_{p}, takes the form of

$$
\begin{aligned}
S_{\mathrm{p}} &= \langle e^{-\alpha(\mathbf{r}_1-\mathbf{A})^2} e^{-\beta(\mathbf{r}_2-\mathbf{B})^2} | r_{12}^p | e^{-\gamma(\mathbf{r}_1-\mathbf{C})^2} e^{-\delta(\mathbf{r}_2-\mathbf{D})^2} \rangle \\
&= G_{\mathrm{AC}} G_{\mathrm{BD}} (\pi/\zeta)^{3/2} (\pi/\eta)^{3/2} \left[\frac{2\,\Gamma(\frac{3}{2}+\frac{p}{2})}{\sqrt{\pi}} \right] \left(\frac{\zeta\eta}{\zeta+\eta} \right)^{-p/2} M\left(-\frac{p}{2}, \frac{3}{2}, -\frac{\zeta\eta}{\zeta+\eta} (\mathbf{P}-\mathbf{Q})^2 \right)
\end{aligned}
\tag{3.49}
$$

This completes the derivation of the general formula for calculating the FB overlap matrix elements over the primitive Gaussian functions.

Note that the FB matrix elements of the Coulomb electron-electron repulsion are very similar in form to those of the FB overlap matrix elements. Thus, calculating the FB electronic repulsion matrix elements using Eq. 3.49 is a straightforward task.

3.3.1.2 Kinetic Integrals

Before we begin to calculate the matrix elements of the Laplacian operator over primitive GTOs, one needs to know the effect of the differential gradient operator on the product of a Gaussian function and the r_{12} correlation factor. It can simply be shown that

$$\nabla_1 \left(r_{12} e^{-\alpha(\mathbf{r}_1-\mathbf{A})^2} \right) = \frac{(\mathbf{r}_1 - \mathbf{r}_2)}{r_{12}} e^{-\alpha(\mathbf{r}_1-\mathbf{A})^2} - 2\alpha r_{12} \left(\mathbf{r}_1 - \mathbf{A}\right) e^{-\alpha(\mathbf{r}_1-\mathbf{A})^2} \tag{3.50}$$

The second term in the expression above can be considered as the result of the effect of a differential gradient operator on the same Gaussian function with respect to the position of the nuclear center, which in this case is A. In other words,

$$\nabla_{\mathbf{A}} \left(r_{12} e^{-\alpha(\mathbf{r}_1-\mathbf{A})^2} \right) = 2\alpha r_{12} \left(\mathbf{r}_1 - \mathbf{A}\right) e^{-\alpha(\mathbf{r}_1-\mathbf{A})^2} \tag{3.51}$$

Therefore, Eq. 3.50 can be further simplified to

$$\nabla_1 \left(r_{12} e^{-\alpha(\mathbf{r}_1-\mathbf{A})^2} \right) = \left[\frac{(\mathbf{r}_1 - \mathbf{r}_2)}{r_{12}^2} - \nabla_{\mathbf{A}} \right] \left(r_{12} e^{-\alpha(\mathbf{r}_1-\mathbf{A})^2} \right) \tag{3.52}$$

In this way, we have constructed a hybrid operator, shown in the square brackets on the right-hand side of Eq. 3.52 that gives us the effect of a differentiation with respect to the coordinates of the electron in an indirect way. This makes the calculation of the matrix elements of kinetic operators much simpler as we demonstrate shortly. Note that, generalizing this result for any power of r_{12}, one can obtain

$$\nabla_1 \left(r_{12}^q e^{-\alpha(\mathbf{r}_1-\mathbf{A})^2} \right) = \left[q \frac{(\mathbf{r}_1 - \mathbf{r}_2)}{r_{12}^2} - \nabla_{\mathbf{A}} \right] \left(r_{12}^q e^{-\alpha(\mathbf{r}_1-\mathbf{A})^2} \right) \tag{3.53}$$

The primitive kinetic integral is

$$T_{\text{pq}} = \langle e^{-\alpha(\mathbf{r}_1-\mathbf{A})^2} e^{-\beta(\mathbf{r}_2-\mathbf{B})^2} r_{12}^p | \left(-\frac{\nabla_1^2}{2} - \frac{\nabla_2^2}{2} \right) | r_{12}^q e^{-\gamma(\mathbf{r}_1-\mathbf{C})^2} e^{-\delta(\mathbf{r}_2-\mathbf{D})^2} \rangle \tag{3.54}$$

Integration by parts gives

$$T_{\text{pq}} = \langle e^{-\alpha(\mathbf{r}_1-\mathbf{A})^2} e^{-\beta(\mathbf{r}_2-\mathbf{B})^2} r_{12}^p | \left(\frac{\nabla_1 \cdot \nabla_1}{2} + \frac{\nabla_2 \cdot \nabla_2}{2} \right) | r_{12}^q e^{-\gamma(\mathbf{r}_1-\mathbf{C})^2} e^{-\delta(\mathbf{r}_2-\mathbf{D})^2} \rangle \tag{3.55}$$

Adopting the convention that the left-side and right-side operators in a dot product like $\mathscr{L} \cdot \mathscr{R}$ can operate on their left and right, respectively, one can transform the operator to sum of differential operators with respect to the Gaussian centers. That is,

$$\begin{aligned} &\nabla_1 \cdot \nabla_1 + \nabla_2 \cdot \nabla_2 \\ &= \left[p \tfrac{(\mathbf{r}_1-\mathbf{r}_2)}{r_{12}^2} - \nabla_{\mathbf{A}} \right] \cdot \left[q \tfrac{(\mathbf{r}_1-\mathbf{r}_2)}{r_{12}^2} - \nabla_{\mathbf{C}} \right] + \left[p \tfrac{(\mathbf{r}_2-\mathbf{r}_1)}{r_{12}^2} - \nabla_{\mathbf{B}} \right] \cdot \left[q \tfrac{(\mathbf{r}_2-\mathbf{r}_1)}{r_{12}^2} - \nabla_{\mathbf{D}} \right] \\ &= \nabla_{\mathbf{A}} \cdot \nabla_{\mathbf{C}} + \nabla_{\mathbf{B}} \cdot \nabla_{\mathbf{D}} + \left(p/r_{12}^2\right) (\mathbf{r}_1 - \mathbf{r}_2) \cdot (\nabla_{\mathbf{D}} - \nabla_{\mathbf{C}}) + \left(q/r_{12}^2\right) (\nabla_{\mathbf{B}} - \nabla_{\mathbf{A}}) \cdot (\mathbf{r}_1 - \mathbf{r}_2) + \left(2pq/r_{12}^2\right) \end{aligned} \tag{3.56}$$

Adding and subtracting Gaussian centers' position vectors from $\mathbf{r}_1$ and $\mathbf{r}_2$ in the parentheses, the last line in Eq. 3.56 can be written as

$$\begin{aligned} &\nabla_1 \cdot \nabla_1 + \nabla_2 \cdot \nabla_2 \\ &= \nabla_{\mathbf{A}} \cdot \nabla_{\mathbf{C}} + \nabla_{\mathbf{B}} \cdot \nabla_{\mathbf{D}} + \left(p/r_{12}^2\right) [(\mathbf{r}_1 - \mathbf{A}) - (\mathbf{r}_2 - \mathbf{B}) + (\mathbf{A} - \mathbf{B})] \cdot (\nabla_{\mathbf{D}} - \nabla_{\mathbf{C}}) \\ &\quad + \left(q/r_{12}^2\right) (\nabla_{\mathbf{B}} - \nabla_{\mathbf{A}}) \cdot [(\mathbf{r}_1 - \mathbf{C}) - (\mathbf{r}_2 - \mathbf{D}) + (\mathbf{C} - \mathbf{D})] + \left(2pq/r_{12}^2\right) \end{aligned} \tag{3.57}$$

Once again, Eq. 3.51 can be used but this time, for the gradient of a Gaussian function without a correlation factor. This casts Eq. 3.57 into its final form

$$\begin{aligned}
&\nabla_1 \cdot \nabla_1 + \nabla_2 \cdot \nabla_2 \\
&= \nabla_{\mathbf{A}} \cdot \nabla_{\mathbf{C}} + \nabla_{\mathbf{B}} \cdot \nabla_{\mathbf{D}} + \left(p/r_{12}^2\right)\left[\nabla_{\mathbf{A}}/2\alpha - \nabla_{\mathbf{B}}/2\beta + (\mathbf{A}-\mathbf{B})\right] \cdot \left(\nabla_{\mathbf{D}} - \nabla_{\mathbf{C}}\right) \\
&\quad + \left(q/r_{12}^2\right)\left(\nabla_{\mathbf{B}} - \nabla_{\mathbf{A}}\right) \cdot \left[\nabla_{\mathbf{C}}/2\gamma - \nabla_{\mathbf{D}}/2\delta + (\mathbf{C}-\mathbf{D})\right] + \left(2pq/r_{12}^2\right)
\end{aligned} \tag{3.58}$$

which has been written only in terms of derivatives with respect to the Gaussian centers. Multiplying Eq. 3.58 by a factor of 1/2 and inserting it into Eq. 3.55, one can obtain the general FB primitive kinetic matrix element as

$$\begin{aligned}
T_{\mathrm{pq}} &= 1/2\left(\nabla_{\mathbf{A}} \cdot \nabla_{\mathbf{C}} + \nabla_{\mathbf{B}} \cdot \nabla_{\mathbf{D}}\right)\mathbf{S}_{p+q} + 1/2\left(p\left[\nabla_{\mathbf{A}}/2\alpha - \nabla_{\mathbf{B}}/2\beta + (\mathbf{A}-\mathbf{B})\right] \cdot \left(\nabla_{\mathbf{D}} - \nabla_{\mathbf{C}}\right)\right. \\
&\quad \left. + q\left(\nabla_{\mathbf{B}} - \nabla_{\mathbf{A}}\right) \cdot \left[\nabla_{\mathbf{C}}/2\gamma - \nabla_{\mathbf{D}}/2\delta + (\mathbf{C}-\mathbf{D})\right] + 2pq\right)\mathbf{S}_{p+q-2}
\end{aligned} \tag{3.59}$$

Therefore, the FB kinetic matrix elements can be written in terms of the FB overlap matrix elements (Eq. 3.49) and differential gradient operators with respect to the Gaussian centers.

3.3.1.3 Nuclear-Attraction Integrals

The diagonal FB nuclear-attraction matrix elements U_p where $p \in \{0,2\}$ can be obtained in closed form as we show here. The most difficult integrals in the FB calculations, however, are the nuclear-attraction integrals with $p=1$ that can be reduced to a straightforward one-dimensional quadrature. [89, 90] Although the U_0 FB nuclear-attraction matrix elements were given in closed form somewhere else, [4, 17] for the sake of clarity and completeness, we adopt our usual strategy of using the Fourier representations (Eqs. 3.35) to evaluate these integrals here again. The $U_0^{(1)}$ FB nuclear-attraction matrix element (for electron 1 focused on center at **P** and attracted by a positive charge centered at **Z**) over the primitive Gaussian functions is

$$
\begin{aligned}
-U_0^{(1)} &= \langle e^{-\alpha(\mathbf{r}_1-\mathbf{A})^2} e^{-\beta(\mathbf{r}_2-\mathbf{B})^2} | \frac{r_{12}^0}{|\mathbf{r}_1-\mathbf{Z}|} | e^{-\gamma(\mathbf{r}_1-\mathbf{C})^2} e^{-\delta(\mathbf{r}_2-\mathbf{D})^2} \rangle \\
&= G_{\mathrm{AC}} G_{\mathrm{BD}} \int\int e^{-\zeta(\mathbf{r}_1-\mathbf{P})^2} \left[\int \left(\frac{\Gamma(1)}{2\pi^2 k^2} \right) e^{i\mathbf{k}\cdot(\mathbf{r}_1-\mathbf{Z})} d\mathbf{k} \right] e^{-\eta(\mathbf{r}_2-\mathbf{Q})^2} d\mathbf{r}_1 d\mathbf{r}_2 \\
&= G_{\mathrm{AC}} G_{\mathrm{BD}} \left(\frac{\Gamma(1)}{2\pi^2} \right) \int k^{-2} e^{-i\mathbf{k}\cdot\mathbf{Z}} \left[\int e^{-\zeta(\mathbf{r}_1-\mathbf{P})^2 + i\mathbf{k}\cdot\mathbf{r}_1} d\mathbf{r}_1 \right] \left[\int e^{-\eta(\mathbf{r}_2-\mathbf{Q})^2} d\mathbf{r}_2 \right] d\mathbf{k} \\
&= G_{\mathrm{AC}} G_{\mathrm{BD}} (\pi/\zeta)^{3/2} (\pi/\eta)^{3/2} \left(\frac{\Gamma(1)}{2\pi^2} \right) \int k^{-2} e^{-i\mathbf{k}\cdot\mathbf{Z}} \left(e^{-\left(k^2/4\zeta\right)} e^{i\mathbf{k}\cdot\mathbf{P}} \right) d\mathbf{k} \\
&= G_{\mathrm{AC}} G_{\mathrm{BD}} (\pi/\zeta)^{3/2} (\pi/\eta)^{3/2} \left(\frac{\Gamma(1)}{2\pi^2} \right) \left[\frac{2\pi^2 \ \mathrm{erf}(\sqrt{\zeta}|\mathbf{P}-\mathbf{Z}|)}{|\mathbf{P}-\mathbf{Z}|} \right] \\
&= G_{\mathrm{AC}} G_{\mathrm{BD}} (\pi/\zeta)^{3/2} (\pi/\eta)^{3/2} \left[\frac{2\,\Gamma(\frac{3}{2}-\frac{1}{2})}{\sqrt{\pi}} \right] \sqrt{\zeta}\, M(\frac{1}{2}, \frac{3}{2}, -\zeta|\mathbf{P}-\mathbf{Z}|^2)
\end{aligned}
\tag{3.60}
$$

in which, we have adopted the Fourier representation of r^{-1} for the nuclear-attraction operator $|\mathbf{r}-\mathbf{Z}|^{-1}$. Also, to obtain the last line of the Eq. 3.60, we have used the relation

$$
\mathrm{erf}(x) = (2/\sqrt{\pi}) \int_0^x e^{-t^2} dt = (2x/\sqrt{\pi})\, M(\frac{1}{2}, \frac{3}{2}, -x^2) \tag{3.61}
$$

which corresponds the CHGF to the more elementary error function erf. [3] Frequently, one faces a form of these Coulomb-interaction integrals over Gaussian functions which includes a class of functions referred to as Boys Functions [4, 17]

$$
F_n(x) = \int_0^1 \exp(-xt^2) t^{2n} dt \tag{3.62}
$$

which are related to the error functions and CHGFs thorough the expressions [4]

$$
F_0(x) = \sqrt{\frac{\pi}{4x}} \mathrm{erf}(\sqrt{x}) \tag{3.63a}
$$

$$
F_n(x) = \frac{M(n+\frac{1}{2}, n+\frac{3}{2}, -x)}{2n+1} \tag{3.63b}
$$

The $U_0^{(2)}$ FB nuclear-attraction matrix element (for electron 2 located at $\mathbf{Q}$ and attracted by a positive charge centered at $\mathbf{Z}$) over the primitive Gaussian functions is

$$\begin{aligned}
-U_0^{(2)} &= \langle e^{-\alpha(\mathbf{r}_1-\mathbf{A})^2} e^{-\beta(\mathbf{r}_2-\mathbf{B})^2} | \frac{r_{12}^0}{|\mathbf{r}_2-\mathbf{Z}|} | e^{-\gamma(\mathbf{r}_1-\mathbf{C})^2} e^{-\delta(\mathbf{r}_2-\mathbf{D})^2} \rangle \\
&= G_{\mathrm{AC}} G_{\mathrm{BD}} (\pi/\zeta)^{3/2} (\pi/\eta)^{3/2} \left[\frac{2\,\Gamma(\frac{3}{2}-\frac{1}{2})}{\sqrt{\pi}} \right] \sqrt{\eta}\, M(\frac{1}{2},\frac{3}{2},-\eta|\mathbf{Q}-\mathbf{Z}|^2)
\end{aligned} \tag{3.64}$$

Thus, U_0 is

$$\begin{aligned}
-U_0 &= -(U_0^{(1)} + U_0^{(2)}) \\
&= \langle e^{-\alpha(\mathbf{r}_1-\mathbf{A})^2} e^{-\beta(\mathbf{r}_2-\mathbf{B})^2} | \frac{r_{12}^0}{|\mathbf{r}_1-\mathbf{Z}|} + \frac{r_{12}^0}{|\mathbf{r}_2-\mathbf{Z}|} | e^{-\gamma(\mathbf{r}_1-\mathbf{C})^2} e^{-\delta(\mathbf{r}_2-\mathbf{D})^2} \rangle \\
&= G_{\mathrm{AC}} G_{\mathrm{BD}} (\pi/\zeta)^{3/2} (\pi/\eta)^{3/2} (2/\sqrt{\pi}) \left[\sqrt{\zeta}\, M(\frac{1}{2},\frac{3}{2},-\zeta|\mathbf{P}-\mathbf{Z}|^2) + \sqrt{\eta}\, M(\frac{1}{2},\frac{3}{2},-\eta|\mathbf{Q}-\mathbf{Z}|^2) \right]
\end{aligned} \tag{3.65}$$

The $U_2^{(1)}$ FB nuclear-attraction matrix element (for electron 1 focused on center at $\mathbf{P}$ and attracted by a positive charge centered at $\mathbf{Z}$) over the primitive Gaussian functions can be calculated in two different ways. The first one is the usual way of using the Fourier representation provided in the set of Eqs. 3.35 for $|\mathbf{r}-\mathbf{Z}|^{-1}$ operator and proceed quite similar to what we did for S_2 case as

$$\begin{aligned}
-U_2^{(1)} &= \langle e^{-\alpha(\mathbf{r}_1-\mathbf{A})^2} e^{-\beta(\mathbf{r}_2-\mathbf{B})^2} | \frac{r_{12}^2}{|\mathbf{r}_1-\mathbf{Z}|} | e^{-\gamma(\mathbf{r}_1-\mathbf{C})^2} e^{-\delta(\mathbf{r}_2-\mathbf{D})^2} \rangle \\
&= G_{\mathrm{AC}} G_{\mathrm{BD}} \int\int \frac{e^{-\zeta(\mathbf{r}_1-\mathbf{P})^2}}{|\mathbf{r}_1-\mathbf{Z}|} \left[r_{12}^2 \right] e^{-\eta(\mathbf{r}_2-\mathbf{Q})^2} d\mathbf{r}_1 d\mathbf{r}_2 \\
&= G_{\mathrm{AC}} G_{\mathrm{BD}} \int\int \frac{e^{-\zeta(\mathbf{r}_1-\mathbf{P})^2}}{|\mathbf{r}_1-\mathbf{Z}|} \left[-\int \nabla_{\mathbf{k}}^2 \delta(\mathbf{k}) e^{i\mathbf{k}\cdot(\mathbf{r}_1-\mathbf{r}_2)} d\mathbf{k} \right] e^{-\eta(\mathbf{r}_2-\mathbf{Q})^2} d\mathbf{r}_1 d\mathbf{r}_2 \\
&= G_{\mathrm{AC}} G_{\mathrm{BD}} \int \left[-\nabla_{\mathbf{k}}^2 \delta(\mathbf{k}) \right] \left[\int \frac{e^{-\zeta(\mathbf{r}_1-\mathbf{P})^2 + i\mathbf{k}\cdot\mathbf{r}_1}}{|\mathbf{r}_1-\mathbf{Z}|} d\mathbf{r}_1 \right] \left[\int e^{-\eta(\mathbf{r}_2-\mathbf{Q})^2 - i\mathbf{k}\cdot\mathbf{r}_2} d\mathbf{r}_2 \right] d\mathbf{k} \\
&= G_{\mathrm{AC}} G_{\mathrm{BD}} (2\pi/\zeta) (\pi/\eta)^{3/2} \int \left[-\nabla_{\mathbf{k}}^2 \delta(\mathbf{k}) \right] M\left(\frac{1}{2},\frac{3}{2},-\zeta\left(\mathbf{P}-\mathbf{Z}+\frac{ik}{2\zeta} \right)^2 \right) \\
&\times e^{i\mathbf{k}\cdot(\mathbf{P}-\mathbf{Q}) - \left(k^2/4\zeta\right) - \left(k^2/4\eta\right)} d\mathbf{k}
\end{aligned} \tag{3.66}$$

To proceed, we need to recall the following property of the Dirac delta "function" [3]

$$\delta(x) = 0 \qquad x \neq 0, \tag{3.67a}$$

$$f(0) = \int_a^b f(x)\delta(x)dx \tag{3.67b}$$

where integration includes the origin and $f(x)$ is any well-behaved function. Considering the special case of Eq. 3.67b,

$$\int_{-\infty}^{\infty} \delta(x)\, dx = 1 \tag{3.68}$$

and integrating by parts, one can get

$$\begin{aligned}
-U_2^{(1)} &= G_{\mathrm{AC}}G_{\mathrm{BD}}\,(2\pi/\zeta)\,(\pi/\eta)^{3/2} \\
&\times \left(-\nabla^2_{\mathbf{k}}\right)\left[e^{i\mathbf{k}\cdot(\mathbf{P}-\mathbf{Q})-\left(k^2/4\zeta\right)-\left(k^2/4\eta\right)} M\left(\frac{1}{2},\frac{3}{2},-\zeta\left(\mathbf{P}-\mathbf{Z}+\frac{ik}{2\zeta}\right)^2\right)\right]_{k=0} \\
&= G_{\mathrm{AC}}G_{\mathrm{BD}}\,(2\pi/\zeta)\,(\pi/\eta)^{3/2} \\
&\times \Bigg\{\left[\left(-\nabla^2_{\mathbf{k}}\right) e^{i\mathbf{k}\cdot(\mathbf{P}-\mathbf{Q})-\left(k^2/4\zeta\right)-\left(k^2/4\eta\right)}\right]_{k=0}\left[M\left(\frac{1}{2},\frac{3}{2},-\zeta\left(\mathbf{P}-\mathbf{Z}+\frac{ik}{2\zeta}\right)^2\right)\right]_{k=0} \\
&-2\left[\nabla_{\mathbf{k}}\, e^{i\mathbf{k}\cdot(\mathbf{P}-\mathbf{Q})-\left(k^2/4\zeta\right)-\left(k^2/4\eta\right)}\right]_{k=0}\cdot\left[\nabla_{\mathbf{k}}\, M\left(\frac{1}{2},\frac{3}{2},-\zeta\left(\mathbf{P}-\mathbf{Z}+\frac{ik}{2\zeta}\right)^2\right)\right]_{k=0} \\
&+\left[e^{i\mathbf{k}\cdot(\mathbf{P}-\mathbf{Q})-\left(k^2/4\zeta\right)-\left(k^2/4\eta\right)}\right]_{k=0}\left[\left(-\nabla^2_{\mathbf{k}}\right) M\left(\frac{1}{2},\frac{3}{2},-\zeta\left(\mathbf{P}-\mathbf{Z}+\frac{ik}{2\zeta}\right)^2\right)\right]_{k=0}\Bigg\} \\
&= G_{\mathrm{AC}}G_{\mathrm{BD}}\,(2\pi/\zeta)\,(\pi/\eta)^{3/2}\Bigg\{\left[(\mathbf{P}-\mathbf{Q})^2+\frac{3}{2\zeta}+\frac{3}{2\eta}\right]M\left(\frac{1}{2},\frac{3}{2},-\zeta|\mathbf{P}-\mathbf{Z}|^2\right) \\
&-\frac{2}{3}(\mathbf{P}-\mathbf{Q})\cdot(\mathbf{P}-\mathbf{Z})\,M\left(\frac{3}{2},\frac{5}{2},-\zeta|\mathbf{P}-\mathbf{Z}|^2\right)-\frac{e^{-\zeta|\mathbf{P}-\mathbf{Z}|^2}}{2\zeta}\Bigg\}
\end{aligned} \tag{3.69}$$

Similarly, for the $U_2^{(2)}$ FB nuclear-attraction matrix element (for electron 2 sitting at **Q** center and attracted by a positive charge centered at **Z**) over the primitive GTOs, we have

$$\begin{aligned}
-U_2^{(2)} &= \langle e^{-\alpha(\mathbf{r}_1-\mathbf{A})^2} e^{-\beta(\mathbf{r}_2-\mathbf{B})^2} | \frac{r_{12}^2}{|\mathbf{r}_2-\mathbf{Z}|} | e^{-\gamma(\mathbf{r}_1-\mathbf{C})^2} e^{-\delta(\mathbf{r}_2-\mathbf{D})^2} \rangle \\
&= G_{\mathrm{AC}} G_{\mathrm{BD}} \,(2\pi/\eta)\,(\pi/\zeta)^{3/2} \left\{ \left[(\mathbf{P}-\mathbf{Q})^2 + \frac{3}{2\zeta} + \frac{3}{2\eta} \right] M(\frac{1}{2},\frac{3}{2},-\eta|\mathbf{Q}-\mathbf{Z}|^2) \right. \\
&\left. - \frac{2}{3}(\mathbf{P}-\mathbf{Q})\cdot(\mathbf{Z}-\mathbf{Q})\, M(\frac{3}{2},\frac{5}{2},-\eta|\mathbf{Q}-\mathbf{Z}|^2) - \frac{e^{-\eta|\mathbf{Q}-\mathbf{Z}|^2}}{2\eta} \right\}
\end{aligned} \tag{3.70}$$

Finally, for the U_2 FB nuclear-attraction matrix element, one can obtain

$$\begin{aligned}
-U_2 &= -(U_2^{(1)} + U_2^{(2)}) \\
&= \langle e^{-\alpha(\mathbf{r}_1-\mathbf{A})^2} e^{-\beta(\mathbf{r}_2-\mathbf{B})^2} | \frac{r_{12}^2}{|\mathbf{r}_1-\mathbf{Z}|} + \frac{r_{12}^2}{|\mathbf{r}_2-\mathbf{Z}|} | e^{-\gamma(\mathbf{r}_1-\mathbf{C})^2} e^{-\delta(\mathbf{r}_2-\mathbf{D})^2} \rangle \\
&= G_{\mathrm{AC}} G_{\mathrm{BD}} \left\{ (2\pi/\zeta)\,(\pi/\eta)^{3/2} \left[\left((\mathbf{P}-\mathbf{Q})^2 + \frac{3}{2\zeta} + \frac{3}{2\eta} \right) M(\frac{1}{2},\frac{3}{2},-\zeta|\mathbf{P}-\mathbf{Z}|^2) \right. \right. \\
&\left. - \frac{2}{3}(\mathbf{P}-\mathbf{Q})\cdot(\mathbf{P}-\mathbf{Z})\, M(\frac{3}{2},\frac{5}{2},-\zeta|\mathbf{P}-\mathbf{Z}|^2) - \frac{e^{-\zeta|\mathbf{P}-\mathbf{Z}|^2}}{2\zeta} \right] + (2\pi/\eta)\,(\pi/\zeta)^{3/2} \\
&\times \left[\left((\mathbf{P}-\mathbf{Q})^2 + \frac{3}{2\zeta} + \frac{3}{2\eta} \right) M(\frac{1}{2},\frac{3}{2},-\eta|\mathbf{Q}-\mathbf{Z}|^2) \right. \\
&\left.\left. - \frac{2}{3}(\mathbf{P}-\mathbf{Q})\cdot(\mathbf{Z}-\mathbf{Q})\, M(\frac{3}{2},\frac{5}{2},-\eta|\mathbf{Q}-\mathbf{Z}|^2) - \frac{e^{-\eta|\mathbf{Q}-\mathbf{Z}|^2}}{2\eta} \right] \right\}
\end{aligned} \tag{3.71}$$

In the second possible way of calculating $U_2^{(1)}$ (or $U_2^{(2)}$), one can rewrite the r_{12}^2 operator in terms of the vectors $\mathbf{r}_1-\mathbf{P}$ and $\mathbf{r}_2-\mathbf{Q}$.

$$\begin{aligned}
-U_2^{(1)} &= \langle e^{-\alpha(\mathbf{r}_1-\mathbf{A})^2} e^{-\beta(\mathbf{r}_2-\mathbf{B})^2} | \frac{r_{12}^2}{|\mathbf{r}_1-\mathbf{Z}|} | e^{-\gamma(\mathbf{r}_1-\mathbf{C})^2} e^{-\delta(\mathbf{r}_2-\mathbf{D})^2} \rangle \\
&= G_{\mathrm{AC}} G_{\mathrm{BD}} \int\!\!\int e^{-\zeta(\mathbf{r}_1-\mathbf{P})^2} \left[\frac{((\mathbf{r}_1-\mathbf{P})-(\mathbf{r}_2-\mathbf{Q})+(\mathbf{P}-\mathbf{Q}))^2}{|\mathbf{r}_1-\mathbf{Z}|} \right] e^{-\eta(\mathbf{r}_2-\mathbf{Q})^2} d\mathbf{r}_1 d\mathbf{r}_2 \\
&= G_{\mathrm{AC}} G_{\mathrm{BD}} \int\!\!\int e^{-\zeta(\mathbf{r}_1-\mathbf{P})^2} \left[\frac{1}{|\mathbf{r}_1-\mathbf{Z}|} \left((\mathbf{r}_1-\mathbf{P})^2 + 2(\mathbf{P}-\mathbf{Q})\cdot(\mathbf{r}_1-\mathbf{P}) + (\mathbf{r}_2-\mathbf{Q})^2 \right.\right. \\
&\left.\left. - 2(\mathbf{P}-\mathbf{Q})\cdot(\mathbf{r}_2-\mathbf{Q}) + (\mathbf{P}-\mathbf{Q})^2 - 2(\mathbf{r}_1-\mathbf{P})\cdot(\mathbf{r}_2-\mathbf{Q}) \right) \right] e^{-\eta(\mathbf{r}_2-\mathbf{Q})^2} d\mathbf{r}_1 d\mathbf{r}_2
\end{aligned} \tag{3.72}$$

Expanding r_{12}^2 in this form results in an expression for $U_2^{(1)}$ integral which is now a sum of six separable integrals

$$
\begin{aligned}
-U_2^{(1)} = & \left(-\frac{\partial}{\partial\zeta}\int\frac{e^{-\zeta(\mathbf{r}_1-\mathbf{P})^2}}{|\mathbf{r}_1-\mathbf{Z}|}d\mathbf{r}_1\right)\left(\int e^{-\eta(\mathbf{r}_2-\mathbf{Q})^2}d\mathbf{r}_2\right) \\
& +2\left((\mathbf{P}-\mathbf{Q})\cdot\frac{\nabla_\mathbf{P}}{2\zeta}\int\frac{e^{-\zeta(\mathbf{r}_1-\mathbf{P})^2}}{|\mathbf{r}_1-\mathbf{Z}|}d\mathbf{r}_1\right)\left(\int e^{-\eta(\mathbf{r}_2-\mathbf{Q})^2}d\mathbf{r}_2\right) \\
& +\left(\int\frac{e^{-\zeta(\mathbf{r}_1-\mathbf{P})^2}}{|\mathbf{r}_1-\mathbf{Z}|}d\mathbf{r}_1\right)\left(-\frac{\partial}{\partial\eta}\int e^{-\eta(\mathbf{r}_2-\mathbf{Q})^2}d\mathbf{r}_2\right) \\
& -2\left(\int\frac{e^{-\zeta(\mathbf{r}_1-\mathbf{P})^2}}{|\mathbf{r}_1-\mathbf{Z}|}d\mathbf{r}_1\right)\left((\mathbf{P}-\mathbf{Q})\cdot\frac{\nabla_\mathbf{Q}}{2\eta}\int e^{-\eta(\mathbf{r}_2-\mathbf{Q})^2}d\mathbf{r}_2\right) \\
& +\left((\mathbf{P}-\mathbf{Q})^2\int\frac{e^{-\zeta(\mathbf{r}_1-\mathbf{P})^2}}{|\mathbf{r}_1-\mathbf{Z}|}d\mathbf{r}_1\right)\left(\int e^{-\eta(\mathbf{r}_2-\mathbf{Q})^2}d\mathbf{r}_2\right) \\
& -2\left(\frac{\nabla_\mathbf{P}}{2\zeta}\int\frac{e^{-\zeta(\mathbf{r}_1-\mathbf{P})^2}}{|\mathbf{r}_1-\mathbf{Z}|}d\mathbf{r}_1\right)\cdot\left(\frac{\nabla_\mathbf{Q}}{2\eta}\int e^{-\eta(\mathbf{r}_2-\mathbf{Q})^2}d\mathbf{r}_2\right)
\end{aligned}
\tag{3.73}
$$

Calculation of integrals in each parentheses is straightforward

$$
\begin{aligned}
&\int\frac{e^{-\zeta(\mathbf{r}_1-\mathbf{P})^2}}{|\mathbf{r}_1-\mathbf{Z}|}d\mathbf{r}_1 = (\pi/\zeta)^{3/2}\frac{\mathrm{erf}(\sqrt{\zeta}|\mathbf{P}-\mathbf{Z}|)}{|\mathbf{P}-\mathbf{Z}|} && \int e^{-\eta(\mathbf{r}_2-\mathbf{Q})^2}d\mathbf{r}_2 = (\pi/\eta)^{3/2} \\
&\frac{\nabla_\mathbf{P}}{2\zeta}\int\frac{e^{-\zeta(\mathbf{r}_1-\mathbf{P})^2}}{|\mathbf{r}_1-\mathbf{Z}|}d\mathbf{r}_1 = \left[\frac{\pi e^{-\zeta|\mathbf{P}-\mathbf{Z}|^2}}{\zeta^2|\mathbf{P}-\mathbf{Z}|^2}-\frac{\pi^{3/2}\mathrm{erf}(\sqrt{\zeta}|\mathbf{P}-\mathbf{Z}|)}{2\zeta^{5/2}|\mathbf{P}-\mathbf{Z}|^3}\right](\mathbf{P}-\mathbf{Z}) && \frac{\nabla_\mathbf{Q}}{2\eta}\int e^{-\eta(\mathbf{r}_2-\mathbf{Q})^2}d\mathbf{r}_2 = \mathbf{0} \\
&-\frac{\partial}{\partial\zeta}\int\frac{e^{-\zeta(\mathbf{r}_1-\mathbf{P})^2}}{|\mathbf{r}_1-\mathbf{Z}|}d\mathbf{r}_1 = \left[\frac{3\pi^{3/2}\mathrm{erf}(\sqrt{\zeta}|\mathbf{P}-\mathbf{Z}|)}{2\zeta^{5/2}|\mathbf{P}-\mathbf{Z}|}-\frac{\pi e^{-\zeta|\mathbf{P}-\mathbf{Z}|^2}}{\zeta^2}\right] && -\frac{\partial}{\partial\eta}\int e^{-\eta(\mathbf{r}_2-\mathbf{Q})^2}d\mathbf{r}_2 = \frac{3\pi^{3/2}}{2\eta^{5/2}}
\end{aligned}
\tag{3.74}
$$

Using the above elementary integrals (Eqs. 3.74) and the relation between CHGFs and error functions (Eq. 3.61), one can simplify the Eq. 3.73 to reach at $U_2^{(1)}$ (same as Eq. 3.69).

So far, we have achieved closed-form expressions for U_0 and U_2 FB nuclear-attraction matrix elements. However, for the U_1 matrix element which is the most difficult integral, we have managed to reduce it to a one-dimensional integral. The $U_1^{(1)}$ matrix element over primitive Gaussian functions is defined as

$$
\begin{aligned}
-U_1^{(1)} &= \langle e^{-\alpha(\mathbf{r}_1-\mathbf{A})^2} e^{-\beta(\mathbf{r}_2-\mathbf{B})^2} | \frac{r_{12}^1}{|\mathbf{r}_1-\mathbf{Z}|} | e^{-\gamma(\mathbf{r}_1-\mathbf{C})^2} e^{-\delta(\mathbf{r}_2-\mathbf{D})^2} \rangle \\
&= G_{\mathrm{AC}} G_{\mathrm{BD}} \int\int \frac{e^{-\zeta(\mathbf{r}_1-\mathbf{P})^2}}{|\mathbf{r}_1-\mathbf{Z}|} \left[r_{12}^1\right] e^{-\eta(\mathbf{r}_2-\mathbf{Q})^2} d\mathbf{r}_1 d\mathbf{r}_2 \\
&= G_{\mathrm{AC}} G_{\mathrm{BD}} \int\int \frac{e^{-\zeta(\mathbf{r}_1-\mathbf{P})^2}}{|\mathbf{r}_1-\mathbf{Z}|} \left[\int \left(-\frac{\Gamma(3)}{2\pi^2 k^4}\right) e^{i\mathbf{k}\cdot(\mathbf{r}_1-\mathbf{r}_2)} d\mathbf{k}\right] e^{-\eta(\mathbf{r}_2-\mathbf{Q})^2} d\mathbf{r}_1 d\mathbf{r}_2 \\
&= G_{\mathrm{AC}} G_{\mathrm{BD}} \int \left[-\frac{\Gamma(3)}{2\pi^2 k^4}\right] \left[\int \frac{e^{-\zeta(\mathbf{r}_1-\mathbf{P})^2}}{|\mathbf{r}_1-\mathbf{Z}|} e^{i\mathbf{k}\cdot\mathbf{r}_1} d\mathbf{r}_1\right] \left[\int e^{-\eta(\mathbf{r}_2-\mathbf{Q})^2} e^{-i\mathbf{k}\cdot\mathbf{r}_2} d\mathbf{r}_2\right] d\mathbf{k} \\
&= G_{\mathrm{AC}} G_{\mathrm{BD}} (2\pi/\zeta)(\pi/\eta)^{3/2} \int \left[-\frac{\Gamma(3)}{2\pi^2 k^4}\right] M\left(\frac{1}{2}, \frac{3}{2}, -\zeta\left(\mathbf{P}-\mathbf{Z}+\frac{ik}{2\zeta}\right)^2\right) \\
&\times e^{i\mathbf{k}\cdot(\mathbf{P}-\mathbf{Q}) - \left(k^2/4\zeta\right) - \left(k^2/4\eta\right)} d\mathbf{k}
\end{aligned}
\tag{3.75}
$$

We now use Eq. 3.61 and substitute the CHGF by its corresponding integral representation

$$
M\left(\frac{1}{2}, \frac{3}{2}, -x^2\right) = \int_0^1 e^{-x^2 t^2} dt \tag{3.76}
$$

to get

$$
\begin{aligned}
-U_1^{(1)} &= G_{\mathrm{AC}} G_{\mathrm{BD}} (2\pi/\zeta)(\pi/\eta)^{3/2} \int \left[-\frac{\Gamma(3)}{2\pi^2 k^4}\right] \left[\int_0^1 \exp\left(-\zeta\left(\mathbf{P}-\mathbf{Z}+\frac{ik}{2\zeta}\right)^2 t^2\right) dt\right] \\
&\times e^{i\mathbf{k}\cdot(\mathbf{P}-\mathbf{Q}) - \left(k^2/4\zeta\right) - \left(k^2/4\eta\right)} d\mathbf{k} \\
&= G_{\mathrm{AC}} G_{\mathrm{BD}} (2\pi/\zeta)(\pi/\eta)^{3/2} \\
&\times \int_0^1 \left[\int \left(-\frac{\Gamma(3)}{2\pi^2 k^4}\right) \exp\left(-\left[\frac{1}{\eta}+\frac{1-t^2}{\zeta}\right]\frac{k^2}{4} + i\mathbf{k}\cdot\left[(\mathbf{P}-\mathbf{Q})-(\mathbf{P}-\mathbf{Z})t^2\right]\right) d\mathbf{k}\right] \\
&\times \exp(-\zeta(\mathbf{P}-\mathbf{Z})^2 t^2) dt
\end{aligned}
\tag{3.77}
$$

The last step of this derivation requires the following integral

$$
\int \left(-\frac{\Gamma(3)}{2\pi^2 k^4}\right) \exp(-\frac{k^2}{4}x + i\mathbf{k}\cdot\mathbf{R})\, d\mathbf{k} = (2/\sqrt{\pi})\, \Gamma\left(\frac{1+3}{2}\right) x^{1/2} M\left(-\frac{1}{2}, \frac{3}{2}, -\frac{R^2}{x}\right) \tag{3.78}
$$

to give us

$$
\begin{aligned}
-U_1^{(1)} &= G_{\mathrm{AC}}G_{\mathrm{BD}}\,(2\pi/\zeta)\,(\pi/\eta)^{3/2} \\
&\times \int_0^1 \left[\int \left(-\frac{\Gamma(3)}{2\pi^2 k^4}\right)\exp\left(-\left[\frac{1}{\eta}+\frac{1-t^2}{\zeta}\right]\frac{k^2}{4}+i\mathbf{k}\cdot\left[(\mathbf{P}-\mathbf{Q})-(\mathbf{P}-\mathbf{Z})t^2\right]\right)d\mathbf{k}\right] \\
&\times \exp(-\zeta(\mathbf{P}-\mathbf{Z})^2t^2)dt \\
&= G_{\mathrm{AC}}G_{\mathrm{BD}}\left(4\pi^{1/2}/\zeta\right)(\pi/\eta)^{3/2}\,\Gamma\left(\frac{1+3}{2}\right) \\
&\times \int_0^1 \left(\frac{1}{\eta}+\frac{1-t^2}{\zeta}\right)^{1/2} M\left(-\frac{1}{2},\frac{3}{2},-\frac{\left[(\mathbf{P}-\mathbf{Q})-(\mathbf{P}-\mathbf{Z})t^2\right]^2}{\frac{1}{\eta}+\frac{1-t^2}{\zeta}}\right)\exp(-\zeta(\mathbf{P}-\mathbf{Z})^2t^2)dt
\end{aligned}
\tag{3.79}
$$

This is the final form for $U_1^{(1)}$ matrix element which has been reduced to a one-dimensional integral which can be calculated using quadrature methods. Similarly, $U_1^{(2)}$ matrix element can be expressed as

$$
\begin{aligned}
-U_1^{(2)} &= G_{\mathrm{AC}}G_{\mathrm{BD}}\left(4\pi^{1/2}/\eta\right)(\pi/\zeta)^{3/2}\,\Gamma\left(\frac{1+3}{2}\right) \\
&\times \int_0^1 \left(\frac{1}{\zeta}+\frac{1-t^2}{\eta}\right)^{1/2} M\left(-\frac{1}{2},\frac{3}{2},-\frac{\left[(\mathbf{P}-\mathbf{Q})-(-\mathbf{Q}+\mathbf{Z})t^2\right]^2}{\frac{1}{\zeta}+\frac{1-t^2}{\eta}}\right)\exp(-\eta(\mathbf{Q}-\mathbf{Z})^2t^2)dt
\end{aligned}
\tag{3.80}
$$

Finally, the U_1 FB nuclear-attraction matrix element is

$$
U_1 = U_1^{(1)} + U_1^{(2)} \tag{3.81}
$$

To proceed with the calculation of U_1 matrix element, we need an accurate way of evaluation of the one-dimensional integral in the last line of Eq. 3.79, Eq. 3.80 and therefore, Eq. 3.81. In numerical analysis, one can approximate the definite integral of a function $f(x)$ through a quadrature rule which expresses that integral as a weighted sum of the function values $f(x_i)$ at specific points in the domain of integration. For a system of orthogonal polynomials $f_n(x)$ of degree n satisfying

$$
\begin{aligned}
\int_a^b f_m(x)f_n(x)W(x)dx &= h_n\delta_{mn} \\
h_n &= \int_a^b f_n^2(x)W(x)dx
\end{aligned}
\tag{3.82}
$$

where $W(x) \geq 0$ is a weight in the interval $[a,b]$, one can consider the fact that $f_n(x)$ has n distinct roots or zeros in the interval $[a,b]$

$$f_n(x_i) = 0 \qquad\qquad 1 \leq i \leq n \tag{3.83}$$

In Eqs. 3.82, if $h_n = 1$, then the polynomials are orthonormal. [81, 91] Based on the fundamental theorem of Gaussian quadrature, the optimal abscissas of the n-point quadrature formulas are precisely the roots of the orthogonal polynomial for the same interval and weighting function $W(x)$. [92] Therefore, one can design a suitable quadrature to have an accurate evaluation of an integral through selecting optimal abscissas x_i for which, we need to calculate $f(x_i)$. Hence, for a general polynomial $f_k(x)$ of degree k [4, 81]

$$f_k(x) = \sum_{i=1}^{k} c_i x^i \tag{3.84}$$

it can be shown that if $k < 2n$, then

$$\int_a^b f_k(x) W(x) dx = \sum_{i=1}^{n} w_i f_k(x_i) \tag{3.85}$$

in which,

$$w_i = \int_a^b W(x) \prod_{\substack{j=1 \\ j\neq i}}^{n} \frac{x - x_j}{x_i - x_j} dx \tag{3.86}$$

The abscissas x_i and weights w_i depend on the number of quadrature points n but are independent of the polynomial $f_k(x)$. [4] An n-point quadrature rule within the framework of Gaussian quadrature will be exact for the calculation of the integrals with the n-fold sum. [4] In order to calculate the (x_i, w_i) pairs, we used *Numerical Differential Equation Analysis* package in *Mathematica 10.4* program [53] to design various n-point quadratures where $n = 5, 10, 15, 20, 30, 40$ and 50. This experiment showed us that adopting a 50-point quadrature, the U_1 FB nuclear-attraction integrals can accurately be calculated for the whole range of bond lengths considered in this work. The table of the calculated abscissas and weights is provided in Appendix B.

3.4 Concluding Remarks

In this chapter, we have presented the main ideas of the CMO theory introduced by FB. [74] In addition to the comparison with other three approximate RHF, UHF and CI wavefunctions (Eqs. 3.1-3.3), for the first time, we have introduced UFB wavefunction (Eq. 3.5) as a new form of a compact explicitly correlated wavefunction. After a short introduction to each of these five RHF, UHF, CI, RFB and UFB ansätze, we embarked on constructing the required Hamiltonian and overlap matrix elements to be able to calculate the electronic energies through solving the Schrödinger equation. We have managed to have all matrix elements in closed form except that of the nuclear-attraction matrix element with linear r_{12} factor. This element has been reduced to a straightforward one-dimensional quadrature. In this way, we are be able to calculate PECs for all five approximate wavefunctions and analyze them separately and thoroughly in the short, intermediate and long internuclear distances. This will be one of the main goals in the next chapter.

CHAPTER 4

Investigation of the Frost-Braunstein Wavefunction for H_2: Application

In the present chapter, we embark on an in-depth investigation the five wavefunctions for H_2 molecule, namely restricted Hartree-Fock (RHF), unrestricted Hartree-Fock (UHF), configuration interaction (CI), restricted Frost-Braunstein (RFB), which is equivalent to the correlated molecular orbital (CMO) ansatz, and unrestricted Frost-Braunstein (UFB). We provide RHF, UHF, CI, RFB and UFB potential energy curves (PECs) for H_2 and analyze them for small, intermediate and large internuclear distances. We will also show that some spectroscopic parameters of the CMO (or RFB) PEC (such as R_e and D_e etc.) and the linear coefficient p in the CMO wavefunction at a specific bond length *reported by FB were inaccurate. Therefore, we provide a much wider range of bond lengths for our analysis and show that there is a pole in the linear coefficient. In exploring the properties of the UFB wavefunction, we have discovered that for a certain range of R values, there are multiple symmetry-broken (SB) solutions. The presence of these multiple solutions cause the UFB PEC to have a kink. We propose a simple model to demonstrate how these SB solutions evolve with increasing R. We indicate that there is a certain range of R for which these SB solutions are higher in energy than that of the symmetric and restricted solution. The discovery of multiple solutions in UFB PEC can have significant impacts on the explicitly correlated methods especially on R12 and F12 calculations performed within the unrestricted regime. The correlation energy curves of the CI and UFB approximations will be compared to that of the near-exact case provided by Rassolov* et al.. *[93] Finally, we perform a thorough asymptotic analysis for the five mentioned wavefunctions and show that the UFB wavefunction within the single-ζ basis shows R^{-8} "dispersion-like" behavior. This can be compared with the correct behavior of R^{-6} due to the dispersion interaction. The generalization of the FB (GFB) wavefunction using r_{12}^n where n is a positive integer, shows that variation of n does not change the R^{-8} behavior of the GFB energy but the coefficient of the R^{-8} term is affected. Therefore, no analytic correlation function of r_{12} can capture the dispersion in the minimal basis.*

4.1 Introduction

In this chapter, we use the results of our derivations of the Hamiltonian and overlap matrix elements presented in chapter 3 to calculate potential energy curves (PECs) for the restricted Hartree-Fock (RHF), unrestricted Hartree-Fock (UHF), configuration interaction (CI), restricted Frost-Braunstein (RFB) and unrestricted Frost-Braunstein (UFB) wavefunctions.

In order to extract the maximum accuracy from each of the wave functions (Eqs. 3.1 – 3.5) at any bond length R, one should fully optimize the exponent ζ, the linear correlation coefficient p, and the mixing parameter t and the amplitudes θ.

As we have seen in Chapter 3, some of the two-electron integrals in FB calculations are problematic, [74] so we have modeled the exponentials (Eq. 3.8) by their STO–nG expansions [94–97] of Gaussian-type orbitals (GTOs) and extrapolated these energies to the Slater-type orbital (STO) limit (*i.e.* $n = \infty$) using

$$E_n \approx E_\infty + a \exp(-\pi n^{\frac{5}{8}}) \tag{4.1}$$

Most of the required Gaussian integrals can be found in closed form [98] and the hardest ones (nuclear-attraction integrals with r_{12}) can be reduced to a straightforward one-dimensional quadrature (Sec. 3.3.1.3). [90] Based on recent convergence analyses, [99–101] we believe that our extrapolated STO–nG results are indistinguishable from those from exact STOs.

At large bond lengths R, the most difficult integrals become exponentially small and the behaviors of the RHF, UHF, CI, RFB and UFB energies can be investigated by asymptotic analysis in which only algebraic (and/or exponential) terms are retained.

Let $\lambda = (\zeta R)^{-1}$. The required Coulomb integrals become

$$\langle AA\,|\,r_{12}^n\,|AA\rangle = \frac{(n+2)!(n+4)(n+6)}{48(2\zeta)^n} \tag{4.2a}$$

$$\left\langle AA\left|\frac{r_{12}^n}{r_{1A}}\right|AA\right\rangle = \frac{(n+2)!(n+4)}{16(2\zeta)^{n-1}} \tag{4.2b}$$

$$\left\langle AA\left|\frac{r_{12}^n}{r_{1B}}\right|AA\right\rangle \sim \frac{(n+2)!(n+4)(n+6)}{48(2\zeta)^n R} \tag{4.2c}$$

$$\langle AB\,|\,r_{12}^n\,|AB\rangle \sim R^n{}_3F_0\left(-\frac{n}{2},-\frac{n+1}{2},4,\lambda^2\right) \tag{4.2d}$$

$$\left\langle AB\left|\frac{r_{12}^n}{r_{1A}}\right|AB\right\rangle \sim \zeta R^n{}_3F_0\left(-\frac{n}{2},-\frac{n+1}{2},3,\lambda^2\right) \tag{4.2e}$$

$$\left\langle AB\left|\frac{r_{12}}{r_{1B}}\right|AB\right\rangle \sim \big(2-(\lambda-2)e^{2R\zeta}\mathrm{Ei}(-2R\zeta)+(\lambda+2)e^{-2R\zeta}\mathrm{Ei}(2R\zeta)\big)/2 \tag{4.2f}$$

$$\left\langle AB\left|\frac{r_{12}^2}{r_{1B}}\right|AB\right\rangle \sim R(1+4\lambda^2) \tag{4.2g}$$

where ${}_3F_0$ is a generalized hypergeometric function and Ei is the exponential integral, [80] and the kinetic integrals are

$$\left\langle r_{12}^m AA\left|-\frac{\nabla^2}{2}\right|r_{12}^n AA\right\rangle = \zeta^2\frac{(q+4)!}{192(2\zeta)^q}\frac{6+5q-(m-n)^2}{(q+1)(q+3)} \tag{4.2h}$$

$$\begin{aligned}\left\langle r_{12}^m AB\left|-\frac{\nabla^2}{2}\right|r_{12}^n AB\right\rangle \sim \zeta^2 R^q\Big[&{}_3F_0\left(-\tfrac{q}{2},-\tfrac{q+1}{2},4,\lambda^2\right)\\ &-\frac{m(m+1)+n(n+1)}{2}\lambda^2{}_3F_0\left(-\tfrac{q-2}{2},-\tfrac{q-1}{2},4,\lambda^2\right)\Big]\end{aligned} \tag{4.2i}$$

where $q = m+n$. We will briefly discuss the asymptotic analysis of the five RHF, UHF, CI, RFB and UFB approximate wavefunctions in the section 4.3 but a more detailed discussion is presented in Sec. 4.5.

4.2 STO-nG Basis Sets

The STOs and GTOs have well-known strengths and weaknesses in describing the expansion of the wavefunction. In order to have the correct behavior of the wavefunction at small and large R, [79] one can model the exponentials (Eq. 3.8) by their STO–nG expansions. [94–97, 102] It is often required to calculate the electronic energies with large enough n values in the STO–nG expansion [97, 102]

$$\phi^S(\zeta;\mathbf{r}) \approx \phi^{CG}(\zeta;\mathbf{r}) = \sum_{\mu=1}^{n} c_\mu \phi^G(\alpha_\mu;\mathbf{r}) \tag{4.3}$$

to be able to extrapolate the calculated energies to the STO limit (*i.e.* $n \to \infty$). In Eq. 4.3, the superscript CG stands for contracted Gaussian function. The STOs, $\phi^S(\zeta;\mathbf{r})$, and GTOs, $\phi^G(\alpha_\mu;\mathbf{r})$, are defined in Eqs. 3.8 and 3.31, respectively. Here, the Slater orbital and Gaussian orbital exponent dependencies are explicitly shown for clarity and completeness. The Eq. 4.3 is exact in the $n \to \infty$ limit. Although the list of necessary coefficients c_μ and exponents α_μ for constructing the STO–nG basis sets can be found in literature, [94–96] the accuracy of these parameters were not enough for our goals. Therefore, devising a suitable method for calculating the coefficients and parameters of the STO–nG expansions to arbitrary precision seemed crucial.

Construction of the STO–nG expansions where $n = 1$, 2 or 3 is easy and fairly straightforward. For example, it is possible to find the coefficients c_μ and exponents α_μ of the STO–nG expansion in a way that they minimize the fitting criterion

$$\begin{aligned} I &= \int [\phi^S(\zeta = 1;\mathbf{r}) - \phi^{CG}(\zeta = 1;\mathbf{r})]^2 d\mathbf{r} \\ &= \int [\phi^S(\zeta = 1;\mathbf{r}) - \sum_{\mu=1}^{n} c_\mu \phi^G(\alpha_\mu;\mathbf{r})]^2 d\mathbf{r} \end{aligned} \tag{4.4}$$

which provides the best fit for the expansion of the STO in terms of GTOs in the least-square (LSQ) sense. [17, 94] In Eq. 4.4, the integration should be performed over all space. Assuming positive exponents, minimization of I can be performed numerically in *Mathematica* [53] with arbitrary precision.

In order to accurately describe the single-ζ basis function and also, to be able to use the extrapolation methods, one needs CG functions composed of larger number of Gaussian functions. However, as one increases n in the STO-nG expansion, the number of linear and nonlinear parameters are also increases. Therefore, minimization of the LSQ integral I becomes more and more difficult because of the high-nonlinearity of the problem and extra dimensions: the basis functions become linearly dependent and the energy becomes a very flat function of the exponents. [79]

To overcome this obstacle we have proposed a method to calculate the optimized coefficients c_μ and exponents α_μ for constructing the STO–nG basis sets with an arbitrary precision. We exemplify this method by constructing the STO-3G basis from STO-2G parameters because the analytic expressions for the integral I can be easily obtained and thus, the accuracy of our method can be checked conveniently.

The analyses of the variationally optimized basis sets show that the ratio of the two successive exponents in such basis sets are approximately constant. [79, 103, 104] Taking this ratio to be a constant reduces the optimization problem to only two parameters regardless of the size of the basis set. Such basis sets are called *even-temperered* basis sets. In even-tempered basis sets, the μth exponent can be given by

$$\zeta_\mu = \alpha\beta^\mu \tag{4.5}$$

$$\ln(\zeta_\mu) = \ln(\alpha) + \mu\ \ln(\beta) \tag{4.6}$$

where $\mu \in \{1,2,3,\ldots,n\}$ and n is the maximum number of Gaussian functions in the STO–nG expansion (Eq. 4.3). The STO–3G basis set can be constructed from STO–2G parameters as follows:

i. Taking the natural logarithm of the STO-2G exponents and fitting them using Eq. 4.6, one can find the even-tempered parameters $\alpha_{\text{STO-3G}}$ and $\beta_{\text{STO-3G}}$ from the intercept and slope of the resulting line, respectively.

ii. A geometric series of three exponents for the STO-3G basis set can be constructed by using Eq. 4.5.

iii. The resulting exponents from the previous step can be inserted into Eq. 4.4 to fit a CG function composed of three Gaussian functions to a STO with the exponent $\zeta = 1$. This results in an expression in terms of three coefficients c_1, c_2 and c_3 as unknowns.

iv. The best coefficients should minimize LSQ integral I. This means that all coefficients satisfy

$$\frac{\partial I}{\partial c_\mu} = 0, \qquad \mu \in \{1,2,3,\ldots,n\} \tag{4.7}$$

This condition leads to a system of n simultaneous equations in n unknowns.

v. The coefficients and exponents that have been obtained in previous steps are now used as initial guesses for minimizing the LSQ integral I defined in Eq. 4.4. The "findminimum" function of the *Mathematica 10.4* program package provides a mean for local optimization of the parameters using initial guesses. This minimization process can be performed with arbitrary precision. [53]

It is important to note that, as mentioned by Hehre *et al.*, [94], the optimized coefficients and exponents resulting from minimizing the LSQ integral I appear to produce basis sets which are not fully normalized. Therefore, the resulting coefficients should be multiplied by appropriate normalization factors. [94] The optimized coefficients c_μ and exponents α_μ for the normalized STO–nG expansion where $n = 8$ and 9 are provided in Appendix D.

4.3 The Electronic Energy

In this section, we discuss the general properties of the calculated electronic energies and the trends in optimized variables in each wavefunction shown in Table 4.1 and the specific characteristics of the RHF, UHF, CI, RFB and UFB PECs for H_2 at short, intermediate and long internuclear distances.

4.3.1 Restricted Hartree-Fock

The RHF electronic energy expression for H_2 is [17]

$$E = 2\langle\psi_1|h|\psi_1\rangle + \langle\psi_1\psi_1|\psi_1\psi_1\rangle \tag{4.8}$$

and Sugiura showed [82] that this can be evaluated in terms of the exponential integral function. [80] The required integral expressions have been given in the Appendix A. Minimizing this energy with respect to ζ, for various bond lengths R, yields the E_{RHF} and ζ_{RHF} in Table 4.1.

Kellner showed [58] that for H_2 molecule at $R = 0$, the optimal energy and exponent are $E_{\text{RHF}} = -(27/16)^2$ and $\zeta_{\text{RHF}} = 27/16$, respectively.

As R increases, the energy E_{RHF} increases monotonically, but the exponent ζ_{RHF} decreases to a minimum (0.8402) at $R \approx 8.4$ and then increases slightly as the bond lengthens further.

Table 4.1 Single-zeta electronic energies E, exponents ζ, mixing parameters t, and linear coefficients p for H_2 at bond length R. The boldface numbers correspond to the lowest energy UFB solution.

	Hartree-Fock					Configuration Interaction			Frost-Braunstein							
R	$-E_{\mathrm{RHF}}$	$-E_{\mathrm{UHF}}$	ζ_{RHF}	ζ_{UHF}	t_{UHF}	$-E_{\mathrm{CI}}$	ζ_{CI}	θ_{CI}	$-E_{\mathrm{RFB}}$	$-E_{\mathrm{SB}}$	ζ_{RFB}	ζ_{SB}	p_{RFB}	p_{SB}	t_{RFB}	t_{SB}
0.00	2.84766		1.6875		0	2.84766	1.6875	0	**2.89112**		**1.8497**		**0.3658**		**0**	
0.50	2.48078		1.4930		0	2.48883	1.4949	0.0526	**2.51779**		**1.6486**		**0.3477**		**0**	
0.60	2.39122		1.4494		0	2.40029	1.4519	0.0602	**2.42680**		**1.6013**		**0.3413**		**0**	
0.70	2.30596		1.4084		0	2.31610	1.4115	0.0684	**2.34014**		**1.5559**		**0.3342**		**0**	
0.80	2.22560		1.3700		0	2.23687	1.3739	0.0772	**2.25846**		**1.5128**		**0.3268**		**0**	
0.90	2.15029		1.3342		0	2.16276	1.3390	0.0866	**2.18195**		**1.4722**		**0.3197**		**0**	
1.00	2.07993		1.3009		0	2.09366	1.3067	0.0966	**2.11052**		**1.4342**		**0.3131**		**0**	
1.10	2.01427		1.2699		0	2.02934	1.2769	0.1072	**2.04393**		**1.3989**		**0.3074**		**0**	
1.20	1.95301		1.2411		0	1.96951	1.2493	0.1185	**1.98191**		**1.3661**		**0.3026**		**0**	
1.30	1.89585		1.2144		0	1.91385	1.2239	0.1305	**1.92413**		**1.3358**		**0.2989**		**0**	
1.32	1.88488		1.2093		0	1.90319	1.2191	0.1330	**1.91306**		**1.3300**		**0.2983**		**0**	
1.34	1.87406		1.2042		0	1.89269	1.2143	0.1355	**1.90214**		**1.3244**		**0.2977**		**0**	
1.36	1.86339		1.1992		0	1.88233	1.2097	0.1380	**1.89137**		**1.3188**		**0.2972**		**0**	
1.37	1.85811		1.1968		0	1.87721	1.2073	0.1393	**1.88605**		**1.3160**		**0.2970**		**0**	
1.38	1.85286		1.1943		0	1.87212	1.2051	0.1406	**1.88076**		**1.3132**		**0.2967**		**0**	
1.39	1.84765		1.1919		0	1.86708	1.2028	0.1419	**1.87551**		**1.3105**		**0.2965**		**0**	
1.40	1.84247		1.1895		0	1.86206	1.2005	0.1432	**1.87029**		**1.3078**		**0.2963**		**0**	
1.42	1.83223		1.1847		0	1.85214	1.1961	0.1458	**1.85997**		**1.3025**		**0.2960**		**0**	
1.44	1.82211		1.1800		0	1.84237	1.1917	0.1485	**1.84978**		**1.2973**		**0.2956**		**0**	
1.46	1.81214		1.1754		0	1.83273	1.1874	0.1512	**1.83974**		**1.2921**		**0.2954**		**0**	
1.48	1.80229		1.1709		0	1.82322	1.1832	0.1539	**1.82984**		**1.2870**		**0.2951**		**0**	
1.50	1.79258		1.1664		0	1.81386	1.1790	0.1567	**1.82008**		**1.2820**		**0.2950**		**0**	
1.60	1.74589		1.1448		0	1.76896	1.1592	0.1709	**1.77321**		**1.2583**		**0.2948**		**0**	
1.70	1.70214		1.1247		0	1.72711	1.1411	0.1859	**1.72942**		**1.2365**		**0.2958**		**0**	
1.80	1.66110		1.1060		0	1.68809	1.1245	0.2017	**1.68847**		**1.2164**		**0.2981**		**0**	
1.90	1.62256		1.0886		0	1.65169	1.1093	0.2184	**1.65015**		**1.1981**		**0.3016**		**0**	
2.00	1.58631		1.0723		0	1.61771	1.0954	0.2359	**1.61424**		**1.1812**		**0.3065**		**0**	
2.10	1.55218		1.0571		0	1.58598	1.0828	0.2542	**1.58058**		**1.1659**		**0.3126**		**0**	
2.20	1.52001		1.0429		0	1.55636	1.0714	0.2734	**1.54900**		**1.1518**		**0.3201**		**0**	
2.27	1.49857		1.0336		0	1.53680	1.0641	0.2873	**1.52804**		**1.1427**		**0.3263**		**0**	
2.28	1.49558	1.49559	1.0323	1.0327	0.0755	1.53408	1.0631	0.2893	**1.52512**		**1.1415**		**0.3272**		**0**	
2.30	1.48965	1.48973	1.0297	1.0311	0.1350	1.52869	1.0612	0.2934	**1.51934**		**1.1390**		**0.3291**		**0**	
2.40	1.46097	1.46249	1.0173	1.0242	0.2807	1.50286	1.0519	0.3142	**1.49148**		**1.1274**		**0.3397**		**0**	
2.50	1.43384	1.43827	1.0057	1.0187	0.3688	1.47873	1.0437	0.3358	**1.46530**		**1.1169**		**0.3519**		**0**	
2.80	1.36077	1.37956	0.9751	1.0080	0.5380	1.41560	1.0242	0.4045	**1.39579**		**1.0912**		**0.4000**		**0**	
3.00	1.31807	1.34907	0.9578	1.0042	0.6147	1.38029	1.0151	0.4527	**1.35609**		**1.0785**		**0.4437**		**0**	
3.04	1.31004	1.34361	0.9546	1.0036	0.6280	1.37380	1.0136	0.4625	**1.34872**		**1.0763**		**0.4538**		**0**	
3.05	1.30805	1.34228	0.9538	1.0035	0.6312	1.37221	1.0132	0.4650	**1.34690**	1.34435	**1.0758**	1.0323	**+0.4564**	0.1108	**0**	0.5018
3.10	1.29829	1.33577	0.9499	1.0029	0.6468	1.36442	1.0115	0.4773	**1.33800**	1.33731	**1.0732**	1.0232	**+0.4699**	0.0710	**0**	0.5725
3.11	1.29637	1.33451	0.9492	1.0027	0.6498	1.36289	1.0111	0.4798	**1.33623**	1.33597	**1.0727**	1.0222	**+0.4726**	0.0672	**0**	0.5806
3.12	1.29445	1.33325	0.9484	1.0026	0.6528	1.36138	1.0108	0.4822	1.33452	**1.33464**	1.0723	**1.0212**	+0.4755	**0.0640**	0	**0.5880**
3.20	1.27948	1.32356	0.9426	1.0019	0.6756	1.34964	1.0084	0.5020	1.32101	**1.32452**	1.0687	**1.0158**	+0.4994	**0.0465**	0	**0.6335**
3.30	1.26157	1.31231	0.9357	1.0011	0.7016	1.33589	1.0059	0.5266	1.30506	**1.31294**	1.0647	**1.0115**	+0.5328	**0.0344**	0	**0.6741**
3.40	1.24451	1.30190	0.9292	1.0005	0.7252	1.32309	1.0038	0.5510	1.29009	**1.30233**	1.0614	**1.0085**	+0.5705	**0.0268**	0	**0.7060**
3.50	1.22824	1.29224	0.9231	1.0001	0.7468	1.31117	1.0022	0.5752	1.27604	**1.29255**	1.0585	**1.0065**	+0.6132	**0.0215**	0	**0.7328**
4.00	1.15739	1.25271	0.8978	0.9993	0.8300	1.26278	0.9981	0.6874	1.21817	**1.25278**	1.0504	**1.0018**	+0.9347	**0.0094**	0	**0.8261**
5.00	1.05497	1.20046	0.8660	0.9996	0.9221	1.20278	0.9984	0.8466	1.14843	**1.20047**	1.0478	**1.0003**	+3.7010	**0.0034**	0	**0.9214**
6.00	0.98690	1.16674	0.8498	0.9999	0.9643	1.16721	0.9995	0.9289	1.11423	**1.16675**	1.0456	**1.0002**	−5.2869	**0.0016**	0	**0.9642**
7.00	0.94012	1.14287	0.8426	1.0000	0.9839	1.14296	0.9999	0.9678	1.09630	**1.14287**	1.0410	**1.0001**	−2.1375	**0.0009**	0	**0.9838**
8.00	0.90691	1.12500	0.8404	1.0000	0.9928	1.12502	1.0000	0.9856	1.08556	**1.12500**	1.0356	**1.0001**	−1.5304	**0.0005**	0	**0.9928**
9.00	0.88250	1.11111	0.8404	1.0000	0.9968	1.11111	1.0000	0.9937	1.07817	**1.11111**	1.0304	**1.0000**	−1.2711	**0.0003**	0	**0.9968**
10.00	0.86392	1.10000	0.8412	1.0000	0.9986	1.10000	1.0000	0.9973	1.07248	**1.10000**	1.0258	**1.0000**	−1.1265	**0.0002**	0	**0.9986**
15.00	0.81197	1.06667	0.8436	1.0000	1.0000	1.06667	1.0000	1.0000	1.05401	**1.06667**	1.0122	**1.0000**	−0.8572	**0.0000**	0	**1.0000**
∞	0.71191	1	0.84375	1	1	1	1	1	1	**1**	1	**1**	−0.625	**0**	0	**1**

At large R, the Eq. 4.8 becomes asymptotic to

$$E \sim \zeta^2 - \frac{27}{16}\zeta - \frac{3}{2R} + \dots \tag{4.9}$$

and minimization of this yields

$$\zeta_{\text{RHF}}(R) \sim \frac{27}{32} - \frac{5 \cdot 3^8}{2^{20}} R^3 \exp\left(-\tfrac{27}{32}R\right) + \dots \tag{4.10}$$

$$E_{\text{RHF}}(R) \sim -\left(\frac{27}{32}\right)^2 - \frac{3}{2R} - \frac{5 \cdot 3^8}{2^{19}} R^2 \exp\left(-\tfrac{27}{32}R\right) + \dots \tag{4.11}$$

Thus, the total energy (including nuclear repulsion)

$$E_{\text{RHF}}^{\text{tot}}(R) \sim -\left(\frac{27}{32}\right)^2 - \frac{1}{2R} - \frac{5 \cdot 3^8}{2^{19}} R^2 \exp\left(-\tfrac{27}{32}R\right) + \dots \tag{4.12}$$

is wrong at $R \to \infty$ limit and the way that it is approached is also incorrect. This is because, in this limit, the RHF description of the molecule is a superposition of atoms and ions. [105]

4.3.2 Unrestricted Hartree-Fock

The UHF electronic energy expression is [17]

$$E = \langle \psi_\alpha | h | \psi_\alpha \rangle + \langle \psi_\beta | h | \psi_\beta \rangle + \langle \psi_\alpha \psi_\beta | \psi_\alpha \psi_\beta \rangle \tag{4.13}$$

and this requires exactly the same one- and two-electron integrals as the RHF energy (Eq. 4.8) presented in Appendix A. Minimizing E_{UHF} with respect to both the exponent ζ and the mixing parameter t at various bond lengths R yields the E_{UHF}, ζ_{UHF} and t_{UHF} values in Table 4.1.

As for RHF at $R = 0$, the optimal energy and exponent are the Kellner values $E_{\text{UHF}} = -(27/16)^2$ and $\zeta_{\text{UHF}} = 27/16$.

As R increases, the energy E_{UHF} increases monotonically, but the exponent ζ_{UHF} decreases to a minimum (0.9993) at $R \approx 4.1$ and then increases at longer bond lengths. The mixing parameter t_{UHF} is zero until the symmetry-breaking point $R \approx 2.28$ and then rises monotonically to unity as R grows.

At large R, the expression (Eq. 4.13) becomes

$$E \sim \zeta^2 - 2\zeta - \frac{1}{R} + \dots \tag{4.14}$$

and minimization of this yields

$$\zeta_{\mathrm{UHF}}(R) \sim 1 - \frac{1}{6}R^3 \exp(-2R) + \dots \tag{4.15}$$

$$t_{\mathrm{UHF}}(R) \sim 1 - \frac{2}{3\pi}R^2 \exp(-R) + \dots \tag{4.16}$$

$$E_{\mathrm{UHF}}(R) \sim -1 - \frac{1}{R} - \frac{1}{6}R^2 \exp(-2R) + \dots \tag{4.17}$$

Thus, the total energy (including nuclear repulsion)

$$E_{\mathrm{UHF}}^{\mathrm{tot}}(R) \sim -1 - \frac{1}{6}R^2 \exp(-2R) + \dots \tag{4.18}$$

is correct at $R \to \infty$ limit but the way that it is approached is incorrect. This is because, in this limit, the UHF description of the molecule is a superposition of singlet- and triplet-coupled atoms without any dispersion interaction.

4.3.3 Configuration Interaction

Since at $R = 0$ the doubly-excited determinant has an infinite energy, the mixing parameter is $\theta_{\mathrm{CI}} = 0$ and the optimal energy and exponent are the RHF values $E_{\mathrm{CI}} = -(27/16)^2$ and $\zeta_{\mathrm{CI}} = 27/16$.

As R increases, the energy E_{CI} increases monotonically but the exponent ζ_{CI} decreases to a minimum (0.9976) at R ≈ 4.3 and then increases at longer bond lengths. The mixing parameter θ_{CI} grows monotonically from zero toward its limit.

At large R, the Hamiltonian matrix is asymptotically

$$H_{\text{CI}} \sim \begin{bmatrix} \zeta^2 - \frac{27}{16}\zeta - \frac{3}{2R} + \dots & \frac{5}{16}\zeta - \frac{1}{2R} + \dots \\ \frac{5}{16}\zeta - \frac{1}{2R} + \dots & \zeta^2 - \frac{27}{16}\zeta - \frac{3}{2R} + \dots \end{bmatrix} \tag{4.19}$$

and minimization of its lowest eigenvalue yields

$$\zeta_{\text{CI}}(R) \sim 1 + \frac{1}{45}\left[6(\gamma + \ln R) - 23\right] R^4 \exp(-2R) \tag{4.20}$$

$$\theta_{\text{CI}}(R) \sim 1 - \frac{4}{3\pi} R^2 \exp(-R) \tag{4.21}$$

$$E_{\text{CI}}(R) \sim -1 - \frac{1}{R} + \frac{1}{45}\left[6(\gamma + \ln R) - 28\right] R^3 \exp(-2R) \tag{4.22}$$

where $\gamma = 0.577215664901\dots$, is the Euler-Mascheroni constant. [106] Thus, the total energy (including nuclear repulsion)

$$E_{\text{CI}}^{\text{tot}}(R) \sim -1 + \frac{1}{45}\left[6(\gamma + \ln R) - 28\right] R^3 \exp(-2R) \tag{4.23}$$

is correct at $R \to \infty$ limit but the way that it is approached is incorrect. Because of the restricted nature of the orbitals in the present CI wavefunction, there is a root around $R \approx 51.3$ for $E_{\text{CI}}^{\text{tot}}$ and around $R \approx 17.3$ for the ζ_{CI}. This means that the CI energy curve within the single-ζ basis has a hump– with a maximum of a very small value of 1.9×10^{-43} above the limit– around $R \approx 51.8$ and goes to its limit, -1, from above. A similar maximum exists in ζ_{RCI} expansion with the value of 1.0×10^{-13} which occurs around $R \approx 17.8$. We have verified that the use of unrestricted CI can cure this small hump but we do not analyze this wavefunction here. Similar behaviors have been observed for RFB as we show in the next subsection. It should be noted that although CI correctly dissociates the molecule into singlet-coupled atoms and recovers some static correlation at moderate bond lengths, it completely lacks any dispersion interaction in this basis.

4.3.4 Restricted Frost-Braunstein

The RFB results shown in Table 4.1 are more accurate and complete than those previously reported by FB [74] which enable us to analyze and understand the behavior of the RFB wavefunction more thoroughly.

Hylleraas showed [28] that for H_2 molecule at $R = 0$, the optimal energy, exponent and linear coefficient are $E_{\mathrm{RFB}} = -2.89112$, $\zeta_{\mathrm{RFB}} = 1.8497$ and $p_{\mathrm{RFB}} = 0.3658$, respectively.

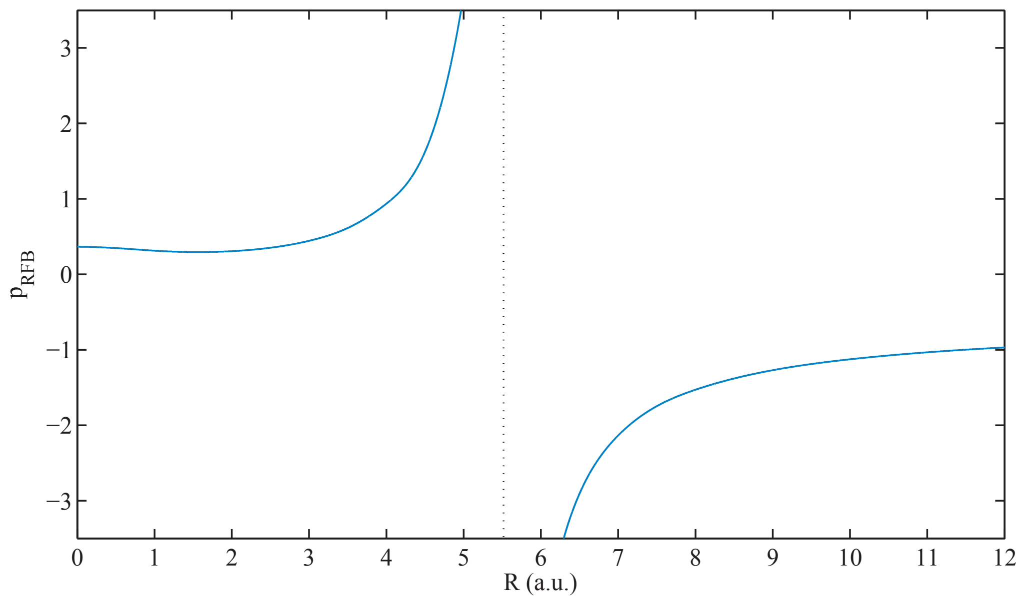

Fig. 4.1 Variation of p_{RFB} with the bond length R.

As R increases, the exponent ζ_{RFB} decreases monotonically but slowly toward unity. The linear coefficient p_{RFB} (see Fig. 4.1) is remarkably constant, and somewhat lower than the Kato cusp [26] value (1/2) until $R \approx 3$, but then increases rapidly and has a pole at $R \approx 5.5$, where p_{RFB} changes sign, just as it does for two electrons on a sphere of increasing radius. [107] The pole occurs when the relative weight of Ψ_{RHF} goes to zero and the RFB wavefunction simply becomes proportional to $r_{12}\Psi_{\text{RHF}}$.

Beyond the pole, the coefficient p_{RFB} is negative and slowly approaches its asymptotic value of $-5/8$. Our analysis of p_{RFB} can be compared with that reported by FB, [74] however, they plotted p_{RFB} only for $R < 5.5$ and, consequently, did not comment on the presence of the pole and sign change of p_{RFB} for longer bond lengths.

The r_{12} factor amplifies the covalent part of the RHF wavefunction but not the ionic part. [74] However, whereas this amplification should grow exponentially [108] with R, it grows only linearly in the RFB wavefunction. Because the ionic contaminant is not removed quickly enough as R grows, the energy E_{RFB} increases monotonically but approaches its limit too slowly.

At large R, the overlap, kinetic, nuclear-attraction and electron-repulsion matrices are asymptotic to

$$S_{\text{RFB}} \sim \begin{bmatrix} 1 & R\left(\frac{1}{2}+\frac{35}{32}\lambda+\lambda^2\right) \\ R\left(\frac{1}{2}+\frac{35}{32}\lambda+\lambda^2\right) & R^2\left(\frac{1}{2}+6\lambda^2\right) \end{bmatrix} \tag{4.24}$$

$$T_{\text{RFB}} \sim \zeta^2 \begin{bmatrix} 1 & R\left(\frac{1}{2}+\frac{25}{32}\lambda+\frac{1}{2}\lambda^2\right) \\ R\left(\frac{1}{2}+\frac{25}{32}\lambda+\frac{1}{2}\lambda^2\right) & R^2\left(\frac{1}{2}+4\lambda^2\right) \end{bmatrix} \tag{4.25}$$

$$U_{\text{RFB}} \sim -\zeta \begin{bmatrix} 2+2\lambda & R\left(1+\frac{23}{8}\lambda+\frac{59}{16}\lambda^2+\lambda^3+\lambda^5+\ldots\right) \\ R\left(1+\frac{23}{8}\lambda+\frac{59}{16}\lambda^2+\lambda^3+\lambda^5+\ldots\right) & R^2\left(1+\lambda+9\lambda^2+10\lambda^3\right) \end{bmatrix} \tag{4.26}$$

$$V_{\text{RFB}} \sim \zeta \begin{bmatrix} \frac{5}{16}+\frac{1}{2}\lambda & R\lambda \\ R\lambda & R^2\left(\frac{1}{2}\lambda+\frac{35}{32}\lambda^2+\lambda^3\right) \end{bmatrix} \tag{4.27}$$

Minimization of the energy yields

$$\zeta_{\mathrm{RFB}}(R) \sim 1 + \frac{367}{160R^2} + \dots \tag{4.28}$$

$$p_{\mathrm{RFB}}(R) \sim -\frac{5}{8} - \frac{127}{64R} + \dots \tag{4.29}$$

$$E_{\mathrm{RFB}}(R) \sim -1 - \frac{1}{R} + \frac{207}{80R^2} + \dots \tag{4.30}$$

Thus, the total energy (including nuclear repulsion)

$$E^{\mathrm{tot}}_{\mathrm{RFB}}(R) \sim -1 + \frac{207}{80R^2} + \dots \tag{4.31}$$

is correct at $R \to \infty$ limit but approaches its limit slowly from above. [74] This is the most serious deficiency of the RFB wave function and arises because, although it correctly dissociates the molecule into singlet-coupled atoms, the ionic contaminant of the RHF wave function is removed far too slowly as the bond is lengthened.

4.3.5 Unrestricted Frost-Braunstein

To our knowledge, this is the first report on the UFB wavefunction for H_2, the analysis of which reveals some new features that have wider implications for explicitly correlated calculations. We searched for stationary points of the UFB energy expression which correspond to either symmetric, $t = 0$, or symmetry-broken (SB), $t \neq 0$, solutions and showed the results in Table 4.1. We define the UFB energy to be the lowest energy solution at each R. The UFB results are shown in bold in Table 4.1.

At $R = 0$, as for RFB, the optimal energy, exponent and linear coefficient are $E_{\mathrm{UFB}} = -2.89112$, $\zeta_{\mathrm{UFB}} = 1.8497$ and $p_{\mathrm{UFB}} = 0.3658$. The E_{UFB} values in Table 4.1 increase monotonically towards their limiting value of 1 as the bond length increases. A SB solution appears around $R \approx 3.05$, however, between $R \approx 3.05$ and $R \approx 3.11$, we observe that this

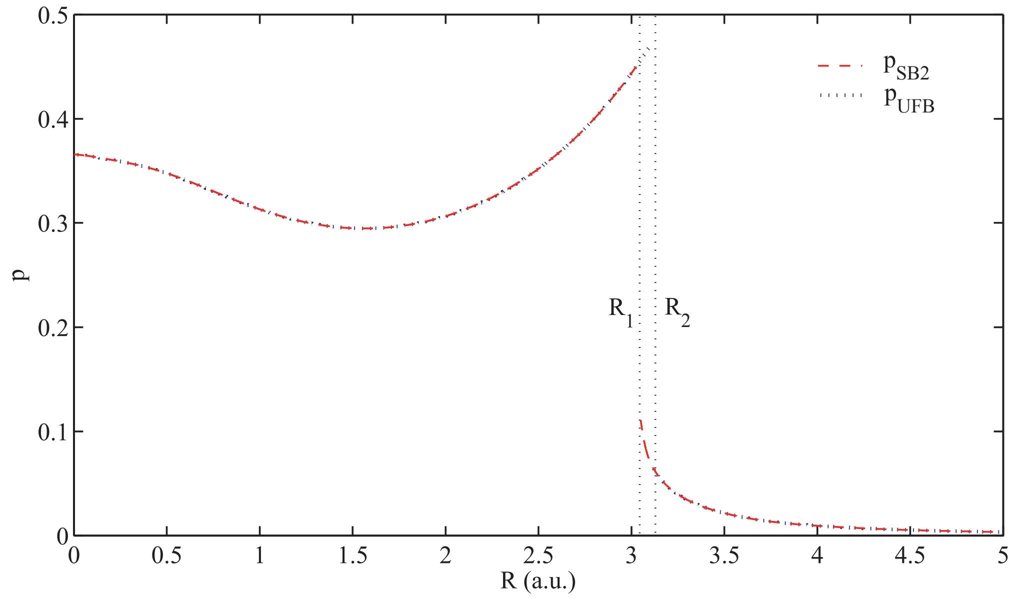

Fig. 4.2 Variation of p_{UFB} and p_{SB2} with the bond length R.

solution is higher than E_{RFB}. This is in contrast to the more familiar HF picture where the SB solution always lies below E_{RHF}.

Up until $R \approx 3.05$, $t_{UFB} = t_{RFB} = 0$ and only the restricted solution exists. At this bond length, a SB solution appears with $t = 0.5018$. Between $3.05 < R < 3.12$ this solution is higher in energy than E_{RFB}, but beyond $R = 3.12$ it drops below E_{RFB} and permits E_{UFB} to split away from the restricted solution. At this bifurcation point, t_{UFB} jumps discontinuously from 0 to 0.5880.

A similar discontinuity exists for the linear coefficient p. The boldface path in Table 4.1 shows that p_{UFB} behaves like p_{RFB} as the bond lengthens until $R = 3.12$ where it shows an abrupt change from $p_{UFB} \approx 0.47$ to 0.0640 (Fig. 4.2). Although, the exponent ζ_{UFB} is monotonically decreasing toward unity, it shows similar jump going from 1.0727 at $R = 3.11$ to 1.0212 at $R = 3.12$. At large R, the overlap, kinetic, nuclear-attraction and electron-repulsion matrices are asymptotic to

$$S_{\text{UFB}} \sim \begin{bmatrix} 1 & R\left(1+2\lambda^2\right) \\ R\left(1+2\lambda^2\right) & R^2\left(1+6\lambda^2\right) \end{bmatrix} \tag{4.32}$$

$$T_{\text{UFB}} \sim \zeta^2 \begin{bmatrix} 1 & R\left(1+\lambda^2\right) \\ R\left(1+\lambda^2\right) & R^2\left(1+4\lambda^2\right) \end{bmatrix} \tag{4.33}$$

$$U_{\text{UFB}} \sim -\zeta \begin{bmatrix} 2+2\lambda & R\left(2+2\lambda+3\lambda^2+2\lambda^3+2\lambda^5+\ldots\right) \\ R(2+2\lambda+3\lambda^2+2\lambda^3+2\lambda^5+\ldots) & R^2\left(2+2\lambda+9\lambda^2+8\lambda^3\right) \end{bmatrix} \tag{4.34}$$

$$V_{\text{UFB}} \sim \zeta \begin{bmatrix} \lambda & R\lambda \\ R\lambda & R^2\left(\lambda+2\lambda^3\right) \end{bmatrix} \tag{4.35}$$

and minimization of the resulting energy yields

$$\zeta_{\text{UFB}}(R) \sim 1+\frac{2}{R^5}+\ldots \tag{4.36}$$

$$t_{\text{UFB}}(R) \sim 1-O[R^2\exp(-R)] \tag{4.37}$$

$$p_{\text{UFB}}(R) \sim \frac{2}{R^4}+\ldots \tag{4.38}$$

$$E_{\text{UFB}}(R) \sim -1-\frac{1}{R}-\frac{4}{R^8}+\ldots \tag{4.39}$$

Thus, the total energy (including nuclear repulsion)

$$E^{\text{tot}}_{\text{UFB}}(R) \sim -1-\frac{4}{R^8}+\ldots \tag{4.40}$$

is correct at $R \to \infty$ limit but approaches its limit, -1, as $O(R^{-8})$, rather than the correct $O(R^{-6})$ behavior that arises due to dispersion. [109] This is because the adopted single-ζ basis lacks any polarization functions and the r_{12} term is only able to capture the induced-quadrupole induced-quadrupole interaction.

4.4 Potential Energy Curves

The data in Table 4.1 have been used to generate RHF, UHF, CI, RFB and UFB PECs that are shown in Fig. 4.3. The UFB curve shows the lowest-energy UFB solution at each bond length, and the corresponding energies are shown in bold in Table 4.1.

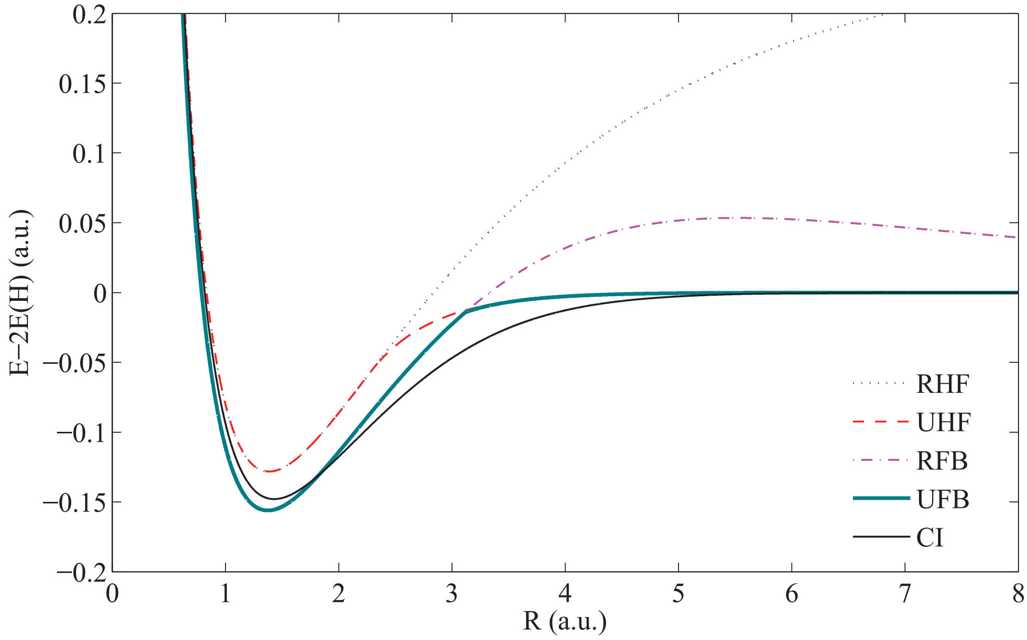

Fig. 4.3 Single-ζ RHF, UHF, RFB , UFB and CI potential energy curves for H_2.

The r_{12} correlation factor in the RFB wavefunction lowers the energy at long bond lengths where the RHF wavefunction performs poorly because of the ionic contamination, however, the growth of r_{12} is far too slow to remove it completely, resulting in slow decay of the energy (Eq. 4.31) and a "hump" in the RFB PEC around $R = 5$. The relaxation of the determinant in the UFB wavefunction is able to cure this hump by breaking the spin-symmetry of the orbitals. For longer bond lengths, the UFB curve becomes very similar to, but distinct from, the UHF curve. One of the most striking features in Fig. 4.3 is the kink in the UFB curve that occurs around $R \approx 3.12$ where the lowest-energy solution switches from the symmetric to a

SB solution. In order to understand the origin of this behavior we consider a simple model system in the following subsection.

4.4.1 UFB/STO-1G Energy Curve: A Simple Model

In this model we approximate each STO with a single uncontracted Gaussian function with exponent $\alpha = 0.27095$. This simplifies the necessary integrals and allows us to perform a exhaustive search for all stationary points of the UFB energy. This model will obviously change the quantitative picture, however, as will be shown, it retains the same qualitative characteristics as our STO model.

Fig. 4.4 shows the UFB/STO-1G PECs for a range of bond lengths that includes three points of interest labeled R_1, R_2 and R_3. Fig. 4.5 shows the UFB energy as a function of the symmetry breaking parameter, t, for a selection of bond lengths. These plots can be used to elucidate the PECs in Fig. 4.4.

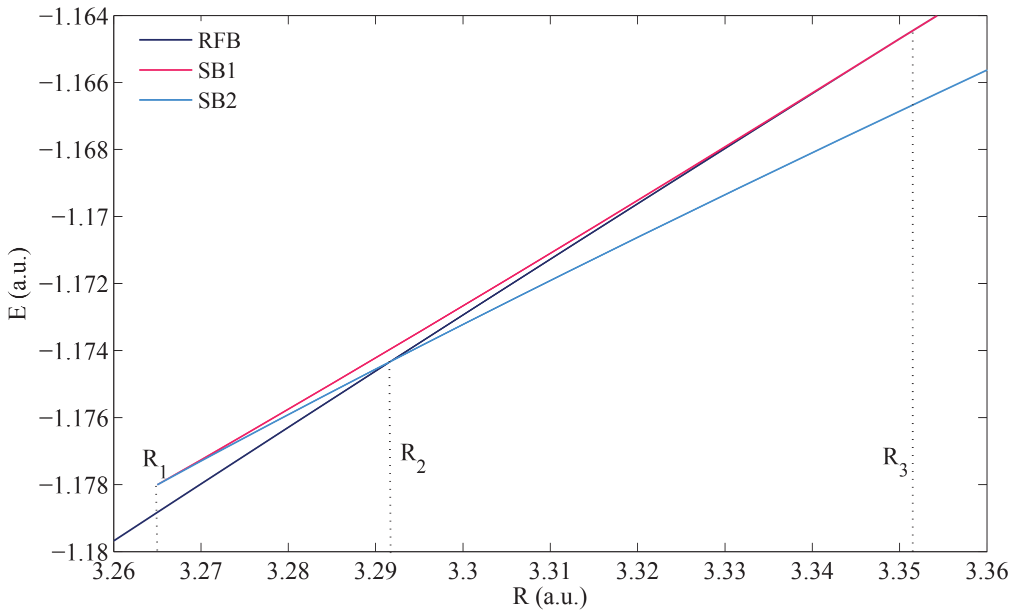

Fig. 4.4 Variation of the RFB and symmetry broken STO-1G electronic energies with R

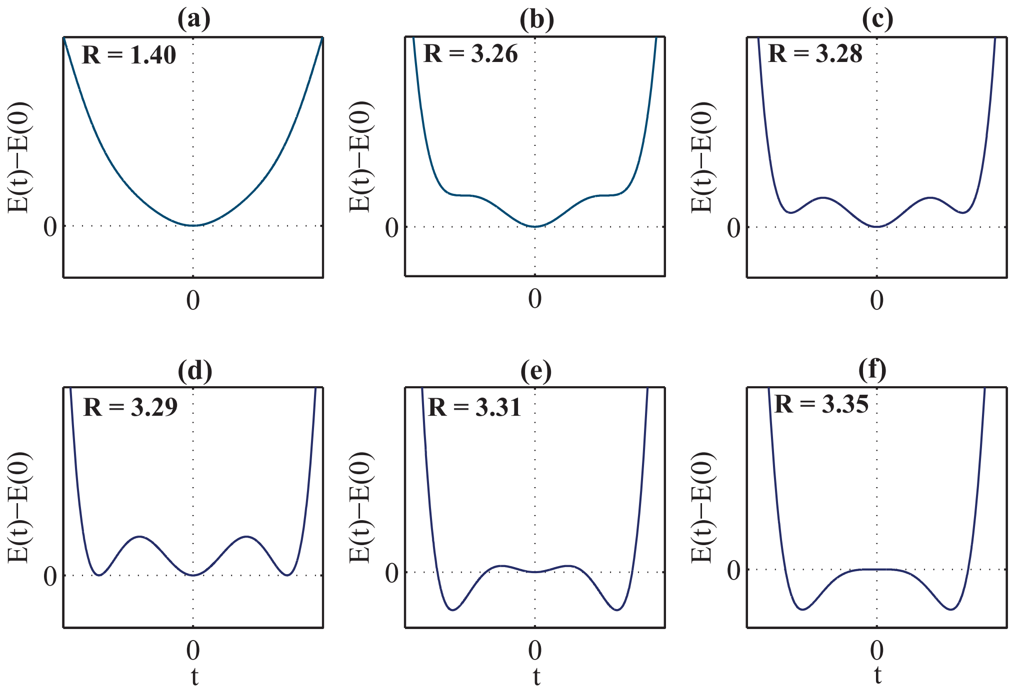

Fig. 4.5 Variation of the UFB/STO-1G energy function with mixing parameter t

At bond lengths shorter than R_1, only the RFB solution exists and this is shown by the single minimum in Fig. 4.5a. At R_1 two equivalent SB solutions appear which correspond to the inflection points shown in Fig. 4.5b. These new solutions are unstable and, as the bond lengthens, each of these bifurcates into one stable and one unstable SB solution, corresponding to the local minima and maxima in Fig. 4.5c, respectively. Figs. 4.4 and 4.5c show that between R_1 and R_2 these SB solutions are all higher in energy than the symmetric RFB solution. At R_2 the stable UFB solutions touch the abscissa (Fig. 4.5d) and become degenerate with the RFB solution. This results in a discontinuous change in the value of t for the UFB energy. Between R_2 and R_3, the difference between the RFB and UFB energies increases, however, in this interval the RFB solution is still RFB→UFB stable, as indicated by the shallow minimum at $t = 0$ in Fig. 4.5e. At R_3 the unstable UFB solutions collapse onto the RFB solution which, at this point, also becomes RFB→UFB unstable. Beyond R_3 only the SB solution is stable and remains the lowest energy solution.

The above analysis is consistent with Fig. 4.3 and the observations made in Subsection 4.3.5. We have verified that in the STO limit the specific values of R_1, R_2 and R_3 are between $3.04 < R_1 < 3.05$, $3.11 < R_2 < 3.12$ and $3.27 < R_3 < 3.28$.

4.4.2 Spectroscopic Parameters

After adding the nuclear repulsion energy $1/R$, one can find the equilibrium bond length R_e, well depth D_e and harmonic vibrational frequency ω_e at the RHF, UHF, CI, RFB and UFB levels. These are given in Table 4.2.

Table 4.2 Equilibrium bond length R_e, harmonic vibrational frequency ω_e and well depth D_e at various levels of theory

	RHF	UHF	CI	RFB	UFB	Exact[a]
R_e / a.u.	1.385	1.385	1.430	1.375	1.375	1.401
ω_e/cm^{-1}	4578	4578	4185	4566	4566	4401
D_e / a.u.	0.41632	0.12823	0.14794	0.15612	0.15612	0.17448

[a] Refs. [110, 111]

Our RFB bond length (1.375 bohr) is much longer than that reported by FB (1.34 bohr) and our well depth (156 mE_h) is slightly larger than theirs (151 mE_h). Both these values are closer to the exact values reported in the literature and we believe, therefore, that the calculations of FB contained significant errors which have been propagated in the literature ever since.

We have also investigated the effects of higher powers of r_{12} in the wavefunction. Adding the r_{12}^2 term to the FB wavefunction introduces an additional degree of freedom and improves the bond length to $R_e = 1.380$ bohr. Improvements to the energy are of the order of a millihartree around the equilibrium bond length and tenths of a millihartree at longer bond lengths. Substituting the linear r_{12} term by the quadratic power, on the other hand, affects the equilibrium bond length by less than 10^{-3} bohr.

4.4.3 Correlation Energies

The correlation energy, E^c, of a method is defined as the difference in energy with respect to UHF. Fig. 4.6 shows the correlation energies as a function of the H_2 bond length for CI and UFB, and compares these to the near-exact curve of Rassolov, Ratner and Pople.[93] The CI and UFB curves were generated using a single Slater basis where all parameters in

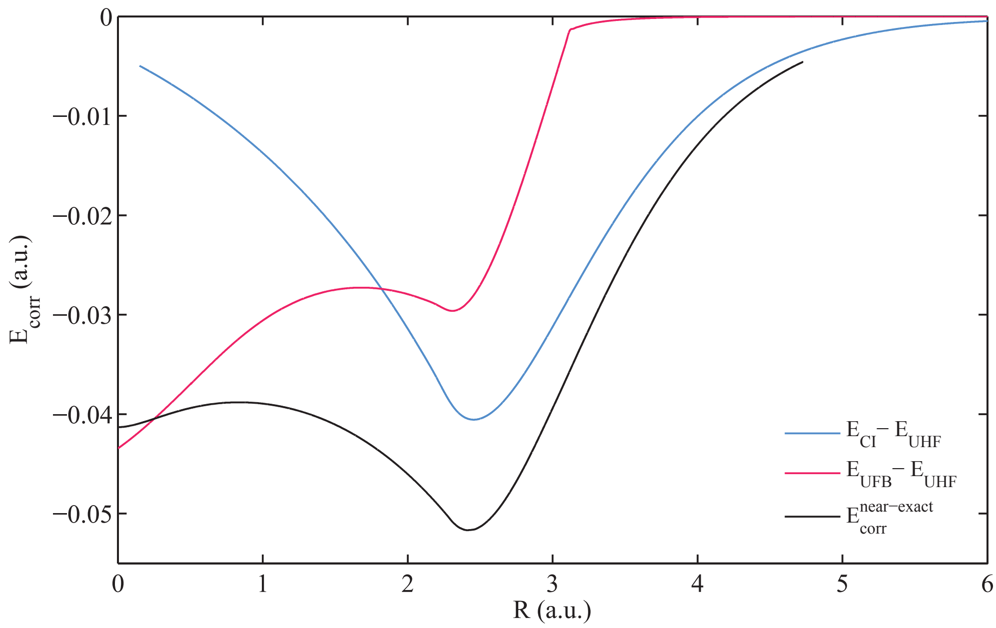

Fig. 4.6 The CI, UFB and near-exact correlation energies for H_2.

the wavefunction, including exponents, were optimized for each bond length. Rassolov *et al.* obtained the near-exact curve using the modified cc-pV6Z basis. [93]

At $R = 0$, the UFB correlation energy ($E^c_{\mathrm{UFB}} = -0.04346$) can be compared to that of the helium atom ($E^c = -0.0420$). [112] The total energy is variational, despite E^c_{UFB} going below the exact value, as the HF references use different basis sets. As R increases, the magnitude of E^c_{UFB} decreases to -0.02728 at $R \approx 1.68$, indicating the electrons in the He atom benefit more from correlation than in the molecule for shorter bond lengths. Beyond $R \approx 1.68$, E^c_{UFB} increases in magnitude slightly before decaying to zero for longer bond lengths, matching the qualitative behavior of the exact E^c curve.

The kink that occurs at $R_2 \approx 3.12$ in Fig. 4.3 is also apparent in Fig. 4.6. Beyond R_2, the correlation energy is predominantly static in nature and the single determinant UFB wavefunction is unable to effectively capture it. Thus, $E^{\mathrm{c}}_{\mathrm{UFB}}$ decays rapidly towards 0 while Ψ_{UFB} approaches Ψ_{UHF}. This is reflected in the behavior of p_{UFB} shown in Fig. 4.2 and Table 4.1.

The similarity of UFB to UHF in the symmetry-broken region can be understood by again considering a single-zeta Gaussian basis in the vicinity of the symmetry breaking point. Let $\theta = t\pi/4$. Using Eqs. 3.7a and 3.7b , one can write

$$\begin{aligned}
\frac{\Psi_{\mathrm{UHF}}}{\Psi_{\mathrm{RHF}}} &= \frac{\psi_\alpha(\mathbf{r}_1)\,\psi_\beta(\mathbf{r}_2)}{\psi_1(\mathbf{r}_1)\,\psi_1(\mathbf{r}_2)} \\
&= \frac{[\psi_1(\mathbf{r}_1)\cos(\theta)+\psi_2(\mathbf{r}_1)\sin(\theta)]\,[\psi_1(\mathbf{r}_2)\cos(\theta)-\psi_2(\mathbf{r}_2)\sin(\theta)]}{\psi_1(\mathbf{r}_1)\,\psi_1(\mathbf{r}_2)} \\
&= \cos^2(\theta)\left[1+\left(\frac{\psi_2(\mathbf{r}_1)}{\psi_1(\mathbf{r}_1)}-\frac{\psi_2(\mathbf{r}_2)}{\psi_1(\mathbf{r}_2)}\right)\tan(\theta)-\frac{\psi_2(\mathbf{r}_1)\,\psi_2(\mathbf{r}_2)}{\psi_1(\mathbf{r}_1)\,\psi_1(\mathbf{r}_2)}\tan^2(\theta)\right]
\end{aligned} \tag{4.41a}$$

Within the simple framework of STO-1G basis, one can write

$$\begin{aligned}
\frac{\psi_2(\mathbf{r})}{\psi_1(\mathbf{r})} &= c\left[\frac{e^{-\alpha\left(\mathbf{r}-\frac{\mathbf{R}}{2}\right)^2}-e^{-\alpha\left(\mathbf{r}+\frac{\mathbf{R}}{2}\right)^2}}{e^{-\alpha\left(\mathbf{r}-\frac{\mathbf{R}}{2}\right)^2}+e^{-\alpha\left(\mathbf{r}+\frac{\mathbf{R}}{2}\right)^2}}\right] \\
&= c\tanh(\alpha\mathbf{R}\cdot\mathbf{r})
\end{aligned} \tag{4.41b}$$

Therefore, for R values which are very close to the symmetry-breaking point, θ is very small and one would be able to obtain

$$\begin{aligned}
\Psi_{\mathrm{UHF}} &= \Psi_{\mathrm{RHF}}\{1+c\;\theta\;[\tanh(\alpha\mathbf{R}\cdot\mathbf{r}_1)-\tanh(\alpha\mathbf{R}\cdot\mathbf{r}_2)]+O(\theta^2)\} \\
&\approx \Psi_{\mathrm{RHF}}\left[1+c\;\theta\;\alpha\;\mathbf{R}\cdot(\mathbf{r_1}-\mathbf{r_2})+O(\theta^2)\right]
\end{aligned} \tag{4.41c}$$

where c is a constant and α is the Gaussian exponent. Thus, to first-order, the transition from RHF to UHF introduces an r_{12}-like term into the wavefunction, leaving the FB correlation term almost redundant.

The Fig. 4.6 shows that the UFB wavefunction can qualitatively reproduce the complex structure of the near-exact correlation energy curve. It also shows that UFB is able to capture more of the correlation energy than CI for bond lengths shorter than $R = 1.82$, where dynamic correlation dominates, but the reverse is true for longer bond lengths where static correlation becomes more important.

4.5 Asymptotic Analysis

Frequently, in many problems arising in physics, the exact analytical solutions are not available for many differential and integral equations. Generally, asymptotic analysis is a branch of analysis which considers both developments in techniques and approximate analytic solutions for problems in which a variable or parameter becomes either very large or small or is in the vicinity of a point where the solution is not analytic. [113] The foundation of modern asymptotic analysis has been laid by Poincaré who gave the precise and formal description of the asymptotic series. [114] Seeking the asymptotic expansion of $f(x)$, for which, we assume a power series form for simplicity of the discussion without loss of generality, one can have [3]

$$x^n R_n(x) = x^n \left[f(x) - s_n(x) \right] \tag{4.42}$$

where in Eq. 4.42, $R_n(x)$ is the corresponding remainder

$$R_n(x) \approx x^{-n-1} \tag{4.43}$$

and $s_n(x)$ is the corresponding partial sum,

$$s_n(x) = a_0 + \frac{a_1}{x} + \frac{a_2}{x^2} + \ldots + \frac{a_n}{x^n} \tag{4.44}$$

respectively. If the conditions

$$\lim_{x\to\infty} x^n R_n(x) = 0 \qquad \text{for fixed } n \tag{4.45}$$

$$\lim_{n\to\infty} x^n R_n(x) = \infty \qquad \text{for fixed } x \tag{4.46}$$

are satisfied, one can write

$$f(x) \sim \sum_{n=0}^{\infty} a_n x^{-n} \tag{4.47}$$

Where the sign $\sim$ which is read "is asymptotic to" has been used instead of $=$ which means "is equal to". The equal sign is valid only in the limit of $x \to \infty$ with restricting the asymptotic series to the limited number of terms. [3]

As mentioned at the end of Sec. 4.1, for large values of R, the most difficult integrals become exponentially small and the behaviors of the RHF, UHF, CI, RFB and UFB energies can be investigated through using the asymptotic analysis techniques. The asymptotic analysis of the optimized exponent ζ, the mixing parameter t, the linear correlation coefficient p, determinant amplitudes θ and the energy of the wavefunctions considered in Eqs. 3.1– 3.5 reveals that, for large R, the decay behaviors can either be exponential or algebraic.

The asymptotic analyses of the RHF, UHF and CI wavefunctions for large R involves the general form for the asymptotic expansion of the total energy

$$E^{\text{tot}}(\zeta,t,R) \sim \sum_{m=-\infty}^{\infty} \sum_{n=0}^{\infty} \left[c_{mn}(\zeta,t) + c'_{mn}(\zeta,t)\ln(R)\right] R^m \exp(-nR) \tag{4.48}$$

where c'_{mn} is zero for RHF and UHF large-R asymptotic expansions whereas it is nonzero for CI asymptotic expansion due to the multiplication of natural logarithms of R with power functions of R which can compete with similar power functions of R in the asymptotic expansion. Note that in order to obtain the asymptotic expression of the total energy at large bond lengths (Eq. 4.48), $\mathrm{Ei}(z)$ has been expanded as

$$\mathrm{Ei}(z) \sim e^z \left(1/z + 1/z^2 + \ldots\right) \tag{4.49}$$

The details of each of the approaches required for obtaining the asymptotic expansions of the RHF, UHF and CI wavefunctions are subjects of the following subsections. In the final subsection, we extend our UFB model to the generalized FB (GFB) wavefunction where the r_{12}^n is the correlation factor and n is a positive integer to see whether it is possible to capture all the London dispersion forces within our minimal basis calculations.

4.5.1 Restricted Hartree-Fock

The energy expression for the RHF wavefunction ($t = 0$) was given in Eq. 4.8. At large R, this energy expression can be expanded as a Taylor series around $\zeta = 27/32$ up to second order as

$$E_{\mathrm{RHF}}^{\mathrm{tot}}(\zeta, R) \sim \sum_{m=-\infty}^{\infty} \sum_{n=0}^{\infty} c_{mn}(\zeta) R^m \exp(-nR) \tag{4.50}$$

Restricting m and n such that $-1 \leq m \leq 4$ and $0 \leq n \leq 1$, Eq. 4.50 becomes

$$E_{\mathrm{RHF}}^{\mathrm{tot}} \sim \left(c_{-10}R^{-1} + c_{00}R^0\right) e^{-0\frac{27}{32}R} + \left(c_{-11}R^{-1} + c_{01}R^0 + c_{11}R^1 + c_{21}R^2 + c_{31}R^3 + c_{41}R^4\right) e^{-1\frac{27}{32}R} \tag{4.51}$$

where the nonzero coefficients can be given as

$$\begin{aligned} c_{-10} &= -\tfrac{1}{2} & c_{00} &= -\left(\tfrac{27}{32}\right)^2 + \left(\zeta - \tfrac{27}{32}\right)^2 \\ c_{-11} &= \tfrac{13}{8} & c_{01} &= -\tfrac{297}{256} - 3\left(\zeta - \tfrac{27}{32}\right) \end{aligned} \tag{4.52}$$

$$c_{11} = -\tfrac{1701}{8192} + \tfrac{171}{256}\left(\zeta - \tfrac{27}{32}\right) + \tfrac{91}{48}\left(\zeta - \tfrac{27}{32}\right)^2 \quad c_{21} = -\tfrac{32805}{524288} - \tfrac{1701}{4096}\left(\zeta - \tfrac{27}{32}\right) - \tfrac{909}{512}\left(\zeta - \tfrac{27}{32}\right)^2$$
$$c_{31} = \tfrac{32805}{524288}\left(\zeta - \tfrac{27}{32}\right) + \tfrac{8505}{16384}\left(\zeta - \tfrac{27}{32}\right)^2 \qquad c_{41} = -\tfrac{32805}{1048576}\left(\zeta - \tfrac{27}{32}\right)^2 \tag{4.53}$$

At the $R \to \infty$ limit, $E_{\text{RHF}}^{\text{tot}} \sim c_{00} \sim -\left(\tfrac{27}{32}\right)^2$. By solving

$$\left(\partial E_{\text{RHF}}^{\text{tot}} / \partial \zeta\right) = 0 \tag{4.54}$$

for ζ, one finds that

$$\zeta_{\text{RHF}} \sim \frac{27}{32} + \left[-\frac{32805\, R^3}{1048576} + \dots\right] e^{-\frac{27}{32}R} + \dots \tag{4.55}$$

4.5.2 Unrestricted Hartree-Fock

Here, we seek to find the leading terms in the asymptotic expansions of ζ_{UHF} and t_{UHF} (Eqs. 4.15 and 4.16, respectively). The UHF energy expression can be written as

$$\begin{aligned} E_{\text{UHF}} = 2h_{11} \cos(\tfrac{t\pi}{4})^2 + 2h_{22} \sin(\tfrac{t\pi}{4})^2 + J_{11} \cos(\tfrac{t\pi}{4})^4 \\ + J_{22} \sin(\tfrac{t\pi}{4})^4 + (2J_{12} - 4K_{12}) \cos(\tfrac{t\pi}{4})^2 \sin(\tfrac{t\pi}{4})^2 \end{aligned} \tag{4.56}$$

in which, J_{ij} and K_{ij} are the Coulomb and exchange integrals. Expanding Eq. 4.56 as a Taylor series around $(\zeta, t) = (1, 1)$ up to second order, one can cast Eq. 4.56 into the form of

$$E_{\text{UHF}}^{\text{tot}}(\zeta, t, R) \sim \sum_{m=-\infty}^{\infty} \sum_{n=0}^{\infty} c_{mn}(\zeta, t) R^m \exp(-nR) \tag{4.57}$$

In order to obtain the ζ_{UHF}, t_{UHF} expansions, it is sufficient to restrict m and n such that $-1 \le m \le 6$ and $0 \le n \le 2$, respectively to get

$$E^{\text{tot}}_{\text{UHF}} \sim \left(c_{-10}R^{-1} + c_{00}R^{0}\right)e^{-0R} + \left(c_{-11}R^{-1} + c_{01}R^{0} + c_{11}R^{1} + c_{21}R^{2} + c_{31}R^{3} + c_{41}R^{4}\right)e^{-1R}$$
$$+ \left(c_{-12}R^{-1} + c_{02}R^{0} + c_{12}R^{1} + c_{22}R^{2} + c_{32}R^{3} + c_{42}R^{4} + c_{52}R^{5} + c_{62}R^{6}\right)e^{-2R} \tag{4.58}$$

where the nonzero coefficients are

$$\begin{aligned}
c_{-10} &= -\tfrac{\pi^2}{8}(t-1)^2 & c_{00} &= -1 + (\zeta-1)^2 + \tfrac{5\pi^2}{64}(t-1)^2\zeta \\
c_{-11} &= -\tfrac{13\pi}{16}(t-1) & c_{01} &= \tfrac{11\pi}{16}(t-1) + \tfrac{3\pi}{2}(\zeta-1)(t-1) \\
c_{11} &= \tfrac{7\pi}{48}(t-1) - \tfrac{19\pi}{48}(\zeta-1)(t-1) & c_{21} &= \tfrac{5\pi}{48}(t-1) + \tfrac{\pi}{2}(\zeta-1)(t-1) \\
c_{31} &= -\tfrac{5\pi}{48}(\zeta-1)(t-1) - \tfrac{55\pi}{96}(\zeta-1)^2(t-1) & c_{41} &= \tfrac{5\pi}{96}(\zeta-1)^2(t-1) \\
c_{-12} &= -\tfrac{1}{8} & c_{02} &= \tfrac{17}{16} + \tfrac{21}{16}(\zeta-1) \\
c_{12} &= \tfrac{7}{12} - \tfrac{23}{24}(\zeta-1) & c_{22} &= c_{02} - \tfrac{11}{24} \\
c_{32} &= \tfrac{11}{72} + \tfrac{5}{72}(\zeta-1) + \left(\tfrac{8\gamma-19}{240}\right)\pi^2(t-1)^2 & c_{42} &= \tfrac{5}{144} + \tfrac{13}{144}(\zeta-1) + \tfrac{5\pi^2}{288}(t-1)^2 \\
& & &\quad - \left(\tfrac{96\gamma-353}{1440}\right)\pi^2(\zeta-1)(t-1)^2 \\
c_{52} &= -\tfrac{5}{72}(\zeta-1) - \tfrac{5\pi^2}{144}(\zeta-1)(t-1)^2 & c_{62} &= \tfrac{5}{72}(\zeta-1)^2 + \tfrac{5\pi^2}{144}(\zeta-1)^2(t-1)^2 \\
&\quad -\tfrac{35}{72}(\zeta-1)^2 + \left(\tfrac{48\gamma-239}{720}\right)\pi^2(t-1)^2(\zeta-1)^2 & &
\end{aligned} \tag{4.59}$$

where, γ is the Euler-Mascheroni constant. [3, 81] Note that at $R \to \infty$ limit, $E^{\text{tot}}_{\text{UHF}} \sim c_{00} \sim -1$. Solving

$$\left(\partial E^{\text{tot}}_{\text{UHF}}/\partial t\right) = 0 \tag{4.60}$$

for t and expanding the result around $\zeta = 1$, one finds that

$$t_{\text{UHF}} \sim 1 + \left[-\frac{2R^2}{3\pi} + \ldots\right]e^{-R} + \ldots \tag{4.61}$$

The differentiation of the energy expression with respect to ζ

$$\left(\partial E_{\mathrm{UHF}}^{\mathrm{tot}}/\partial\zeta\right)=0 \tag{4.62}$$

provides us with

$$\zeta_{\mathrm{UHF}}\sim 1+\left[-\frac{R^3}{6}+\dots\right]e^{-2R}+\dots \tag{4.63}$$

4.5.3 Configuration Interaction

The energy expression for the CI wavefucntion was given in Eq. 3.23. At large bond lengths, the CI energy expression can be expanded as a Taylor series around $(\zeta,\theta)=(1,1)$ up to second order and be cast into the form of Eq. 4.48. Restricting m and n such that $-1\leq m\leq 6$ and $0\leq n\leq 2$, one can get

$$\begin{aligned}E_{\mathrm{CI}}^{\mathrm{tot}}\sim &\left(c_{-10}R^{-1}+c_{00}R^0\right)e^{-0R}+\left(c_{-11}R^{-1}+c_{01}R^0+c_{11}R^1+c_{21}R^2+c_{31}R^3+c_{41}R^4\right)e^{-1R}\\ &+\Big[c_{-12}R^{-1}+c_{02}R^0+c_{12}R^1+c_{22}R^2+c_{32}R^3+c_{42}R^4+c_{52}R^5+c_{62}R^6\\ &+\left(c'_{-12}R^{-1}+c'_{02}R^0+c'_{12}R^1+c'_{22}R^2+c'_{32}R^3+c'_{42}R^4+c'_{52}R^5\right)\ln(R)\Big]e^{-2R}\end{aligned} \tag{4.64}$$

where the nonzero coefficients can be given as

$$c_{-10}=-\tfrac{\pi^2}{16}(\theta-1)^2 \qquad c_{00}=-1+(\zeta-1)^2+\tfrac{5\pi^2}{128}(\theta-1)^2\zeta$$

$$c_{-11}=-\tfrac{13\pi}{16}(\theta-1) \qquad c_{01}=\tfrac{11\pi}{16}(\theta-1)+\tfrac{3\pi}{2}(\zeta-1)(\theta-1)$$

$$c_{11}=\tfrac{7\pi}{48}(\theta-1)-\tfrac{19\pi}{48}(\zeta-1)(\theta-1)-\tfrac{91\pi}{96}(\zeta-1)^2(\theta-1) \qquad c_{21}=\tfrac{5\pi}{48}(\theta-1)+\tfrac{\pi}{2}(\zeta-1)(\theta-1)+\tfrac{131\pi}{96}(\zeta-1)^2(\theta-1)$$

$$c_{31}=-\tfrac{5\pi}{48}(\zeta-1)(\theta-1)-\tfrac{55\pi}{96}(\zeta-1)^2(\theta-1) \qquad c_{41}=\tfrac{5\pi}{96}(\zeta-1)^2(\theta-1)$$

$$c_{-12}=\tfrac{(193+384\gamma)}{320}-\tfrac{21}{160}(\zeta-1)-\tfrac{55}{128}(\zeta-1)^2 \qquad c_{02}=\tfrac{(99+192\gamma)}{80}+\tfrac{389}{160}(\zeta-1)+\tfrac{21}{160}(\zeta-1)^2$$

$$
\begin{aligned}
c_{12} &= \tfrac{(80\gamma-57)}{40} - \tfrac{(133+32\gamma)}{40}(\zeta-1) \\
&-\tfrac{(719+64\gamma)}{160}(\zeta-1)^2 + \tfrac{\pi^2}{48}(\zeta-1)^2(\theta-1)^2 \\
&+\tfrac{\pi^2}{24}(\zeta-1)(\theta-1)^2 + \tfrac{\pi^2}{48}(\theta-1)^2 \\
c_{22} &= \tfrac{(32\gamma-45)}{40} - \tfrac{4(\gamma-6)}{5}(\zeta-1)^2 - \\
&\tfrac{(192\gamma-113)}{120}(\zeta-1) + \tfrac{7\pi^2}{384}(\zeta-1)^2(\theta-1)^2 \\
&+\tfrac{23\pi^2}{384}(\zeta-1)(\theta-1)^2 + \tfrac{13\pi^2}{384}(\theta-1)^2 \\
c_{32} &= \tfrac{(8\gamma-19)}{60} + \tfrac{11}{5}(\zeta-1)^2 - \\
&\tfrac{(64\gamma-107)}{60}(\zeta-1) - \tfrac{3\pi^2}{64}(\zeta-1)^2(\theta-1)^2 \\
&+\tfrac{5\pi^2}{576}(\zeta-1)(\theta-1)^2 + \tfrac{11\pi^2}{576}(\theta-1)^2 \\
c_{42} &= \tfrac{5}{72} + \tfrac{2(11+12\gamma)}{45}(\zeta-1)^2 - \tfrac{(96\gamma-433)}{360}(\zeta-1) \\
&-\tfrac{\pi^2}{24}(\zeta-1)^2(\theta-1)^2 - \tfrac{19\pi^2}{1152}(\zeta-1)(\theta-1)^2 \\
&+\tfrac{5\pi^2}{1152}(\theta-1)^2 \\
c_{52} &= \tfrac{(48\gamma-319)}{180}(\zeta-1)^2 - \tfrac{5}{36}(\zeta-1) \\
&-\tfrac{\pi^2}{192}(\zeta-1)^2(\theta-1)^2 - \tfrac{5\pi^2}{576}(\zeta-1)(\theta-1)^2 \\
c_{62} &= \tfrac{5}{36}(\zeta-1)^2 + \tfrac{5\pi^2}{576}(\zeta-1)^2(\theta-1)^2 \\
c'_{-12} &= \tfrac{6}{5} \\
c'_{02} &= 2c'_{-12} \\
c'_{12} &= 2 - \tfrac{4}{5}(\zeta-1) - \tfrac{2}{5}(\zeta-1)^2 \\
c'_{22} &= \tfrac{4}{5} - \tfrac{8}{5}(\zeta-1) - \tfrac{4}{5}(\zeta-1)^2 \\
c'_{32} &= \tfrac{2}{15} - \tfrac{16}{15}(\zeta-1) \\
c'_{42} &= -\tfrac{4}{15}(\zeta-1) + \tfrac{8}{15}(\zeta-1)^2 \\
c'_{52} &= \tfrac{4}{15}(\zeta-1)^2
\end{aligned}
\tag{4.65}
$$

At the $R \to \infty$ limit, $E_{\mathrm{CI}}^{\mathrm{tot}} \sim c_{00} \sim -1$. Solving

$$\left(\partial E_{\mathrm{CI}}^{\mathrm{tot}}/\partial\theta\right) = 0 \tag{4.66}$$

for θ, one finds that

$$\theta_{\mathrm{CI}} \sim 1 + \left[-\frac{4R^2}{3\pi} + \ldots\right] e^{-R} + \ldots \tag{4.67}$$

The differentiation of the E_{RCI} expression with respect to ζ

$$\left(\partial E_{\mathrm{CI}}^{\mathrm{tot}}/\partial\zeta\right) = 0 \tag{4.68}$$

results in

$$\zeta_{\mathrm{CI}} \sim 1 + \left[\frac{[6(\gamma+\ln(R)) - 23]R^4}{45} + \ldots\right] e^{-2R} + \ldots \tag{4.69}$$

4.5.4 Generalized Frost-Braunstein

In order to investigate the possibility of capturing the correct dispersion behavior of R^{-6} in the energy at large R within our minimal basis model, we have proposed the GFB ansatz with r_{12}^n as the correlation factor. The GFB wavefunction can be defined as

$$\Psi_{\text{GFB}} = \psi_\alpha(\mathbf{r}_1,t)\psi_\beta(\mathbf{r}_2,t)\left[1+p\left(\frac{r_{12}}{R}\right)^n\right] \qquad \forall n \in \mathbb{N} \tag{4.70}$$

where $\mathbb{N}$ is the set of all positive integers (natural numbers) and the spin-unrestricted MOs ψ_α and ψ_β were defined in Eqs. 3.7a and 3.7b, respectively. Note that we have scaled the correlation factor by R^{-n} to make it dimensionless and to simplify the matrix elements. In the present analysis, because we have targeted the algebraic decay of E_{GFB}, ζ_{GFB} and p_{GFB}, the overlap S_{AB} between two STO basis functions ϕ_{A}^S and ϕ_{B}^S in Eqs. 3.6a and 3.6b, which decays exponentially, can be neglected. Hence, letting $x = 1/R$ and $\lambda = x/\zeta$, the asymptotic dependencies of E_{GFB}, ζ_{GFB} and p_{GFB} can be obtained through minimizing the GFB energy expression

$$E_{\text{GFB}} = \frac{\langle\Psi_{\text{GFB}}|\mathscr{H}|\Psi_{\text{GFB}}\rangle}{\langle\Psi_{\text{GFB}}|\Psi_{\text{GFB}}\rangle} \tag{4.71}$$

where, the t dependency has been separated out in the overlap matrix

$$S_{\text{GFB}} = S' - \tfrac{1}{2}\cos^2\left(\tfrac{\pi t}{2}\right)S'' \tag{4.72}$$

and likewise, for T_{GFB}, U_{GFB} and V_{GFB}. The necessary matrices are given by

$$\mathbf{S}' \sim \begin{bmatrix} 1 & 1+(n)_2\,\lambda^2+\frac{5}{8}(n-2)_4\,\lambda^4+\dots \\ 1+(n)_2\,\lambda^2+\frac{5}{8}(n-2)_4\,\lambda^4+\dots & 1+(2n)_2\,\lambda^2+\dots \end{bmatrix} \tag{4.73}$$

$$\mathbf{T}' \sim \zeta^2\begin{bmatrix} 1 & 1+\frac{1}{2}(n)_2\,\lambda^2+\frac{1}{8}(n-2)_4\,\lambda^4+\dots \\ 1+\frac{1}{2}(n)_2\,\lambda^2+\frac{1}{8}(n-2)_4\,\lambda^4+\dots & 1+\frac{1}{3}(3n)_2\,\lambda^2+\dots \end{bmatrix} \tag{4.74}$$

$$\mathbf{U}' \sim -2\zeta \begin{bmatrix} 1 & \begin{matrix} 1+\lambda+\frac{3}{4}(n)_2\,\lambda^2+n^2\,\lambda^3+\frac{3}{8}(n-2)_4\,\lambda^4 \\ +n(n-2)[\frac{5}{8}(n-1)^2-1]\lambda^5+\ldots \end{matrix} \\ \begin{matrix} 1+\lambda+\frac{3}{4}(n)_2\,\lambda^2+n^2\,\lambda^3+\frac{3}{8}(n-2)_4\,\lambda^4 \\ +n(n-2)[\frac{5}{8}(n-1)^2-1]\lambda^5+\ldots \end{matrix} & 1+\lambda+\frac{3}{4}(2n)_2\,\lambda^2+\ldots \end{bmatrix} \tag{4.75}$$

$$\mathbf{V}' \sim x \begin{bmatrix} 1 & 1+(n-1)_2\,\lambda^2+\frac{5}{8}(n-3)_4\,\lambda^4+\ldots \\ 1+(n-1)_2\,\lambda^2+\frac{5}{8}(n-3)_4\,\lambda^4+\ldots & 1+\ldots \end{bmatrix} \tag{4.76}$$

and

$$\mathbf{S}'' \sim \begin{bmatrix} 0 & S_{12}-\frac{(n+4)\ (n+6)\ \Gamma(n+3)}{3\times 2^{n+4}}\lambda^n \\ S_{12}-\frac{(n+4)\ (n+6)\ \Gamma(n+3)}{3\times 2^{n+4}}\lambda^n & S_{22}-\frac{(2n+4)\ (2n+6)\ \Gamma(2n+3)}{3\times 2^{2n+4}}\lambda^{2n} \end{bmatrix} \tag{4.77}$$

$$\mathbf{T}'' \sim \begin{bmatrix} 0 & T_{12}+\frac{\zeta^2\ (n-6)\ \Gamma(n+5)}{3\times 2^{n+4}\ (n+3)}\lambda^n \\ T_{12}+\frac{\zeta^2\ (n-6)\ \Gamma(n+5)}{3\times 2^{n+4}\ (n+3)}\lambda^n & T_{22}-\frac{\zeta^2\ (5n+3)\ \Gamma(2n+5)}{3\times 2^{2n+3}\ (2n+1)\ (2n+3)}\lambda^{2n} \end{bmatrix} \tag{4.78}$$

$$\mathbf{U}'' \sim \begin{bmatrix} 0 & U_{12}+\frac{\zeta\ (n+4)\ [6+(n+6)\lambda]\ \Gamma(n+3)}{3\times 2^{n+3}}\lambda^n \\ U_{12}+\frac{\zeta\ (n+4)\ [6+(n+6)\lambda]\ \Gamma(n+3)}{3\times 2^{n+3}}\lambda^n & U_{22}+\frac{\zeta\ (2n+4)\ [6+(2n+6)\lambda]\ \Gamma(2n+3)}{3\times 2^{2n+3}}\lambda^{2n} \end{bmatrix} \tag{4.79}$$

$$\mathbf{V}'' \sim \begin{bmatrix} V_{11}-\frac{5}{8}\zeta & V_{12}-\frac{\zeta\ (n+3)\ (n+5)\ \Gamma(n+2)}{3\times 2^{n+3}}\lambda^n \\ V_{12}-\frac{\zeta\ (n+3)\ (n+5)\ \Gamma(n+2)}{3\times 2^{n+3}}\lambda^n & V_{22}-\frac{\zeta\ (2n+3)\ (2n+5)\ \Gamma(2n+2)}{3\times 2^{2n+3}}\lambda^{2n} \end{bmatrix} \tag{4.80}$$

where $\Gamma(a)$ and $(a)_k$ are the Gamma function and Pochhammer symbol, respectively. At large R, one can assume that the optimal values of ζ, p and t will be close to 1, 0 and 1, respectively. Thus, it is possible to consider the Taylor expansion of E_{GFB} around the point $(\zeta,p,t)=(1,0,1)$

$$E_{\text{GFB}} = E_0+\mathbf{g}^\dagger\mathbf{z}+\frac{1}{2}\mathbf{z}^\dagger\mathbf{A}\mathbf{z}+\ldots \tag{4.81}$$

where the step $\mathbf{z}$, the gradient $\mathbf{g}$ and the Hessian $\mathbf{A}$ are

$$\mathbf{z} = \begin{bmatrix} \Delta\zeta \\ \Delta p \\ \Delta t \end{bmatrix} \qquad \mathbf{g} = \begin{bmatrix} \frac{\partial E}{\partial \zeta} \\ \frac{\partial E}{\partial p} \\ \frac{\partial E}{\partial t} \end{bmatrix} \qquad \mathbf{A} = \begin{bmatrix} \frac{\partial^2 E}{\partial \zeta^2} & \frac{\partial^2 E}{\partial \zeta \partial p} & \frac{\partial^2 E}{\partial \zeta \partial t} \\ \frac{\partial^2 E}{\partial p \partial \zeta} & \frac{\partial^2 E}{\partial p^2} & \frac{\partial^2 E}{\partial p \partial t} \\ \frac{\partial^2 E}{\partial t \partial \zeta} & \frac{\partial^2 E}{\partial t \partial p} & \frac{\partial^2 E}{\partial t^2} \end{bmatrix} \tag{4.82}$$

respectively and the partial derivatives are evaluated at $(\zeta, p, t) = (1, 0, 1)$. The step that minimizes the energy truncated at second order satisfies

$$\mathbf{Az} = -\mathbf{g} \tag{4.83}$$

and gives the energy $E_{\text{GFB}} = E_0 + \Delta E$ where

$$\Delta E = -\frac{1}{2}\mathbf{g}^\dagger \mathbf{A} \mathbf{g} \tag{4.84}$$

Using elementary calculus, one finds that the asymptotic forms of the gradient and the Hessian are

$$\mathbf{g} \sim \begin{bmatrix} 0 \\ 4n(n-2)x^5 \\ 0 \end{bmatrix} \qquad \mathbf{A} \sim \begin{bmatrix} 2 & -n(n+1)x^2 & 0 \\ -n(n+1)x^2 & 2n^2x^2 & 0 \\ 0 & 0 & \frac{\pi^2}{32}(5-8x) \end{bmatrix} \tag{4.85}$$

Solving Eq. 4.83 and evaluating Eq. 4.84, one discovers that

$$\Delta\zeta \sim -(n-2)(n+1)x^5 \tag{4.86}$$

$$\Delta p \sim -\frac{2(n-2)}{n}x^3 \tag{4.87}$$

$$\Delta t = 0 \tag{4.88}$$

$$\Delta E \sim -4(n-2)^2 x^8 \tag{4.89}$$

Considering the scale factor R^{-n} in Eq. 4.70 and letting $n = 1$, Eqs. 4.36–4.40 can be reproduced.

The result of this analysis shows that no analytic correlation function of r_{12} can capture the dispersion in our minimal basis model.

4.6 Concluding Remarks

We have revisited the CMO model for H_2, first considered by Frost and Braunstein in 1951, extended it to the unrestricted case and analyzed its large-R behavior for any positive integer power of r_{12}.

For RFB we considered much longer bond lengths than FB and have shown the presence of a pole in the correlation coefficient p_{RFB} at $R \approx 5.5$. The coefficient changes sign at this point and approaches an asymptote of $-5/8$ as $R \to \infty$, contrary to FB who stated p_{RFB} "is extremely large at internuclear distances greater than 5.0 a.u. ." [74] We also obtained values for the equilibrium bond length and well depth that differ from, and we believe are more accurate than those of FB.

UFB provides a significant improvement over RFB past the symmetry breaking point where it is able to completely remove the hump in the RFB energy curve. The UFB model also displays several surprising features including the presence of multiple solutions, a non-smooth PEC, SB solutions that are higher in energy than the restricted solution, and RFB$\to$UFB stability in the presence of lower-energy UFB solutions.

We have considered higher powers of r_{12} and found the energetic effects of their inclusion are small. The existence of multiple solutions for other powers of r_{12} was also observed.

The asymptotic analysis of the RHF, UHF, CI, RFB and UFB wavefunctions shows that none of the PECs has the correct $O(R^{-6})$ decay. The UFB energy demonstrates dispersion-like $O(R^{-8})$ decay which is an improvement over the CI and UHF with exponential decays. Also, the large-R analysis of the GFB wavefunction in which, r_{12}^n is the correlation factor and n is a positive integer, reveals that no analytic function of r_{12} can capture the dispersion within the minimal basis.

Whether or not these phenomena prevail in other explicitly correlated methods is an important question for the R12 and F12 community to address.

CHAPTER 5

Conclusion

In the present thesis, to attack the correlation problem, we have mainly focused on the explicitly correlated wavefunction based methods. Our work begins with the analysis of Nakatsuji's highly-accurate free-complement (FC) method which is based on the theory of the structure of the exact wavefunction. In this analysis, we have demonstrated that the structure of the FC wavefunction –at least– at lower orders, is far from being optimal. In comparison with the conventional FC method, we have shown that fewer number of complement functions can be used to achieve lower energies for the ground state of He atom. This is important because the number of complement functions in the FC method rapidly increases with increasing the order.

In the experiments on the first triplet excited state of the He atom, we have discovered the presence of permanents, in addition to the determinants, in the FC expansion of the wavefunction. These permanents are important for the energy convergence. For example, in the calculation of the excited state of the He atom, adding one permanent to the conventional 4-terms FC expansion can improve the energy by ≈ 2 mE_{h} at first order. Although keeping the permanents in the FC expansion seems to be energetically favorable, their computational cost becomes a major drawback at higher orders. This can be a possible reason explaining why permanents have either been overlooked or discarded by Nakatsuji.

Armed with our knowledge from strengths and weaknesses of the FC method, we have considered three possible compact ansätze with various correlation functions which can be applied to many electron systems. Our main focus on the wavefunction with the linear correlation factor for a better understanding of the mechanism of work of modern R12 and F12 approaches has led us to the investigation of the correlated molecular orbital (CMO) theory of the Frost and Braunstein (FB). We have revisited their work within both restricted (R) and unrestricted formalisms (U) using single-ζ basis where we have derived all necessary matrix elements in closed form except that of the nuclear-attraction with linear r_{12}. We have managed to reduce this matrix element to an accurate one-dimensional quadrature.

The analytic expressions and accurate quadrature enabled us to reproduce the FB results for a wider range of bond lengths in H_2. Hence, we observed the presence of a pole in the correlation coefficient p_{RFB} at $R \approx 5.5$. The coefficient changes sign at this point and approaches an asymptote of $-5/8$ as $R \to \infty$, contrary to FB who stated p_{RFB} "*is extremely large at internuclear distances greater than 5.0 a.u.* ." [74] We also obtained values for the equilibrium bond length and well depth that differ from, and we believe are more accurate than those of FB.

Introducing the unrestricted FB (UFB) ansatz for the first time, we compared its performance with those of RFB, restricted Hartree-Fock (RHF), unrestricted Hartree-Fock (UHF) and configuration interaction (CI) wavefunctions. Our UFB wavefunction provides significant improvements over the RFB where after the symmetry breaking point, it completely removes the hump in the RFB potential energy curve (PEC). UFB also shows surprising characteristics such as the presence of multiple solutions, non-smooth PEC, symmetry-broken solutions that are higher in energy than the restricted solution and RFB$\rightarrow$UFB stability in the presence of lower UFB solutions. These phenomena, particularly, the presence of the multiple solutions can have remarkable impacts on the explicitly correlated methods especially on R12 and F12 calculations within the unrestricted formalism: a converged result at some bond lengths which has been identified as a minimum point on the potential energy surface may not be the lowest possible solution, i.e. the global minimum.

Our detailed large-R asymptotic analysis of the RHF, UHF, CI, RFB and UFB wavefunctions indicates that only RHF is unable to get the dissociation limit of the energy correct. Of the other four methods, E_{UHF} and E_{UFB} both approach the correct limit from below, whereas E_{RFB} and E_{CI} approach it from above. At large R, E_{CI} is never more than $2 \times 10^{-43} E_h$ above the limit. We have verified that use of the unrestricted orbitals in the CI wavefunction can remove this small hump as well. We showed that none of these five PECs has the correct $O(R^{-6})$ decay. The UFB energy demonstrates dispersion-like $O(R^{-8})$ decay which is an improvement over the CI and UHF with exponential decays. Considering the generalized FB (GFB) wavefunction where r_{12}^n is the correlation factor and n is a positive integer, we have shown that no analytic function of r_{12} can capture the dispersion within the minimal basis. This raises the question about the possibility of capturing the correct dispersion decay by adding p functions to our basis set.

We have also found that the energetic effects of inclusion of the higher powers of r_{12} are small. The existence of multiple solutions for other powers of r_{12} was also observed.

CHAPTER 6

Responses to Examiners' Questions

The present chapter tries to address and highlight some important questions raised by examiners. We use **Q** for question and **A** for answer throughout this part.

1. **Q**: *Eq. 4.4 assumes that there is an even weight in the fit at all values of distance. Is there any merit for small n of applying a distance-related weighting function so that the fit is more accurate for particular regions (e.g. near the core)?*

   A: It could well be a possibility. However, the present case provides a simple fit which has extensively been used in textbooks and literature. Since in our study, the required values of n are 8 and 9, this bottom-to-top fitting procedure is not a bottleneck and inserting further complexity into the this process is not a necessity.

2. **Q**: *Exponents and coefficients are given to 50 significant figures. Was any special treatment required in Mathematica for this given that a typical double precision code would only yield about a third of this number of digits in a precise manner?*

   A: No. Mathematica in its local minimization code, "FindMinimum", adopts an "automatic" approach by default. This approach chooses the direct search methods that do not require derivatives of functions wherever the default derivative-based methods face difficulties. The procedure proposed in the text helps FindMinimum code to find the correct local minimum by providing good initial guesses.

3. **Q**: *Why one should be worried about the linear correlation factor, "r_{12}" and how does this term affect the total energy values for complex systems?*

   A: Because of the linear dependence of the exact wavefunction on the interelectronic separation r_{12} in the region of electron coalescence, the inclusion of r_{12} is a natural way to account for the same characteristic in the trial wavefunction. This strategy leads to a rapid convergence of the energy toward the basis set limit for which the traditional algebraic methods fail seriously.

4. **Q**: *Using the FB ansatz, can one get a reliable and accurate total energy of a particular system even in its splitted form. For e.g.,*

$$E_{\text{Tot}} = E_{\text{Kinetic}} + E_{\text{Nuc-electron}} + E_{\text{Exchange}} + E_{\text{Nuc-Nuc}} + E_{\text{Coulomb}} + E_{\text{Correlation}} + \dots \tag{6.1}$$

   If so, how?

   A: The addition of the second determinant which is explicitly multiplied by the linear correlation factor leads to an extra degree of variational flexibility in the trial wavefunction. This consequently lowers the energy of the FB wavefunction in comparison with that of the HF method which can account for the first four terms in the splitted energy equation provided by the examiner. Thus, one expects to see the major effect on the Coulomb-correlation part.

5. **Q**: *Why focus so much on "minimal basis" and rather try some higher basis sets also?*

   A: The minimal basis models enable one to deal with analytic and closed forms for the most if not all parts of the analysis. In addition to the simplicity in the calculations, the main (qualitative) features of the analysis will remain the same for larger basis sets. This fact has been shown in chapter 3 and implied at the end of the second paragraph of the page 104.

6. **Q**: *Will this UFB ansatz be feasible and bring correct descriptions of the nature of the wavefunction present in complex systems like radicals? If so, how?*

   A: Yes, it is possible. In the subsections 3.8.6 and 3.8.7 of Ref. [17] two illustrative cases were provided that we can build our UFB approach on them: CH_3 radical and H_2 molecule. As we have shown in Chapters 3 and 4 for H_2 molecule, by adding an unrestricted determinant multiplied by the r_{12} factor to the first single unrestricted wavefunction, one can obtain the 2×2 matrix eigenvalue equation to achieve variational solutions. The same story can happen for methyl radical; however, the calculation of many-electron integrals will be an important issue.

7. **Q**: *Has this UFB ansatz some conformational effects as well?*

   A: Yes as is shown in subsection 4.4.2. Table 4.2 shows that the obtained spectroscopic parameters (including the equilibrium bond length) are different for FB ansätze compared with those of other traditional methods.

8. **Q**: *What if one goes beyond 2 electron system and looks for finding the reliable and accurate PECs for Li_2, CH_4, etc? How difficult it is to solve beyond 2 e^- systems and whether high precision in the energy value for a particular system really matters in a bigger perspective?*

A: As mentioned in Section 1.2, page 12, dealing with many-electron integrals is one of the main drawbacks of explicitly correlated methods (including FB). Because in principle, analytic integration is not always possible for arbitrary functions, this issue has restricted the use of explicitly correlated methods for highly accurate calculations on large systems.

Although numerical proofs can mirror the accuracy of the method, usually in practical uses there is a balance between the cost and accuracy. In addition, accurate results close to their non-relativistic limit can be compared with the experimental data to elicit relativistic and quantum electrodynamic contributions. These can be further used to calculate important physical and spectroscopic constants.

References

[1] W. Kutzelnigg. Theory of electron correlation. *Prog. Theor. Chem. Phys.*, 13 (In Explicitly Correlated Wave Functions in Chemistry and Physics: Theory and Applications):3–90, 2003.

[2] W. Feller. *An Introduction to Probability Theory and its Elementary Applications*. Wiley, New York, USA, 1950.

[3] G. B. Arfken, H. J. Weber, and F. E. Harris. *Mathematical Methods for Physicists*. Academic Press, Boston, 7th edition, 2012.

[4] T. Helgaker, P. Jørgensen, and J. Olsen. *Molecular Electronic Structure Theory*. Wiley, New York, 2000.

[5] C. Hättig, W. Klopper, A. Köhn, and D. P. Tew. Explicitly correlated electrons in molecules. *Chem. Rev.*, 112:4–74, 2012.

[6] L. Kong, F. A. Bischoff, and E. F. Valeev. Explicitly correlated R12/F12 methods for electronic structure. *Chem. Rev.*, 112:75–107, 2012.

[7] P. O. Löwdin. *Adv. Chem. Phys.*, 22:207, 1959.

[8] J. A. Pople and J. S. Binkley. Correlation energies for ahn molecules and cations. *Mol. Phys.*, 29(2):599–611, 1975.

[9] W. Kutzelnigg and D. Mukherjee. Cumulant expansion of the reduced density matrixes. *J. Chem. Phys.*, 110(6):2800–2809, 1999.

[10] D. A. Mazziotti. Approximate solution for electron correlation through the use of schwinger probes. *Chem. Phys. Lett.*, 289(5–6):419 – 427, 1998.

[11] D. A. Mazziotti. 3,5-contracted schrödinger equation: Determining quantum energies and reduced density matrices without wave functions. *Int. J. Quantum Chem.*, 70(4-5):557–570, 1998.

[12] D. A. Mazziotti. Contracted schrödinger equation: Determining quantum energies and two-particle density matrices without wave functions. *Phys. Rev. A*, 57:4219–4234, 1998.

[13] D. A. Mazziotti. Comparison of contracted schrödinger and coupled-cluster theories. *Phys. Rev. A*, 60:4396–4408, 1999.

[14] R. Kubo. Generalized cumulant expansion method. *J. Phys. Soc. Jpn.*, 17(7):1100–1120, 1962.

[15] W. Kutzelnigg, G. Del Re, and G. Berthier. Correlation coefficients for electronic wave functions. *Phys. Rev.*, 172:49–59, Aug 1968.

[16] W. Kutzelnigg. Electron correlation and electron pair theories. 41 (New Concepts I in Topics in Current Chemistry), 1973.

[17] A. Szabo and N. S. Ostlund. *Modern Quantum Chemistry*. McGraw-Hill, New York, 1989.

[18] R. McWeeny. *Methods of Molecular Quantum Mechanics*. Academic Press, London, England, 2nd edition, 2001.

[19] J. C. Slater. Note on hartree's method. *Phys. Rev.*, 35:210–211, Jan 1930.

[20] V. Fock. Näherungsmethode zur lösungdes quantenmechanischen mehrkörperproblems. *Z. Phys.*, 61(1):126–148, 1930.

[21] R. Pauncz. *Spin Eigenfunctions: Construction and Use*. Plenum Press, New York, USA, 1979.

[22] D. M. Collins. *Z. Naturforsch*, 48a:68, 1993.

[23] E. Schrödinger. *Ann. Physik*, 79:361, 1926.

[24] H. Nakatsuji. Discovery of a general method of solving the schrödinger and dirac equations that opens a way to accurately predictive quantum chemistry. *Acc. Chem. Res.*, 45(9):1480–90, 2012.

[25] T. Kato. Fundamental poperties of hamiltonian operators of schrödinger type. *Trans. Amer. Math. Soc.*, 70:195–211, 1951.

[26] T. Kato. On the eigenfunctions of many-particle systems in quantum mechanics. *Comm. Pure. Appl. Math.*, 10:151–177, 1957.

[27] J. C. Slater. Central fields and rydberg formulas in wave mechanics. *Phys. Rev.*, 31(3):0333–0343, 1928.

[28] E. A. Hylleraas. Neue berechnung der energie des heliums im grundzustande, sowie des tiefsten terms von ortho-helium (New calculation of the energy of helium in the ground-state, and the deepest terms of ortho-helium). *Z. Phys.*, 54(5-6):347–366, 1929.

[29] H. M. James and A. S. Coolidge. The ground state of lithium. *Phys. Rev.*, 49:688–95, 1936.

[30] A. Preiskorn and W. Woznicki. Superposition of correlated configurations method - the ground-state of h-3+. *Chem. Phys. Lett.*, 86(4):369–373, 1982.

[31] J. Rychlewski and J. Komasa. Explicitly correlated functions in variational calculations. *Prog. Theor. Chem. Phys.*, 13(In Explicitly Correlated Wave Functions in Chemistry and Physics):91–147, 2003.

[32] W. Kutzelnigg. r12-dependent terms in the wave function as closed sums of partial wave amplitudes for large l. *Theor. Chim. Acta*, 68:445–469, 1985.

[33] W. Klopper, F. R. Manby, S. Ten-no, and E. F. Valeev. R12 methods in explicitly correlated molecular electronic structure theory. *Int. Rev. Phys. Chem.*, 25(3):427–468, 2006.

[34] S. Ten-no and J. Noga. Explicitly correlated electronic structure theory from r12/f12 ansatze. *WIREs Comput. Mol. Sci.*, 2(1):114–125, 2012.

[35] W. Klopper and J. Noga. Linear R12 terms in coupled cluster theory. *Prog. Theor. Chem. Phys.*, 13(In Explicitly Correlated Wave Functions in Chemistry and Physics):149–183, 2003.

[36] H. Nakatsuji. Structure of the exact wave function. *J. Chem. Phys.*, 113(8):2949–2956, 2000.

[37] H. Nakatsuji and E. R. Davidson. Structure of the exact wave function. II. iterative configuration interaction method. *J. Chem. Phys.*, 115(5):2000–2006, 2001.

[38] H. Nakatsuji. Structure of the exact wave function. III. exponential ansatz. *J. Chem. Phys.*, 115(6):2465–2475, 2001.

[39] H. Nakatsuji. Structure of the exact wave function. IV. excited states from exponential ansatz and comparative calculations by the iterative configuration interaction and extended coupled cluster theories. *J. Chem. Phys.*, 116(5):1811–1824, 2002.

[40] H. Nakatsuji and M. Ehara. Structure of the exact wave function. V. iterative configuration interaction method for molecular systems within finite basis. *J. Chem. Phys.*, 117(1):9–12, 2002.

[41] P. Jørgensen and J. Simons. *Second-Quantization Based Methods in Quantum Chemistry*. Academic Press, New York, USA, 1981.

[42] H. Nakatsuji. Inverse schrödinger equation and the exact wave function. *Phys. Rev. A*, 65(5):052122, 2002.

[43] H. Nakatsuji. Scaled schrödinger equation and the exact wave function. *Phys. Rev. Lett.*, 93(3):030403, 2004.

[44] B. L. Hammond, W. A. Lester Jr., and P. J. Reynolds. *Monte Carlo Methods in Ab Initio Quantum Chemistry*. World Scientific, Singapore, 1994.

[45] H. Nakatsuji, H. Nakashima, Y. Kurokawa, and A. Ishikawa. Solving the schrödinger equation of atoms and molecules without analytical integration based on the free iterative-complement-interaction wave function. *Phys. Rev. Lett.*, 99(24):240402, 2007.

[46] H. Nakatsuji and H. Nakashima. Free-complement local-schrödinger-equation method for solving the schrödinger equation of atoms and molecules: Basic theories and features. *J. Chem. Phys.*, 142(8), 2015.

[47] H. Nakashima and H. Nakatsuji. Solving the schrödinger equation for helium atom and its isoelectronic ions with the free iterative complement interaction (ICI) method. *J. Chem. Phys.*, 127(22):224104, 2007.

[48] A. Ishikawa, H. Nakashima, and H. Nakatsuji. Solving the schrödinger and dirac equations of hydrogen molecular ion accurately by the free iterative complement interaction method. *J. Chem. Phys.*, 128(12):124103, 2008.

[49] A. Ishikawa, H. Nakashima, and H. Nakatsuji. Accurate solutions of the schrödinger and dirac equations of , hd+, and ht+: With and without born–oppenheimer approximation and under magnetic field. *Chem. Phys.*, 401(0):62–72, 2012.

[50] H. Nakashima, Y. Hijikata, and H. Nakatsuji. Solving the electron and electron-nuclear schrödinger equations for the excited states of helium atom with the free iterative-complement-interaction method. *J. Chem. Phys.*, 128(15):154108, 2008.

[51] W. G. Baber and H. R. Hasse. *Proc. Cambridge Philos. Soc.*, 31:564, 1935.

[52] V. Magnasco. *Elementary Quantum Mechanics: Mathematical Methods and Applications*. Elsevier, New York, USA, 2nd edition, 2013.

[53] Wolfram Research Inc. Mathematica: Version 10.4, 2016.

[54] L. J. Schaad and W. V. Hicks. Equilibrium bond length in h2+. *J. Chem. Phys.*, 53(2):851–852, 1970.

[55] J. C. Slater. Atomic shielding constants. *Phys. Rev.*, 36:57–64, 1930.

[56] X. Pan, V. Sahni, Massa L., and K. D. Sen. New expression for the expectation value integral for a confined helium atom. *Comput. Theor. Chem.*, 965(1):202 – 205, 2011.

[57] T. Kinoshita. Ground state of the helium atom. *Physical Review*, 105(5):1490–1502, 1957.

[58] G. W. Kellner. Die ionisierungsspannung des heliums nach der schrodingerschen theorie. *Z. Phys.*, 44:91–109, 1927.

[59] J. H. Bartlett. The helium wave equation. *Phys. Rev.*, 51:661–669, 1937.

[60] T. H. Gronwall. The helium wave equation. *Phys. Rev.*, 51:655–660, 1937.

[61] V. A. Fock. On the schrödinger equation of the helium atom. *Izv. Akad. Nauk. SSSR, Ser. Fiz.*, 18:161, 1954.

[62] I. V. Komarov L. D. Faddeev, L. A. Khalfin, editor. *V.A. Fock - Selected Works: Quantum Mechanics and Quantum Field Theory*. CRC Press, New York, USA, 2004.

[63] T. Koga and K. Matsui. Optimal Hylleraas wavefunctions. *Z. Phys. D*, 27:97–102, 1993.

[64] T. Muir. *A Treatise on the Theory of Determinants*. Dover Publications, New York, USA, 1960.

[65] E. W. Weisstein. Permanent, from mathworld–a wolfram web resource, http://mathworld.wolfram.com/permanent.html.

[66] T. Koga. Hylleraas six-term wavefunction: Correction. *J. Chem. Phys.*, 93(5):3720, 1990.

[67] T. Koga. Hylleraas and Kinoshita wavefunctions: Revision and correction. *J. Chem. Phys.*, 94(8):5530, 1991.

[68] T. Koga. Hylleraas wavefunctions revisited. *J. Chem. Phys.*, 96(2):1276, 1992.

[69] T. Koga and S. Morishita. Optimal Kinoshita wavefunctions for heliumlike atoms. *Z. Phys. D*, 34:71–74, 1995.

[70] T. Koga. Optimal Kinoshita wavefunctions with half-integer powers. *J. Chem. Phys.*, 104(16):6308, 1996.

[71] S. Ten-no. Initiation of explicitly correlated slater-type geminal theory. *Chem. Phys. Lett.*, 398(1–3):56 – 61, 2004.

[72] H. M. James and A. S. Coolidge. The ground state of the hydrogen molecule. *J. Chem. Phys.*, 1(12):825–835, 1933.

[73] A. A. Frost, J. Braunstein, and W. Schwemer. Correlated molecular orbitals. *J. Am. Chem. Soc.*, 70:3292–3295, 1948.

[74] A. A. Frost and J. Braunstein. Hydrogen molecule energy calculation by correlated molecular orbitals. *J. Chem. Phys.*, 19:1133–1138, 1951.

[75] C. C. J. Roothaan. New developments in molecular orbital theory. *Rev. Mod. Phys.*, 23:69–89, 1951.

[76] G. G. Hall. The molecular orbital theory of chemical valency. viii. a method of calculating ionization potentials. *Proc. Roy. Soc. (London)*, A205:541–552, 1951.

[77] J. A. Pople and R. K. Nesbet. Self-consistent orbitals for radicals. *J. Chem. Phys.*, 22:571–572, 1954.

[78] S. Wang. The problem of the normal hydrogen molecule in the new quantum mechanics. *Phys. Rev.*, 31:579–586, 1928.

[79] F. Jensen. *Introduction to Computational Chemistry*. Wiley, England, 2007.

[80] F. W. J. Olver, D. W. Lozier, R. F. Boisvert, and C. W. Clark, editors. *NIST Handbook of Mathematical Functions*. Cambridge University Press, New York, 2010.

[81] M. Abramowitz and I. A. Stegun, editors. *Handbook of Mathematical Functions*. Dover Publications, New York, 2007.

[82] Y. Sugiura. Uber die eigenschaften des wasserstoffmolekuls im grundzustande. *Z. Phys.*, 45:484–492, 1927.

[83] W. Kutzelnigg and III Morgan, J. D. Rates of convergence of the partial-wave expansions of atomic correlation energies. *J. Chem. Phys.*, 96(6):4484–508, 1992.

[84] W. Kutzelnigg. Correction. *J. Chem. Phys.*, 97(11):8821–8821, 1992.

[85] C. Schwartz. Importance of angular correlations between atomic electrons. *Phys. Rev.*, 126:1015–19, 1962.

[86] B. Klahn and III Morgan, J. D. Rates of convergence of variational calculations and of expectation values. *J. Chem. Phys.*, 81(1):410–33, 1984.

[87] R. N. Hill. Rates of convergence and error estimation formulas for the rayleigh-ritz variational method. *J. Chem. Phys.*, 83(3):1173–96, 1985.

[88] S. Fournais, M. Hoffmann-Ostenhof, T. Hoffmann-Ostenhof, and T. O. Sorensen. Sharp regularity results for coulombic many-electron wave functions. *Commun. Math. Phys.*, 255(1):183–227, 2005.

[89] Secrest D. Stroud A.H. *Gaussian quadrature formulas*. Prentice-Hall series in automatic computation. PH, 1966.

[90] G. M. J. Barca, P. F. Loos, and P. M. W. Gill. Efficient computation of three-electron integrals over gaussian basis functions, in preparation.

[91] E. W. Weisstein. Orthogonal polynomials, http://mathworld.wolfram.com /orthogonalpolynomials.html.

[92] E. W. Weisstein. Gaussian quadrature, http://mathworld.wolfram.com /gaussianquadrature.html.

[93] V. A. Rassolov, M. A. Ratner, and J. A. Pople. Electron correlation in chemical bonds. *J. Chem. Phys.*, 112:4014–4019, 2000.

[94] W. J. Hehre, R. F. Stewart, and J. A. Pople. Self-consistent molecular-orbital methods. I. use of gaussian expansions of slater-type atomic orbitals. *J. Chem. Phys.*, 51:2657–2664, 1969.

[95] R. López, G. Ramírez, J. M. García de la Vega, and J. Fernández Rico. Large gaussian expansions of sto's for the calculation of many-center molecular integrals with slater basis. *J. Chim. Phys.*, 84:696–698, 1987.

[96] J. Fernández Rico, G. Ramírez, R. López, and J. I. Fernández-Alonso. Accurate gaussian expansion of stos. test of many-center slater integrals. *Coll. Czech. Chem. Commun.*, 53:2250–2265, 1988.

[97] A. S. P. Gomes and R. Custodio. Exact gaussian expansions of slater-type atomic orbitals. *J. Comput. Chem.*, 23:1007–1012, 2002.

[98] P. M. W. Gill. Molecular integrals over gaussian basis functions. *Adv. Quantum Chem.*, 25:141–205, 1994.

[99] W. Kutzelnigg. Theory of the expansion of wave functions in a gaussian basis. *Int. J. Quantum Chem.*, 51:447–463, 1994.

[100] L. K. McKemmish and P. M. W. Gill. Gaussian expansions of orbitals. *J. Chem. Theory Comput.*, 8:4891–4898, 2012.

[101] W. Kutzelnigg. Expansion of a wave function in a gaussian basis. i. local versus global approximation. *Int. J. Quantum Chem.*, 113:203–217, 2013.

[102] J. M. Foster and S. F. Boys. A quantum variational calculation for hcho. *Rev. Mod. Phys.*, 32:303–304, Apr 1960.

[103] M. W. Schmidt and K. Ruedenberg. Effective convergence to complete orbital bases and to the atomic hartree–fock limit through systematic sequences of gaussian primitives. *J. Chem. Phys.*, 71(10):3951–3962, 1979.

[104] D. F. Feller and K. Ruedenberg. Systematic approach to extended even-tempered orbital bases for atomic and molecular calculations. *Theoret. Chim. Acta*, 52(3):231–251, 1979.

[105] C. A. Coulson. The energy and screening constants of the hydrogen molecule. *Trans. Faraday Soc.*, 33:1479–1492, 1937.

[106] D. E. Knuth. *Math. Comput.*, 16:275, 1962.

[107] P. F. Loos and P. M. W. Gill. Ground state of two electrons on a sphere. *Phys. Rev. A*, 79:062517, 2009.

[108] S. Weinbaum. The normal state of the hydrogen molecule. *J. Chem. Phys.*, 1:593–596, 1933.

[109] J. Mitroy and V. D. Ovsiannikov. Generating van der waals coefficients to arbitrary orders of the atom–atom interaction. *Chem. Phys. Lett.*, 412:76–81, 2005.

[110] K. P. Huber and G. Herzberg. *Molecular spectra and molecular structure*, volume IV. Constants of diatomic molecules. van Nostrand Reinhold, New York, 1979.

[111] W. Kolos, K. Szalewicz, and H. J. Monkhorst. New born-oppenheimer potential energy curve and vibrational energies for the electronic ground state of the hydrogen molecule. *J. Chem. Phys.*, 84:3278–3283, 1986.

[112] H. A. Bethe and E. E. Salpeter. *Quantum Mechanics of One- and Two-Electron Atoms*. Springer, Berlin, 1957.

[113] J. D. Murray. *Asymptotic Analysis*. Springer, New York, USA, 1984.

[114] H. Poincaré. Sur les intégrales irrégulières. *Acta Mathematica*, 8(1):295–344, 1886.

APPENDIX A

The One- and Two-Electron Integrals Over Slater-Type Orbitals for H_2

Following the famous results of Hitler-London work on H_2, Sugiura [82] managed to present closed form analytic expressions for all necessary integrals arising from the MO calculation of the PEC of H_2 molecule. We present the results of his work here for the sake of completeness allowing the interested reader to calculate and reproduce the RHF, UHF and CI electronic energies and PECs for H_2 molecule presented in Chapter 4.

Let $X = \zeta R$ where ζ is the exponent of the STO basis functions. The two-center overlap integrals over Slater orbitals can be evaluated directly in confocal elliptical coordinates

[4, 78, 82, 52] or using the Fourier convolution theorem [3] and can be expressed as

$$S_{AB} = (1+X+X^2/3)\exp(-X) \tag{A.1}$$

The one- and two-center kinetic and nuclear-attraction one-electron integrals are

$$T_{AA} = \langle A| -\frac{\nabla^2}{2}|A\rangle = \frac{X^2}{2} \tag{A.2}$$
$$T_{AB} = \langle A| -\frac{\nabla^2}{2}|B\rangle = \frac{X^2}{2}\left(1+X-\frac{X^2}{3}\right)\exp(-X) \tag{A.3}$$
$$U_{AA} = \langle A| -r_A^{-1} - r_B^{-1}|A\rangle = -(1+X)[1-\exp(-2X)] \tag{A.4}$$
$$U_{AB} = \langle A| -r_A^{-1} - r_B^{-1}|B\rangle = -2X(1+X)\exp(-X) \tag{A.5}$$

and the two-electron Coulomb repulsion integrals are expressed as

$$\langle AA|AA\rangle = \frac{5X}{8} \tag{A.6}$$
$$\langle AB|AB\rangle = 1-\left(1+\frac{11}{8}X+\frac{3}{4}X^2+\frac{1}{6}X^3\right)\exp(-2X) \tag{A.7}$$
$$\langle AA|AB\rangle = \left(\frac{5}{16}+\frac{1}{8}X+X^2\right)\exp(-X)-\left(\frac{5}{16}+\frac{1}{8}X\right)\exp(-3X) \tag{A.8}$$
$$\langle AA|BB\rangle = \left(\frac{5}{8}X-\frac{23}{20}X^2-\frac{3}{5}X^3-\frac{1}{15}X^4\right)\exp(-2X)+\frac{6}{5}\left[(\ln(R)+\gamma)S_{AB}(X)^2\right. \tag{A.9}$$
$$\left. - 2\mathrm{Ei}(-2\mathrm{X})S_{AB}(X)S_{AB}(-X)+\mathrm{Ei}(-4\mathrm{X})S_{AB}(-X)^2\right] \tag{A.10}$$

where γ is the Euler-Mascheroni constant and Ei is the exponential integral. [4, 78, 82, 52] In order to be able to write all these integral expressions in terms of X only, we have to make some changes in our core Hamiltonian h, Coulomb J and exchange K integrals as

$$h_{11} = \frac{1}{R^2}\left[\frac{T_{AA}+T_{AB}}{1+S_{AB}}\right]+\frac{1}{R}\left[\frac{U_{AA}+U_{AB}}{1+S_{AB}}\right] \tag{A.11}$$

$$h_{22} = \frac{1}{R^2}\left[\frac{T_{\mathrm{AA}} - T_{\mathrm{AB}}}{1 - S_{\mathrm{AB}}}\right] + \frac{1}{R}\left[\frac{U_{\mathrm{AA}} - U_{\mathrm{AB}}}{1 - S_{\mathrm{AB}}}\right] \tag{A.12}$$

$$J_{11} = \frac{1}{R}\left[\frac{2\langle AA|AA\rangle + 2\langle AB|AB\rangle + 8\langle AA|AB\rangle + 4\langle AA|BB\rangle}{4(1 + S_{\mathrm{AB}})^2}\right] \tag{A.13}$$

$$J_{22} = \frac{1}{R}\left[\frac{2\langle AA|AA\rangle + 2\langle AB|AB\rangle - 8\langle AA|AB\rangle + 4\langle AA|BB\rangle}{4(1 - S_{\mathrm{AB}})^2}\right] \tag{A.14}$$

$$J_{12} = \frac{1}{R}\left[\frac{2\langle AA|AA\rangle + 2\langle AB|AB\rangle + 0\langle AA|AB\rangle - 4\langle AA|BB\rangle}{4(1 + S_{\mathrm{AB}})(1 - S_{\mathrm{AB}})}\right] \tag{A.15}$$

$$K_{12} = \frac{1}{R}\left[\frac{2\langle AA|AA\rangle - 2\langle AB|AB\rangle + 0\langle AA|AB\rangle + 0\langle AA|BB\rangle}{4(1 + S_{\mathrm{AB}})(1 - S_{\mathrm{AB}})}\right] \tag{A.16}$$

APPENDIX $\mathcal{B}$

The Abscissas and Weights of the Gaussian Quadrature for the U_1 Nuclear-Attraction Integrals

As we have mentioned in Subsubsection. 3.3.1.3, an n-point quadrature rule within the framework of Gaussian quadrature will be exact for all polynomials up to degree $2n-1$. [4] In other words, the Gaussian quadrature approximates the definite integral as a linear combination of values of its integrand calculated at optimal abscissas. [81]

$$\int_a^b f(x)dx \approx \sum_i w_i f(x_i) \tag{B.1}$$

We have used *Numerical Differential Equation Analysis* package in *Mathematica 10.4* program [53] to design a 50-point quadrature and calculate the (x_i, w_i) pairs on the interval $[0, 1]$ (the last line of Eq. 3.79 and Eq. 3.80). Table B.1 shows the calculated optimal abscissas and weights for this 50-point Gaussian quadrature using which, we have managed to calculate U_1 FB nuclear-attraction integrals accurately.

Table B.1 The optimal abscissas x_i and weights w_i for 50-point Gaussian quadrature on the interval $[0,1]$.

,

x_i	w_i
0.0005667978	0.0014543113
0.0029840153	0.0033798996
0.0073229580	0.0052952742
0.0135678074	0.0071904114
0.0216945224	0.0090577804
0.0316716905	0.0108901216
0.0434607217	0.0126803368
0.0570160102	0.0144214968
0.0722851153	0.0161068641
0.0892089646	0.0177299178
0.1077220835	0.0192843783
0.1277528489	0.0207642315
0.1492237656	0.0221637522
0.1720517672	0.0234775257
0.1961485364	0.0247004692
0.2214208477	0.0258278515
0.2477709275	0.0268553109
0.2750968325	0.0277788724
0.3032928441	0.0285949628
0.3322498773	0.0293004249
0.3618559031	0.0298925294
0.3919963816	0.0303689854
0.4225547050	0.0307279498
0.4534126492	0.0309680337
0.4844508308	0.0310883083
0.5155491692	0.0310883083
0.5465873508	0.0309680337
0.5774452950	0.0307279498
0.6080036184	0.0303689854
0.6381440969	0.0298925294
0.6677501227	0.0293004249
0.6967071559	0.0285949628
0.7249031675	0.0277788724
0.7522290725	0.0268553109
0.7785791523	0.0258278515
0.8038514636	0.0247004692
0.8279482328	0.0234775257
0.8507762344	0.0221637522
0.8722471511	0.0207642315
0.8922779165	0.0192843783
0.9107910354	0.0177299178
0.9277148847	0.0161068641
0.9429839898	0.0144214968
0.9565392783	0.0126803368
0.9683283095	0.0108901216
0.9783054776	0.0090577804
0.9864321926	0.0071904114
0.9926770420	0.0052952742
0.9970159847	0.0033798996
0.9994332022	0.0014543113

APPENDIX C

Asymptotic Expressions for Coulomb Integrals Over Slater Functions: Derivation

To be able to analyze the behavior of RHF, UHF, CI, RFB and UFB energies for large R, we need to derive the large-R expressions for two classes of integrals: $\langle \mathrm{AA}|\hat{\mathscr{O}}|\mathrm{AA}\rangle$ and $\langle \mathrm{AB}|\hat{\mathscr{O}}|\mathrm{AB}\rangle$ shown in Eqs. 4.2a– 4.2i. Here, instead of using the symbol ϕ_{A}^{S} to show the Slater basis functions focused on center A, defined in Eq. 3.8a, we only use the letter A for brevity.

At large R, the one-center overlap integrals over the STOs can be calculated as

$$
\begin{aligned}
&\langle \mathrm{AA}|r_{12}^{n}|\,\mathrm{AA}\rangle \\
&= \int_0^\infty \int_0^\infty \left(\frac{\zeta^3}{\pi} e^{-2\zeta r_1}\right) \left[\frac{(r_1+r_2)^{n+2} - |r_1-r_2|^{n+2}}{2(n+2) r_1 r_2}\right] \left(\frac{\zeta^3}{\pi} e^{-2\zeta r_2}\right) \left(4\pi r_1^2\right) \left(4\pi r_2^2\right) dr_1 dr_2 \\
&= \frac{(n+4)(n+6)(n+2)!}{48(2\zeta)^n}
\end{aligned}
\tag{C.1}
$$

in which, we have used cosine rule to represent r_{12}^{n} in the square brackets where both electrons are focused on the same center. The one-center nuclear-attraction integrals become

$$
\begin{aligned}
&\langle \mathrm{AA}\big|r_{12}^{n}\, r_{1A}^{-1}\big|\,\mathrm{AA}\rangle \\
&= \int_0^\infty \int_0^\infty \left(\frac{\zeta^3}{\pi} \frac{e^{-2\zeta r_1}}{r_1}\right) \left[\frac{(r_1+r_2)^{n+2} - |r_1-r_2|^{n+2}}{2(n+2) r_1 r_2}\right] \left(\frac{\zeta^3}{\pi} e^{-2\zeta r_2}\right) \left(4\pi r_1^2\right) \left(4\pi r_2^2\right) dr_1 dr_2 \\
&= \frac{(n+4)(n+2)!}{16(2\zeta)^{n-1}}
\end{aligned}
\tag{C.2}
$$

and

$$
\begin{aligned}
&\langle \mathrm{AA}\big|r_{12}^{n}\, r_{1B}^{-1}\big|\,\mathrm{AA}\rangle \\
&\sim \int_0^\infty \int_0^\infty \left(\frac{\zeta^3}{\pi} \frac{e^{-2\zeta r_1}}{R}\right) \left[\frac{(r_1+r_2)^{n+2} - |r_1-r_2|^{n+2}}{2(n+2) r_1 r_2}\right] \left(\frac{\zeta^3}{\pi} e^{-2\zeta r_2}\right) \left(4\pi r_1^2\right) \left(4\pi r_2^2\right) dr_1 dr_2 \\
&\sim \frac{(n+4)(n+6)(n+2)!}{48(2\zeta)^n R}
\end{aligned}
\tag{C.3}
$$

Considering the integral,

$$
\begin{aligned}
&\langle \mathrm{AA}|\frac{r_2^2 - r_1^2}{r_1} r_{12}^{n}|\mathrm{AA}\rangle \\
&= \int_0^\infty \int_0^\infty \left(\frac{\zeta^3}{\pi} e^{-2\zeta r_1}\right) \left[\frac{(r_1+r_2)^{n+2} - |r_1-r_2|^{n+2}}{2(n+2) r_1 r_2}\right] \left[\frac{r_2^2 - r_1^2}{r_1}\right] \left(\frac{\zeta^3}{\pi} e^{-2\zeta r_2}\right) \left(4\pi r_1^2\right) \left(4\pi r_2^2\right) dr_1 dr_2 \\
&= \frac{(n+6)(n+4)!}{48(2\zeta)^{n+1}}
\end{aligned}
\tag{C.4}
$$

and using Eqs. C.1 and C.2, the large-R kinetic matrix elements can be expressed as

$$\langle \mathrm{AA}r_{12}^{m}| -\nabla^2/2 | r_{12}^{n}\mathrm{AA}\rangle$$
$$= m\,n\,\langle \mathrm{AA}\,|r_{12}^{m+n-2}|\,\mathrm{AA}\rangle + \frac{m+n}{2}\zeta\left[\langle \mathrm{AA}|\left(\frac{r_2^2-r_1^2}{r_1}r_{12}^{m+n-2} - \frac{r_{12}^{m+n}}{r_1}\right)|\mathrm{AA}\rangle\right] + \zeta^2\,\langle \mathrm{AA}\,|r_{12}^{m+n}|\,\mathrm{AA}\rangle$$
$$= m\,n\left[\frac{(m+n+2)(m+n+4)(m+n)!}{48(2\zeta)^{m+n-2}}\right] + \frac{m+n}{2}\zeta\left[\frac{(m+n+4)(m+n+2)!}{48(2\zeta)^{m+n-1}} - \frac{(m+n+4)(m+n+2)!}{16(2\zeta)^{m+n-1}}\right]$$
$$+\zeta^2\frac{(m+n+4)(m+n+6)(m+n+2)!}{48(2\zeta)^{m+n}}$$
$$= \frac{(m+n+4)!}{192(2\zeta)^{m+n-2}}\frac{-(m-n)^2+5(m+n)+6}{(m+n+1)(m+n+3)}$$
$$= \zeta^2\frac{(q+4)!}{192(2\zeta)^q}\frac{6+5q-(m-n)^2}{(q+1)(q+3)} \tag{C.5}$$

where $q=m+n$. The derivation of asymptotic expressions for two-center integrals $\langle \mathrm{AB}|\hat{\mathscr{O}}|\mathrm{AB}\rangle$ begins with considering the long range r_{12}^n potentials

$$\langle \mathrm{A}\,|r_{12}^n|\,\mathrm{A}\rangle = \int_0^\infty \left(\frac{\zeta^3}{\pi}e^{-2\zeta r}\right)\left[\frac{(x+r)^{n+2}-|x-r|^{n+2}}{2(n+2)rx}\right]\left(4\pi r^2\right)dr$$
$$= x^n\,{}_3F_0\left(-\tfrac{n}{2}, -\tfrac{n+1}{2}, 2, \tfrac{1}{\zeta^2x^2}\right) \tag{C.6}$$

and

$$\langle \mathrm{A}|r_{12}^n r^{-1}|\mathrm{A}\rangle = \int_0^\infty \left(\frac{\zeta^3}{\pi}\frac{e^{-2\zeta r}}{r}\right)\left[\frac{(x+r)^{n+2}-|x-r|^{n+2}}{2(n+2)rx}\right]\left(4\pi r^2\right)dr$$
$$= \zeta x^n\,{}_3F_0\left(-\tfrac{n}{2}, -\tfrac{n+1}{2}, 1, \tfrac{1}{\zeta^2x^2}\right) \tag{C.7}$$

where x is a point at which we calculate the potential and ${}_3F_0$ is the generalized hypergeometric function. Armed with these tools, one can derive the two-center integrals at large R

first of which, is the overlap integral

$$\begin{aligned}
&\langle \mathrm{AB}\,|r_{12}^n|\,\mathrm{AB}\rangle \\
&= \int_0^\infty \int_0^\pi \left(\frac{\zeta^3}{\pi} e^{-2\zeta r}\right) \left[x^n \, {}_3F_0\left(-\tfrac{n}{2}, -\tfrac{n+1}{2}, 2, \tfrac{1}{\zeta^2 x^2}\right)\right] (2\pi r^2) \sin(\theta) d\theta dr
\end{aligned} \tag{C.8}$$

where $x = \sqrt{r^2 + R^2 - 2rR\cos(\theta)}$. Considering this form of x, we change the variable θ to t at large R to get

$$\begin{aligned}
&\langle \mathrm{AB}\,|r_{12}^n|\,\mathrm{AB}\rangle \\
&\sim \int_0^\infty \left(\frac{\zeta^3}{\pi} e^{-2\zeta r}\right) \left[\frac{1}{R\,r} \int_{R-r}^{R+r} t^{n+1} \, {}_3F_0\left(-\tfrac{n}{2}, -\tfrac{n+1}{2}, 2, \tfrac{1}{\zeta^2 t^2}\right) dt\right] (2\pi r^2)\, dr \\
&\sim \int_{-\infty}^\infty t^{n+1} \, {}_3F_0\left(-\tfrac{n}{2}, -\tfrac{n+1}{2}, 2, \tfrac{1}{\zeta^2 t^2}\right) \int_{|R-t|}^\infty \left(\frac{\zeta^3}{\pi} \frac{e^{-2\zeta r}}{R\,r}\right) (2\pi r^2)\, dr\, dt \\
&\sim \frac{\zeta}{2R} \int_{-\infty}^\infty t^{n+1} \, {}_3F_0\left(-\tfrac{n}{2}, -\tfrac{n+1}{2}, 2, \tfrac{1}{\zeta^2 t^2}\right) (1 + 2\zeta\,|t-R|)\, e^{-2\zeta|t-R|} dt \\
&\sim R^n \, {}_3F_0\left(-\tfrac{n}{2}, -\tfrac{n+1}{2}, 4, \lambda^2\right)
\end{aligned} \tag{C.9}$$

where $\lambda = (\zeta R)^{-1}$. Again, let $x = \sqrt{r^2 + R^2 - 2rR\cos(\theta)}$. At large R, the two-center nuclear-attraction integral $\langle \mathrm{AB}\left|r_{12}^n\, r_{1A}^{-1}\right|\mathrm{AB}\rangle$ becomes

$$\begin{aligned}
&\langle \mathrm{AB}\left|r_{12}^n\, r_{1A}^{-1}\right|\mathrm{AB}\rangle \\
&= \int_0^\infty \int_0^\pi \left(\frac{\zeta^3}{\pi} \frac{e^{-2\zeta r}}{r}\right) \left[x^n \, {}_3F_0\left(-\tfrac{n}{2}, -\tfrac{n+1}{2}, 2, \tfrac{1}{\zeta^2 x^2}\right)\right] (2\pi r^2) \sin(\theta) d\theta dr \\
&\sim \int_0^\infty \left(\frac{\zeta^3}{\pi} \frac{e^{-2\zeta r}}{r}\right) \left[\frac{1}{R\,r} \int_{R-r}^{R+r} t^{n+1} \, {}_3F_0\left(-\tfrac{n}{2}, -\tfrac{n+1}{2}, 2, \tfrac{1}{\zeta^2 t^2}\right) dt\right] (2\pi r^2)\, dr \\
&\sim \int_{-\infty}^\infty t^{n+1} \, {}_3F_0\left(-\tfrac{n}{2}, -\tfrac{n+1}{2}, 2, \tfrac{1}{\zeta^2 t^2}\right) \int_{|R-t|}^\infty \left(\frac{\zeta^3}{\pi} \frac{e^{-2\zeta r}}{R\,r^2}\right) (2\pi r^2)\, dr\, dt \\
&\sim \frac{\zeta^2}{R} \int_{-\infty}^\infty t^{n+1} \, {}_3F_0\left(-\tfrac{n}{2}, -\tfrac{n+1}{2}, 2, \tfrac{1}{\zeta^2 t^2}\right) e^{-2\zeta|t-R|} dt
\end{aligned}$$

$$\sim \zeta R^n \, {}_3F_0\left(-\tfrac{n}{2}, -\tfrac{n+1}{2}, 3, \lambda^2\right) \tag{C.10}$$

Derivation of a general asymptotic form for the large-R two-center nuclear-attraction integral $\langle \mathrm{AB} \left| r_{12}^n \, r_{1B}^{-1} \right| \mathrm{AB} \rangle$ was difficult (Chapter 3). However, providing a simple form for the required large-R FB integrals, *i.e.*, $n = 1, 2$ is rather a simpler task. Therefore,

$$\begin{aligned}
&\langle \mathrm{AB} \left| r_{12}^n \, r_{1B}^{-1} \right| \mathrm{AB} \rangle \\
&= \int_0^\infty \int_0^\pi \left(\frac{\zeta^3}{\pi} e^{-2\zeta r} \right) \left[\frac{x^n \, {}_3F_0\left(-\frac{n}{2}, -\frac{n+1}{2}, 2, \frac{1}{\zeta^2 x^2}\right)}{x} \right] \left(2\pi r^2\right) \sin(\theta) d\theta dr \\
&\sim \int_0^\infty \left(\frac{\zeta^3}{\pi} e^{-2\zeta r} \right) \left[\frac{1}{R\, r} \int_{R-r}^{R+r} t^n \, {}_3F_0\left(-\tfrac{n}{2}, -\tfrac{n+1}{2}, 2, \tfrac{1}{\zeta^2 t^2}\right) dt \right] \left(2\pi r^2\right) dr \\
&\sim \int_{-\infty}^\infty t^n \, {}_3F_0\left(-\tfrac{n}{2}, -\tfrac{n+1}{2}, 2, \tfrac{1}{\zeta^2 t^2}\right) \int_{|R-t|}^\infty \left(\frac{\zeta^3}{\pi} \frac{e^{-2\zeta r}}{R\, r} \right) \left(2\pi r^2\right) dr\, dt \\
&\sim \frac{\zeta}{2R} \int_{-\infty}^\infty t^n \, {}_3F_0\left(-\tfrac{n}{2}, -\tfrac{n+1}{2}, 2, \tfrac{1}{\zeta^2 t^2}\right) \left(1 + 2\zeta\, |t - R|\right) e^{-2\zeta |t-R|} dt \\
&\sim \frac{\zeta}{2R} \int_{-\infty}^\infty (t+R)^n \, {}_3F_0\left(-\tfrac{n}{2}, -\tfrac{n+1}{2}, 2, \tfrac{1}{\zeta^2 (t+R)^2}\right) \left(1 + 2\zeta\, |t|\right) e^{-2\zeta |t|} dt \\
&\sim \frac{\zeta}{2R} \int_0^\infty \left[(t+R)^n \, {}_3F_0\left(-\tfrac{n}{2}, -\tfrac{n+1}{2}, 2, \tfrac{1}{\zeta^2 (t+R)^2}\right) + (t-R)^n \, {}_3F_0\left(-\tfrac{n}{2}, -\tfrac{n+1}{2}, 2, \tfrac{1}{\zeta^2 (t-R)^2}\right) \right] \\
&\times \left(1 + 2\zeta t\right) e^{-2\zeta t} dt
\end{aligned} \tag{C.11}$$

For $n = 1$ and $n = 2$, the last line of Eq. C.11 gives us

$$\langle \mathrm{AB} \left| r_{12}^1 \, r_{1B}^{-1} \right| \mathrm{AB} \rangle \sim 1 + \frac{e^{-2/\lambda} (\lambda + 2) \mathrm{Ei}(2/\lambda) - e^{2/\lambda} (\lambda - 2) \mathrm{Ei}(-2/\lambda)}{2} \tag{C.12}$$

$$\langle \mathrm{AB} \left| r_{12}^2 \, r_{1B}^{-1} \right| \mathrm{AB} \rangle \sim R(1 + 4\lambda^2) \tag{C.13}$$

The last piece of this puzzle is to find the asymptotic form for the two-center kinetic integrals at large R. Let $r_{12} = \sqrt{(x_1 - x_2)^2 + (y_1 - y_2)^2 + (z_1 - z_2 + R)^2}$ in cartesian coordinate representation. Hence,

$$\begin{aligned}
&\langle \mathrm{AB} r_{12}^{m} \big| -\nabla^2/2 \big| r_{12}^{n} \mathrm{AB}\rangle \\
&\sim m\,n\,\langle \mathrm{AB} \big| r_{12}^{m+n-2} \big| \mathrm{AB}\rangle - (m+n)\zeta \left[\langle \mathrm{AB} | \left(\frac{\mathbf{r}_1 \cdot \mathbf{r}_{12}}{r_1 r_{12}} \right) r_{12}^{m+n-1} | \mathrm{AB}\rangle \right] + \zeta^2 \langle \mathrm{AA} \big| r_{12}^{m+n} \big| \mathrm{AA}\rangle \\
&\sim m\,n\, R^{m+n-2}\ {}_3F_0 \left(-\frac{m+n-2}{2}, -\frac{m+n-1}{2}, 4, \lambda^2 \right) - \frac{(m+n)(m+n+1)}{2}\ R^{m+n-2} \qquad \text{(C.14)} \\
&\times\ {}_3F_0 \left(-\frac{m+n-2}{2}, -\frac{m+n-1}{2}, 4, \lambda^2 \right) + \zeta^2 R^{m+n}\ {}_3F_0 \left(-\frac{m+n}{2}, -\frac{m+n+1}{2}, 4, \lambda^2 \right) \\
&\sim \zeta^2 R^q \left[{}_3F_0 \left(-\tfrac{q}{2}, -\tfrac{q+1}{2}, 4, \lambda^2 \right) - \frac{m(m+1)+n(n+1)}{2} \lambda^2\ {}_3F_0 \left(-\tfrac{q-2}{2}, -\tfrac{q-1}{2}, 4, \lambda^2 \right) \right]
\end{aligned}$$

in which, $q = m+n$. This completes the derivation of the asymptotic Coulomb integrals (Eqs. 4.2a– 4.2i) presented in Sec. 4.1.

APPENDIX $\mathcal{D}$

The Optimized Exponents and Coefficients of the Normalized STO–nG ($n = 8$ and 9) Basis Sets

The optimized coefficients c_μ and exponents α_μ for the normalized STO–8G and STO-9G basis sets with 50 digits of accuracy were provided. The FB energies coming from using these basis sets can be inserted into the extrapolation formula (Eq. 4.1) to generate the energies of the STO limit shown in Table. 4.1.

Table D.1 The optimized coefficients c_μ and exponents α_μ for the normalized STO–8G and STO-9G basis sets with 50 digits of accuracy.

STO–8G[a]	
α	c
0.05294063219612877407590404531825833686974580920368	0.06159114103594007165419067222992023596723162162760
0.11411093914576128958207231113803884962429811496615	0.28926573961700110005391982624318303075830038536218
0.25095283946544758317118260754823038593293207926644	0.37771677784243995500522560358261889346386276699603
0.58614745871630809649653825872333198123400030810827	0.252225784851252167271869896786599144069513401026312
1.49607112612184879324242206609521511123608208627998	0.11338308049676186194793734609840049085266956540708
4.34394734098301884687044391060137396262141976497179	0.03869067095533864773877664218392844051939735119872
15.5129625353833245014877346317084720281863525070565	0.01016635917759106500858108742752961123752407590058
84.5781563304406770590678409055393935088756726398960	0.00182370874833257093744490240295919175527615983461
STO–9G[b]	
α	c
0.04871801506557735797062111219364367552718703599658	0.04314490380873961139814080432234256840108336100652
0.10062742545217766294878249007977075831411028659920	0.23686448857304026920325212523468951691840360490622
0.20983718788815403667888907200606906698190701153062	0.36005346406702117141158709981610607608651011021242
0.45777954606316785905647268580932835118834143339861	0.27809252741551742796685912125319101118117887345303
1.06675720198887886138350929618098405746975848416130	0.14441580948375998769046390245073120484715020926114
2.72064070449320203961959658705296139790408761328535	0.05785760093216795317734752895802535186366017109473
7.89709680352458606141785051980472966498912298335807	0.01880603607172245550921171344382047920337239458818
28.1979359285303948144123573063484874981579191173210	0.00485157901398688303634389638778571280642574335418
153.728624496781949239120447559239741240730553099218	0.00086527795259664212785177622289366393002048494083

[a] $I = 5.41 \times 10^{-8}$.
[b] $I = 1.27 \times 10^{-8}$.